

**DAHLGREN DIVISION  
NAVAL SURFACE WARFARE CENTER**

Dahlgren, Virginia 22448-5100



---

**NSWCDD/TR-99/19**

**A SIMPLIFIED METHOD FOR PREDICTING  
AERODYNAMICS OF MULTI-FIN WEAPONS**

**BY FRANK G. MOORE    ROY M. MCINVILLE    DAVID I. ROBINSON**  
**WEAPONS SYSTEMS DEPARTMENT**

**MARCH 1999**

Approved for public release; distribution is unlimited.

**1 9 9 9 0 4 1 5 0 1 8**

**DTIC QUALITY INSPECTED 4**

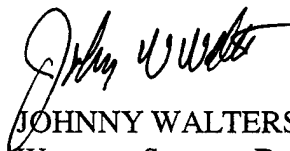
REPORT DOCUMENTATION PAGE			Form Approved OMB No. 0704-0188	
Public reporting burden for this collection of information is estimated to average 1 hour per response, including the time for reviewing instructions, search existing data sources, gathering and maintaining the data needed, and completing and reviewing the collection of information. Send comments regarding this burden or any other aspect of this collection of information, including suggestions for reducing this burden, to Washington Headquarters Services, Directorate for Information Operations and Reports, 1215 Jefferson Davis Highway, Suite 1204, Arlington, VA 22202-4302, and to the Office of Management and Budget, Paperwork Reduction Project (0704-0188), Washington, DC 20503.				
1. AGENCY USE ONLY (Leave blank)	2. REPORT DATE  March 1999	3. REPORT TYPE AND DATES COVERED  Final		
4. TITLE AND SUBTITLE  A Simplified Method for Predicting Aerodynamics of Multi-Fin Weapons		5. FUNDING NUMBERS		
6. AUTHOR(s)  Frank G. Moore, Roy M. McInville, David I. Robinson				
7. PERFORMING ORGANIZATION NAME(S) AND ADDRESS(ES) Commander Naval Surface Warfare Center Dahlgren Division (Code G04) 17320 Dahlgren Road Dahlgren, VA 22448-5100		8. PERFORMING ORGANIZATION REPORT NUMBER  NSWCDD/TR-99/19		
9. SPONSORING/MONITORING AGENCY NAME(S) AND ADDRESS(ES)		10. SPONSORING/MONITORING AGENCY REPORT NUMBER		
11. SUPPLEMENTARY NOTES				
12a. DISTRIBUTION/AVAILABILITY STATEMENT  Approved for public release; distribution is unlimited.		12b. DISTRIBUTION CODE		
13. ABSTRACT (Maximum 200 words) A new semiempirical method was developed to compute aerodynamics of multi-fin missile configurations using cruciform missile aerodynamics as a baseline. The method was developed using full Euler Computational Fluid Dynamics codes to compare computations with wind tunnel data bases for cruciform missiles as a function of Mach number, angle of attack, and aspect ratio. The Euler codes were then used for the same freestream conditions and missile configurations except the number of fins were increased from four to six and eight respectively. A table of coefficients was then formed for the aerodynamics of six- and eight-fin configurations compared to that of four-fin cases for use in the aeroprediction code or other semiempirical codes. It was concluded that this approach worked well except for subsonic Mach numbers at moderate to large angles of attack, where the Euler codes failed to predict the leeward plane flow field adequately. It is believed that full Navier-Stokes solutions could be used to improve upon this semiempirical model. Engineering judgement, in conjunction with low angle-of-attack Euler solutions were used in the regions where Euler solutions were suspect. In comparing the new semiempirical method to a limited amount of wind tunnel data on several configurations, it was concluded that the model worked well at all the conditions where data was available. However, additional wind tunnel data at higher angles of attack on six- and eight-fin configurations is needed before the method can be truly validated.				
14. SUBJECT TERMS  aerodynamics, Aeroprediction Code, multi-fin configurations			15. NUMBER OF PAGES  80	
			16. PRICE CODE	
17. SECURITY CLASSIFICATION OF REPORTS  UNCLASSIFIED	18. SECURITY CLASSIFICATION OF THIS PAGE  UNCLASSIFIED	19. SECURITY CLASSIFICATION OF ABSTRACT  UNCLASSIFIED	20. LIMITATION OF ABSTRACT  UL	

## FOREWORD

The 1998 version of the aeroprediction code (AP98) was limited to configurations that had either planar (two) or cruciform (four) fins. Occasionally, due to launcher constraints or other design considerations, airframe designers would like to have the option of investigating tradeoffs of multiple fins (six or eight) for aerodynamic stability. This report documents an approximate approach to allow these tradeoffs to be accomplished with the AP98 in conjunction with hand calculations. This approximate approach will be integrated into the aeroprediction code and transitioned later as a part of the 2002 version of the code.

The work described in this report was supported through the Office of Naval Research through the Surface Weapons Systems Technology Program managed at the Naval Surface Warfare Center, Dahlgren Division (NSWCDD) by Mr. Robin Staton. Tasking from this program was provided by Mr. Roger Horman and Mr. John Fraysse. Also, some support was provided by the Marine Corps Weaponry Technology Program managed at NSWCDD by Mr. Bob Stiegler. The authors express appreciation for support received in this work.

Approved by:



JOHNNY WALTERS, Deputy Head  
Weapons Systems Department

## CONTENTS

<u>Section</u>	<u>Page</u>
1.0 INTRODUCTION .....	1
2.0 SUMMARY OF METHODS FOR PLANAR AND CRUCIFORM CONFIGURATIONS .....	3
3.0 MODIFICATIONS FOR SIX- AND EIGHT-FIN CONFIGURATIONS .....	5
3.1 SLENDER BODY THEORY PREDICTIONS FOR MULTIFIN AERODYNAMICS .....	6
3.2 COMPUTATIONAL FLUID DYNAMICS (CFD) PREDICTIONS FOR MULTIFIN AERODYNAMICS .....	13
4.0 AERODYNAMIC SMOOTHER .....	35
5.0 COMPARISON OF NEW METHOD FOR MULTIFIN AERODYNAMICS TO EXPERIMENT .....	39
6.0 CONCLUSIONS .....	52
7.0 REFERENCES .....	53
8.0 SYMBOLS AND DEFINITIONS .....	56
DISTRIBUTION .....	(1)

## ILLUSTRATIONS

<u>Figure</u>		<u>Page</u>
1	TYPICAL WEAPON DESIGN AND CONTROL ALTERNATIVES .....	2
2	AP98 METHODS FOR BODY-ALONE AERODYNAMICS .....	4
3	AP98 METHODS FOR DYNAMIC DERIVATIVES (REFERENCES 16 AND 17) .....	4
4	AP98 METHODS FOR WING-ALONE AND INTERFERENCE AERODYNAMICS .....	5
5	LT AND SBT IMPLICATIONS FOR AERODYNAMICS, SINGLE WING OF SPAN $b$ .....	7
6	LT AND SBT IMPLICATIONS OF AERODYNAMICS, CRUCIFORM WINGS OF SPAN $b$ .....	8
7	LT AND SBT IMPLICATIONS OF AERODYNAMICS, THREE WINGS OF SPAN $b$ .....	9
8	LT AND SBT IMPLICATIONS OF AERODYNAMICS, FOUR WINGS OF SPAN $b$ .....	10
9	EFFECT OF BODY RADIUS ON DAMPING IN ROLL FOR FIXED SPAN (TAKEN FROM REFERENCE 24) .....	12
10	EFFECT OF BODY RADIUS ON DAMPING IN PITCH FOR FIXED SPAN WINGS .....	12
11A	FRONT VIEW OF MISSILE AS AOA GOES FROM 0 TO 90 DEG ILLUSTRATING WING-TO-WING BLOCKAGE EFFECTS ( $\Lambda_{LE} = 0$ DEG) .....	14
11B	FRONT VIEW OF MISSILE AS AOA GOES FROM 0 TO 90 DEG ILLUSTRATING WING-TO-WING BLOCKAGE EFFECTS ( $\Lambda_{LE} \neq 0$ DEG) .....	15
12	QUALITATIVE VIEW OF NORMAL FORCE FACTOR FOR MULTIPLE FINS .....	17
13	GENERAL OPERATIONAL BOUNDARY OF ZEUS CODE .....	18
14	AXIAL AND RADIAL GRIDS USED IN GASP COMPUTATIONS .....	19
15	RATIO OF NORMAL FORCE OF SIX AND EIGHT FINS TO THAT OF FOUR FINS BASED ON CFD .....	29
16	STATIC AERODYNAMICS OF A BODY-TAIL CONFIGURATION ILLUSTRATING DISCONTINUITIES AROUND $M = 2.0$ AND $6.0$ ( $\alpha = 1$ DEG, $\Phi = 0$ DEG) .....	36
17	USE OF AERODYNAMIC SMOOTHER TO ELIMINATE DISCONTINUITY IN VALUE OF $C_i$ AT $M = 2$ AND $6$ .....	38

## ILLUSTRATIONS (Continued)

<u>Figure</u>		<u>Page</u>
18	NORMAL FORCE COEFFICIENT AND CENTER OF PRESSURE FOR CONFIGURATION OF FIGURE 16 USING AERODYNAMIC SMOOTHER .....	38
19	SCHEMATIC OF M829 PROJECTILE CONFIGURATION (FROM REFERENCE 32) .....	40
20	COMPARISON OF NEW MULTIFIN METHOD TO CFD AND EXPERIMENT FOR FIGURE 19 CONFIGURATION .....	41
21	SCHEMATIC OF M735 PROJECTILE CONFIGURATION (FROM REFERENCE 34) .....	42
22	COMPARISON OF NEW MULTIFIN METHOD TO CFD AND EXPERIMENT FOR FIGURE 21 CONFIGURATION .....	43
23	SCHEMATIC OF EIGHT-FIN GUIDED PROJECTILE (FROM REFERENCE 34) .....	45
24	NORMAL FORCE COEFFICIENT COMPARISONS FOR BODY ALONE OF FIGURE 23 .....	46
25	NORMAL FORCE COEFFICIENT COMPARISONS FOR FOUR-FIN GUIDED PROJECTILE OF FIGURE 23 .....	48
26	NORMAL FORCE COEFFICIENT COMPARISONS FOR EIGHT-FIN GUIDED PROJECTILE OF FIGURE 23 .....	50

# TABLES

<u>Table</u>		<u>Page</u>
1	EULER CFD CALCULATIONS FROM ZEUS <sup>++29</sup> AND <span style="border: 1px solid black;">GASP<sup>28</sup></span> CODES .....	20
2	COMPARISON OF CFD RESULTS TO NASA DATA BASE FOR FOUR-FIN CONFIGURATION .....	25
3	APPROXIMATED VALUES OF THE FACTORS $F_6$ AND $F_8$ OBTAINED FROM SMOOTHED VALUES OF THE ZEUS <sup>++</sup> AND GASP CODE COMPUTATIONS AND ENGINEERING JUDGEMENT .....	34

## 1.0 INTRODUCTION

Many weapon designs are constrained by their launcher. Launchers such as guns or shoulder-launched configurations tend to be circular in shape. This circular shape puts a constraint on the weapon when it is fin-stabilized versus spin-stabilized. These constraints typically mean that to get adequate stability, a four-fin configuration may need large spans in order to get adequate lifting surface area on the tail fins. The large span fins can have adverse impact on the rest of the weapon design in terms of either reducing the rocket motor length or warhead size or both. This is because the fins are either folded forward and into the projectile or rocket, or folded rearward. In either case, the fins pop up or out after exit from the launcher to provide the static and dynamic stability required for successful flight.

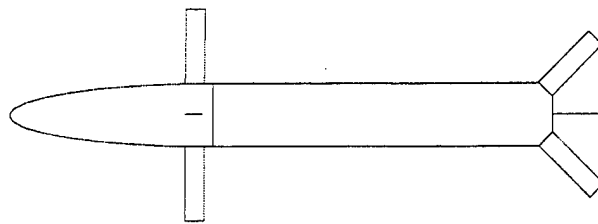
One option to reduce the span of a four-fin projectile or missile, and hence to reduce the impact on the rocket motor or warhead, is to increase the number of tail fins from four to six or eight. This design alternative could prove attractive when the fins are folded rearward and pop up after launch. That is because one could obtain the same level of static stability with a shorter length round, or the extra length could be used for additional rocket motor or warhead, etc. As a result of this desire to investigate various multi-tail-fin alternatives for providing static stability on a given design, an effort was undertaken to define a method that could be used in conjunction with the 1998 version of the aeroprediction code (AP98) to compute aerodynamics of multifin weapons. Of particular interest here are the aerodynamics of six- and eight-fin configurations, since the AP98<sup>1</sup> can already consider two- and four-fin cases. This new methodology will be integrated into the next version of the aeroprediction code (APC) and transitioned to users as AP02.

Typical weapon configuration design and control alternatives, for which aerodynamics are desired, are shown in Figure 1. These configurations define the general requirements to be considered in the analytical development methodology for multifin configurations. In general, one can have a body-tail configuration that is either guided or unguided. If it is unguided, four, six, or eight tail fins can be assumed. On the other hand, if it is tail-controlled, the author is not aware of any tail control alternatives other than for cruciform (four) fins. Hence, this will be the requirement for tail-controlled weapons.

Canard or wing-body-tail configurations have more options for control than body-tail. The control can be from the canards or wings, in which case there will be two or four canards (wings) present and either four, six, or eight tail surfaces. Here, the tail surfaces are used exclusively for stability. For the tail control option, the forward set of lifting surfaces can have two, four, six, or eight fins, but again, the tail controls are assumed to be cruciform. In effect, the above alternative design and control constraints are placed on the aerodynamics methodology from a practical standpoint.



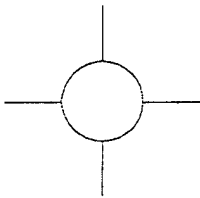
# WEAPON DESIGN



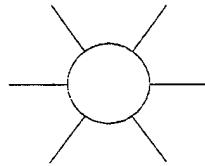
Top View of Cruciform  
Canard/Tail Case

Canards, Wings  
0, 2, or 4 Fins

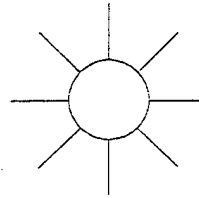
Tails  
4, 6, or 8 Fins



4 Fin



6 Fin



8 Fin

Rear View

## WEAPON CONTROL ALTERNATIVES

### Body - Tail

Unguided : 4, 6, or 8 Fins

Guided : 4 Fins

### Canard or Wing - Body - Tail

Canard Control : 2 or 4 Canards and  
4, 6, or 8 Tails

Tail Control : 2, 4, 6, or 8 Canards  
and 4 Tails

FIGURE 1. TYPICAL WEAPON DESIGN AND CONTROL ALTERNATIVES

The above set of requirements had to do with the practical configurations that aerodynamics are desired for. A second set of requirements in the analytical methodology development has to do with the methodology development approach in the APC. This latter set of requirements is driven by the APC logic and how to most cost-effectively integrate multifin computations into a code set up for two- or four-fin alternatives. The APC logic requirement thus leads one to define factors by which the two- or four-fin aerodynamics can be multiplied so as to make the minimum amount of changes to the APC.

The goal of the present report is therefore to develop factors by which the aerodynamics of two- and four-fin configurations can be multiplied so as to give acceptable accuracy for aerodynamics of the six- and eight-fin cases shown in Figure 1.

## 2.0 SUMMARY OF METHODS FOR PLANAR AND CRUCIFORM CONFIGURATIONS

Reference 1 summarizes the theoretical methodology of the AP98 and the interested reader is referred to that reference for the details of the methodology. However, it is believed that a brief summary or overview of the methodology is appropriate in order to lead into the modifications necessary to consider six- and eight-fin configurations as shown in Figure 1.

Basically, the aeroprediction code uses a component buildup approach to calculate the aerodynamics. By component buildup is meant that the code breaks the configuration down into body alone, wing or tail alone, and mutual interference aerodynamics. Various theoretical or empirical methods are then used to calculate the aerodynamics of these configuration components in a given Mach number regime, and then they are added together to obtain the total configuration aerodynamics. This is as opposed to a Computational Fluid Dynamics (CFD) code where all the aerodynamics are computed simultaneously for all configuration components, including the mutual interference between components.

The APC is considered a semiempirical code. It is semiempirical because it combines theoretical methods and empirical methods to form an overall prediction tool. At low angles of attack (AOAs), mostly analytical methods based on slender body theory (SBT), linear theory (LT), or second-order perturbation methods are used to calculate the aerodynamics. To include the nonlinear aerodynamics that occur at moderate to high AOA, several large wind tunnel data bases are utilized. Figures 2–4 show the theoretical methods that are used to calculate a given force or moment at a given Mach number region. Also shown on the figure are the references associated with each method for those interested in more details.

The APC has shown that it can calculate aerodynamics of most tactical weapon configurations with average accuracies of  $\pm 10$  percent for  $C_A$  and  $C_N$  and  $\pm 4$  percent of body length for  $X_{CP}$ . By “average” is meant enough AOAs and Mach numbers are considered to get a good statistical sample. Dynamic derivatives are less accurate and an average accuracy of  $\pm 20$  percent is

probably more appropriate for low AOAs. No nonlinear methods have been incorporated for higher AOA dynamic derivatives.

COMPONENT/ MACH NUMBER REGION	SUBSONIC $M_\infty < 0.8$	TRANSONIC $0.8 \leq M_\infty < 1.2$	LOW SUPERSONIC $1.2 \leq M_\infty \leq 1.8$	MOD/HIGH SUPERSONIC $1.8 \leq M_\infty \leq 6.0$	HYPERSONIC $M_\infty > 6.0$
NOSE WAVE DRAG	EMPIRICAL (Ref. 2)	SEMIEMPIRICAL BASED ON EULER SOLUTIONS (Ref. 11)	SECOND-ORDER VAN DYKE PLUS MNT (Ref. 2)	SOSET PLUS IMNT (Ref. 9)	SOSET PLUS IMNT MODIFIED FOR REAL GASES (Ref. 6)
BOATTAIL OR FLARE WAVE DRAG	---	WU AND AOYOMA (Ref. 2)	SECOND-ORDER VAN DYKE (Ref. 10)	SOSET (Ref. 8)	SOSET FOR REAL GASES (Ref. 6)
SKIN FRICTION DRAG	VAN DRIEST II (Ref. 12)				
BASE DRAG	IMPROVED EMPIRICAL METHOD (Ref. 13)				
AXIAL FORCE AT $\alpha$	IMPROVED EMPIRICAL METHOD (Ref. 4)				
AEROHEATING INFORMATION	---			SOSET PLUS IMNT FOR REAL GASES (Ref. 14)	
INVISCID LIFT AND PITCHING MOMENT	EMPIRICAL (Ref. 2)	SEMIEMPIRICAL BASED ON EULER SOLUTIONS (Ref. 11)	TSIEN FIRST- ORDER CROSSFLOW (Ref. 5)	SOSET (Ref. 8)	SOSET FOR REAL GASES (Ref. 6)
VISCOUS LIFT AND PITCHING MOMENT	IMPROVED ALLEN AND PERKINS CROSSFLOW (Ref. 15)				
NONAXISYMMETRIC BODY AERO ( $\Phi = 0, 45^\circ$ )	MODIFIED JORGENSEN (Ref. 7)				
NONLINEAR ST. LOADS AVAIL. ( $\Phi = 0, 45^\circ$ )	NO		YES (Ref. 3)		

FIGURE 2. AP98 METHODS FOR BODY-ALONE AERODYNAMICS

COMPONENT/ MACH NUMBER REGION	SUBSONIC $M_\infty < 0.8$	TRANSONIC $0.8 \leq M_\infty \leq 1.2$	LOW SUPERSONIC $1.2 \leq M_\infty \leq 1.8$	MOD/HIGH SUPERSONIC $1.8 \leq M_\infty \leq 6.0$	HYPERSONIC $M_\infty > 6.0$
BODY ALONE	EMPIRICAL				
WING AND INTERFERENCE ROLL DAMPING MOMENT	LIFTING SURFACE THEORY	EMPIRICAL	LINEAR THIN WING THEORY	LINEAR THIN WING OR STRIP THEORY	
WING MAGNUS MOMENT	ASSUMED ZERO				
WING AND INTERFERENCE PITCH DAMPING MOMENT	LIFTING SURFACE THEORY	EMPIRICAL	LINEAR THIN WING THEORY	LINEAR THIN WING OR STRIP THEORY	

FIGURE 3. AP98 METHODS FOR DYNAMIC DERIVATIVES (REFERENCES 16 AND 17)

COMPONENT/ MACH NUMBER REGION	SUBSONIC $M_\infty < 0.8$	TRANSONIC $0.8 \leq M_\infty \leq 1.2$	LOW SUPERSONIC $1.2 \leq M_\infty \leq 1.8$	MOD/HIGH SUPERSONIC $1.8 \leq M_\infty \leq 6.0$	HYPERSONIC $M_\infty > 6.0$
WAVE DRAG		EMPIRICAL (Ref. 18)	LINEAR THEORY PLUS MNT (Ref. 18)	SHOCK EXPANSION (SE) PLUS MNT ALONG STRIPS (Ref. 9)	SE PLUS MNT FOR REAL GASES ALONG STRIPS (Ref. 9)
SKIN FRICTION DRAG	VAN DRIEST II (Ref. 12)				
TRAILING EDGE SEPARATION DRAG	EMPIRICAL (Ref. 18)				
BODY BASE PRESSURE CAUSED BY TAIL FINS	IMPROVED EMPIRICAL (Ref. 13)				
INVISCID LIFT AND PITCHING MOMENT					
• LINEAR	• LIFTING SURFACE THEORY (Ref. 18)	• EMPIRICAL (Ref. 18)	• 3DTWT (Ref. 18)	• 3DTWT OR SE (Ref. 18 or 9)	• 3DTWT OR SE (Ref. 18 or 6)
• NONLINEAR	• EMPIRICAL (Ref. 19, 20)				
WING-BODY, BODY- WING INTERFERENCE ( $\Phi = 0, 45^\circ$ )					
• LINEAR	• SLENDER BODY THEORY OR LINEAR THEORY MODIFIED FOR SHORT AFTERBODIES (Ref. 19, 20)				
• NONLINEAR	• EMPIRICAL (Ref. 19, 20)				
WING-BODY, INTERFERENCE DUE TO $\delta$ ( $\Phi = 0, 45^\circ$ )					
• LINEAR	• SLENDER BODY THEORY (Ref. 20)				
• NONLINEAR	• EMPIRICAL (Ref. 19, 20)				
WING-TAIL INTERFERENCE ( $\Phi = 0, 45^\circ$ )	LINE VORTEX THEORY WITH MODIFICATIONS FOR $K_{W(B)}$ TERM AND NONLINEARITIES (Ref. 20)				
AEROHEATING	NONE PRESENT			SE PLUS MNT (Ref. 21)	SE PLUS MNT REAL GASES (Ref. 21)
NONAXISYMMETRIC BODY AERO ( $\Phi = 0, 45^\circ$ )	IMPROVED NELSON ESTIMATE FOR AP98 (Ref. 7, 22, 23)				
NONLINEAR ST. LOADS AVAIL. ( $\Phi = 0, 45^\circ$ )	NO		YES (Ref. 3)		

FIGURE 4. AP98 METHODS FOR WING-ALONE AND INTERFERENCE AERODYNAMICS

### 3.0 MODIFICATIONS FOR SIX- AND EIGHT-FIN CONFIGURATIONS

Section 2.0 of this report summarized the methods used for aerodynamic computations of planar (two-fin) and cruciform (four-fin) weapon configurations. This section will define approximations necessary to allow the methods of Section 2.0 to be used for six- and eight-fin configuration aerodynamics. As discussed in the Introduction, one of the requirements for this

methodology is to try to define multiplication factors for six- and eight-fin aerodynamics compared to two- or four-fin cases. This will then allow the methods of Section 2.0 to be used directly with minimum modifications.

The first approach will be to investigate SBT implications for multifin aerodynamics. Then CFD and experimental data will be utilized for higher AOA effects on multifin aerodynamics.

### 3.1 SLENDER BODY THEORY PREDICTIONS FOR MULTIFIN AERODYNAMICS

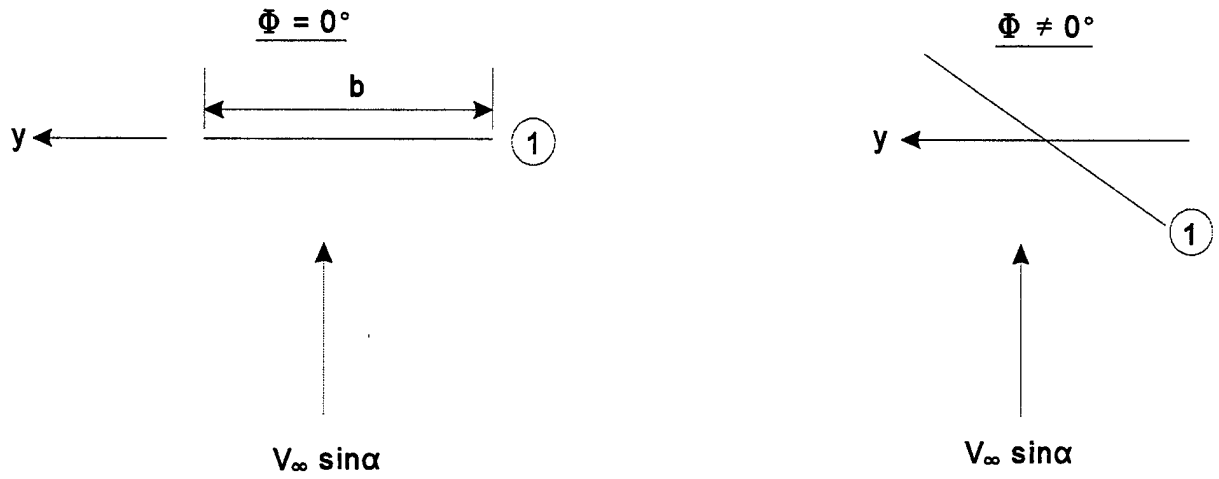
Slender body theory will consider the wings and the mutual interference effects separately. The body-alone aerodynamics are unaffected by the number of fins present, and therefore the methods of Figures 2–4 will stay the same as those in the AP98. References 24 and 25 are the primary sources of material utilized for this part of the report. As pointed out in References 24 and 25, SBT assumes very slender configurations flying at small AOA. As a result of this assumption, aerodynamics are Mach-number independent. However, it is believed SBT can give a reasonable estimate of the ratio of aerodynamics of six and eight fins to four fins, even though the absolute values may be in error.

#### 3.1.1 Wing Alone

Figures 5–8 present the SBT results for one to four wings (two to eight fins) at both the  $\Phi = 0$  and nonzero roll orientations. Results are presented for normal force, axial force, center of pressure, side force and roll damping moment of a wing alone. Figure 5 is for a planar wing (two fins) and shows that a side force exists in any roll orientation but zero. On the other hand, if the missile is cruciform or has more than two wings present (Figures 6–8), the side force is zero near zero AOA. As already mentioned, the Figure 5–8 results are for small AOA. Nonlinear AOA effects will be discussed later.

Figure 6 gives the results for cruciform or four-fin configurations. Note that SBT gives normal force equal to that of a planar configuration at any roll orientation. However, for a cruciform missile, axial force of the wings is double that of the single-wing case and roll damping is 1.62 times that of the single-fin case. While pitch damping moments are not shown on Figures 5–8, they correlate directly with the normal force of the wing alone, and as a result, it will be assumed the pitch damping moment factors for multiple-wing aerodynamics are the same as those for the normal force coefficient.

If the missile has three or four wings (six or eight fins respectively) as shown in Figures 7 and 8, the normal force factors over the single wing case are 1.5 and 2.0 respectively. The axial force factors for the wings are directly proportional to the number of wings (three and four respectively). The roll damping factors for the three- and four-wing cases are 2 and 2.3 respectively, compared to the single-fin case. Figures 6–8 give the aerodynamics relative to a planar fin case because that is the way they are computed in the APC, and hence, to go to a multifin case, factors applied to the planar wing configuration are necessary.



$$(C_{N_w})_{\Phi=0} = (C_{N_w})_1$$

$$(C_{N_w})_{\Phi \neq 0} = (C_{N_w})_{\Phi=0} \cos^2 \Phi$$

$$(C_{A_w})_{\Phi=0} = (C_{A_w})_1$$

$$(C_{A_w})_{\Phi \neq 0} = (C_{A_w})_{\Phi=0}$$

$$(X_{cp})_{\Phi=0} = (X_{cp})_1$$

$$(X_{cp})_{\Phi \neq 0} \approx (X_{cp})_{\Phi=0}$$

$$(C_y)_{\Phi=0} = 0$$

$$(C_y)_{\Phi \neq 0} = -(C_{N_w})_{\Phi=0} \sin^2 \Phi$$

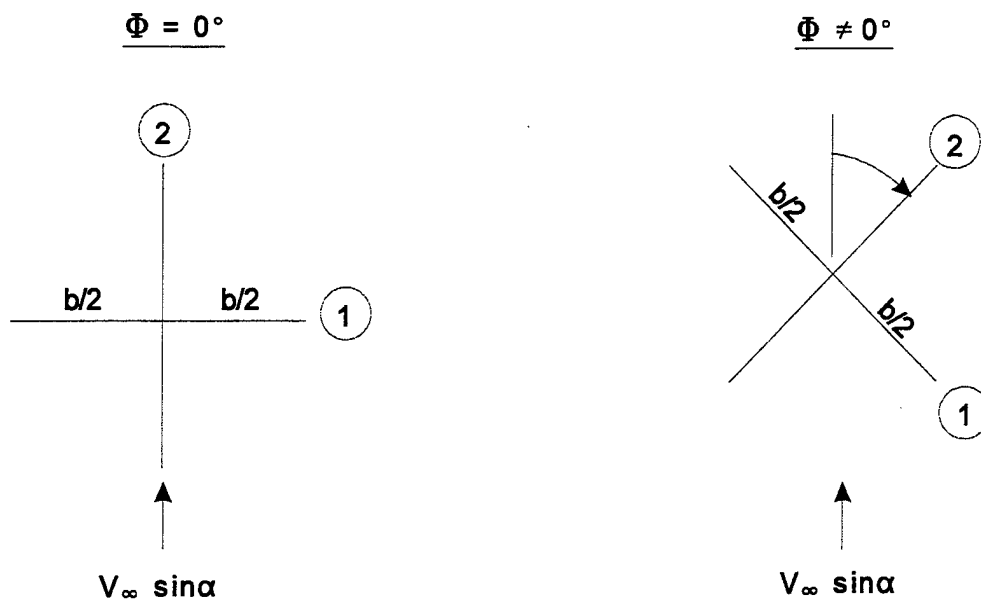
$$(C_{l_p})_{\Phi=0} = (C_{l_p})_1$$

$$(C_{l_p})_{\Phi \neq 0} = (C_{l_p})_{\Phi=0}$$

FOR  $\Phi = 45^\circ$

$$(C_{N_w})_{\Phi=45^\circ} = (C_y)_{\Phi=45^\circ} = \frac{1}{2}(C_{N_w})_{\Phi=0^\circ}$$

FIGURE 5. LT AND SBT IMPLICATIONS FOR AERODYNAMICS, SINGLE WING OF SPAN  $b$



$$(C_{N_w})_{\Phi=0} = (C_{N_w})_1$$

$$(C_{N_w})_{\Phi \neq 0} = (C_{N_w})_1 [\sin^2 \Phi + \cos^2 \Phi] = (C_{N_w})_1$$

$$(C_{A_w})_{\Phi=0} = 2(C_{A_w})_1$$

$$(C_{A_w})_{\Phi \neq 0} = 2(C_{A_w})_1$$

$$(X_{cp})_{\Phi=0} = (X_{cp})_1$$

$$(X_{cp})_{\Phi \neq 0} \cong (X_{cp})_1$$

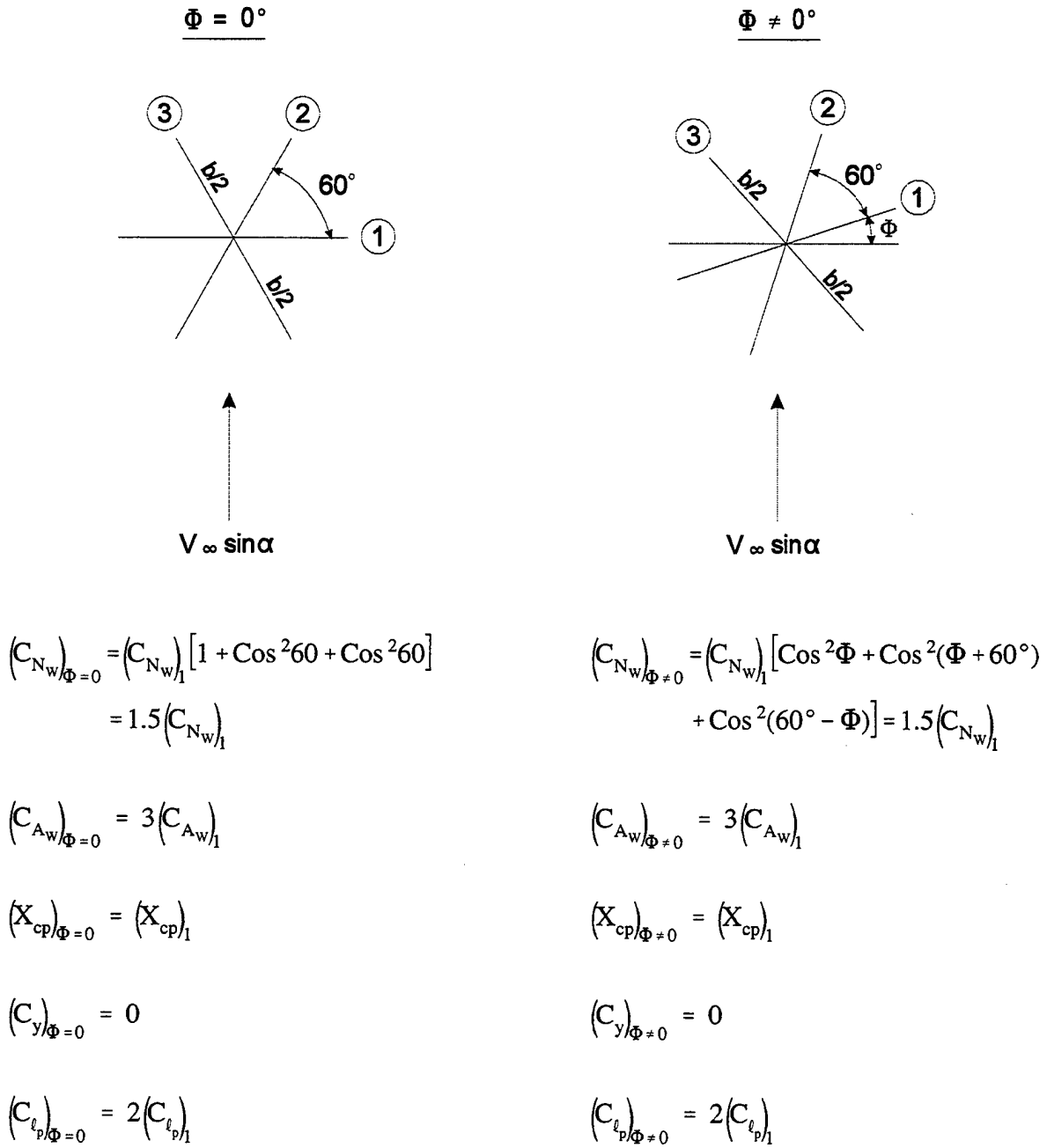
$$(C_y)_{\Phi=0} = 0$$

$$(C_y)_{\Phi \neq 0} = 0$$

$$(C_{l_p})_{\Phi=0} = 1.62(C_{l_p})_1$$

$$(C_{l_p})_{\Phi \neq 0} = 1.62(C_{l_p})_1$$

FIGURE 6. LT AND SBT IMPLICATIONS OF AERODYNAMICS, CRUCIFORM WINGS OF SPAN  $b$

FIGURE 7. LT AND SBT IMPLICATIONS OF AERODYNAMICS, THREE WINGS OF SPAN  $b$



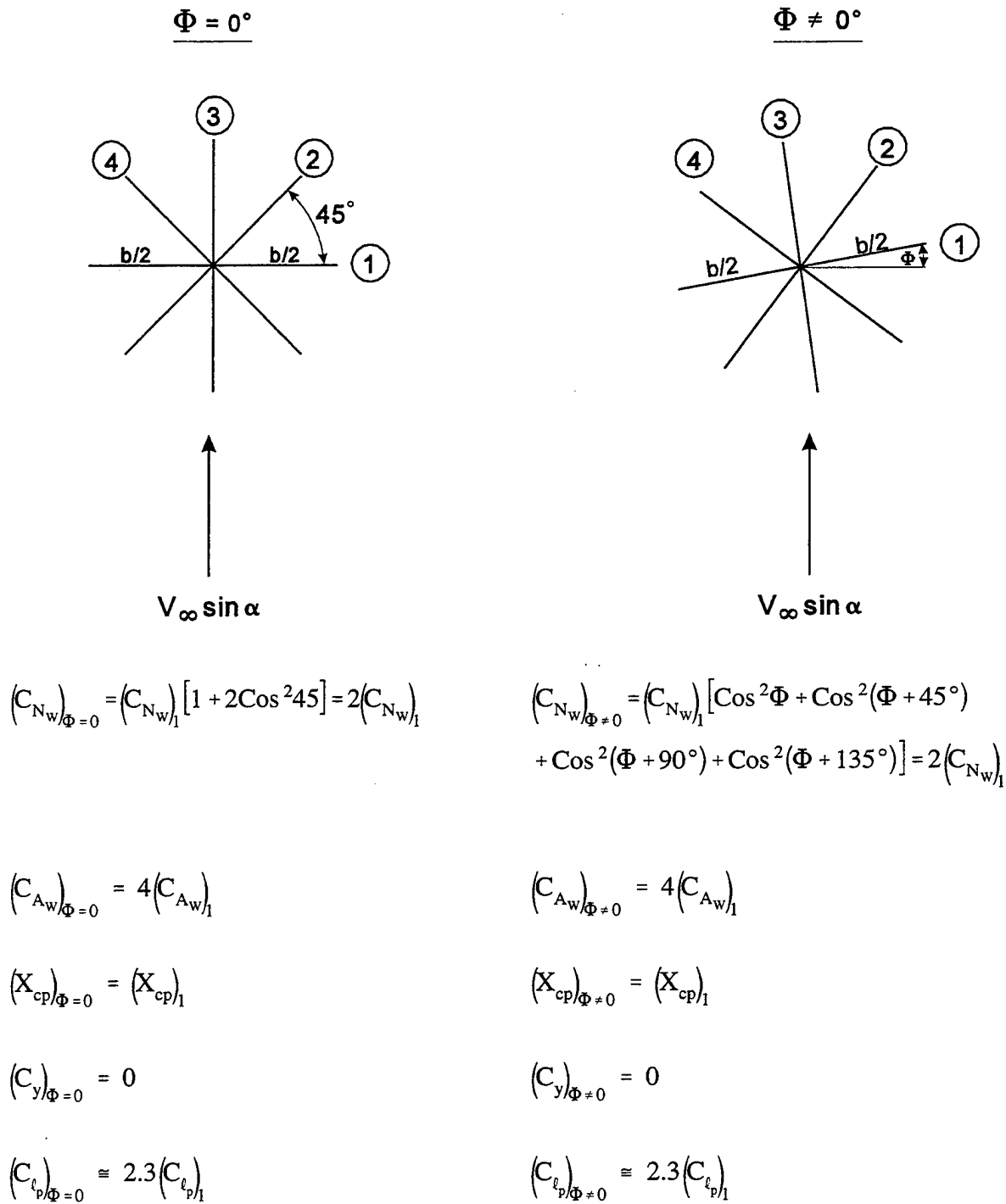


FIGURE 8. LT AND SBT IMPLICATIONS OF AERODYNAMICS, FOUR WINGS OF SPAN  $b$

### 3.1.2 Wing-Body

Wing-body aerodynamics are significantly different from body-alone or wing-alone. This difference is because the body induces an additional upwash onto the fin and the fin induces a higher pressure onto the body. The result of these effects is, in general, a higher loading on both the fin and body than if each were investigated separately. This higher loading dissipates as AOA increases.<sup>3</sup> Since the latest version of the APC<sup>1</sup> has all these nonlinearities included, the assumption is that the factors used for the multifin options on normal force will be used for the interference effects as well.

That is,

$$\left[ C_{N_{W(B)}}, C_{N_{B(W)}}, C_{N_{T(V)}} \right]_{6,8 \text{ Fin}} = (F_6, F_8) \left[ C_{N_{W(B)}}, C_{N_{B(W)}}, C_{N_{T(V)}} \right]_{4 \text{ Fin}} \quad (1)$$

The factors  $F_6$  and  $F_8$  are 1.5 and 2.0, respectively, for the six- and eight-fin cases using SBT at low AOA. These factors will be modified later for all AOA using CFD codes, in conjunction with experimental data.

The axial force methodology for the wing-body will remain as currently available in the AP98, except for the changes already discussed for the multifin factors of Figures 6–8.

For roll damping moments, the present methodology in the AP98 assumes the fins go to the centerline of the body and body interference effects are accounted for by Figure 9. Figure 9 is taken from Reference 24 and it basically says that for two- or four-fin cases, the wing-body roll damping is nearly independent of  $r/s$  for values up to 0.4. After that, the roll damping goes to the body-alone value in a nearly linear fashion as  $r/s$  approaches 1.0. The only assumption made here is that for six or eight fins, the curve of Figure 9 for four fins can be used directly. This assumption is based on the fact that SBT shows little difference between two- and four-fin wing-body roll damping as a function of  $r/s$ , as seen in Figure 9.

As far as pitch damping moment is concerned, the computational procedure is similar to that of the roll damping. The wings are assumed to extend to the centerline of the body and then the method of Bryson<sup>26</sup> is used to account for the interference effects of the body in the presence of the wing. Since the wings are assumed to extend to the centerline of the body and the number of wings will be accounted for by the factor of the normal force of the wing alone, this wing-body interference factor will be less than one. Figure 10 gives the slender body theory results for two, four, six and eight wings. As seen in Figure 10, increasing the number of fins from two to eight has very little effect for small values of  $r/s$  ( $r/s \leq 0.4$ ), but wing-body interference has an increasing effect for all fins as  $r/s$  approaches 0.6 to 0.8.

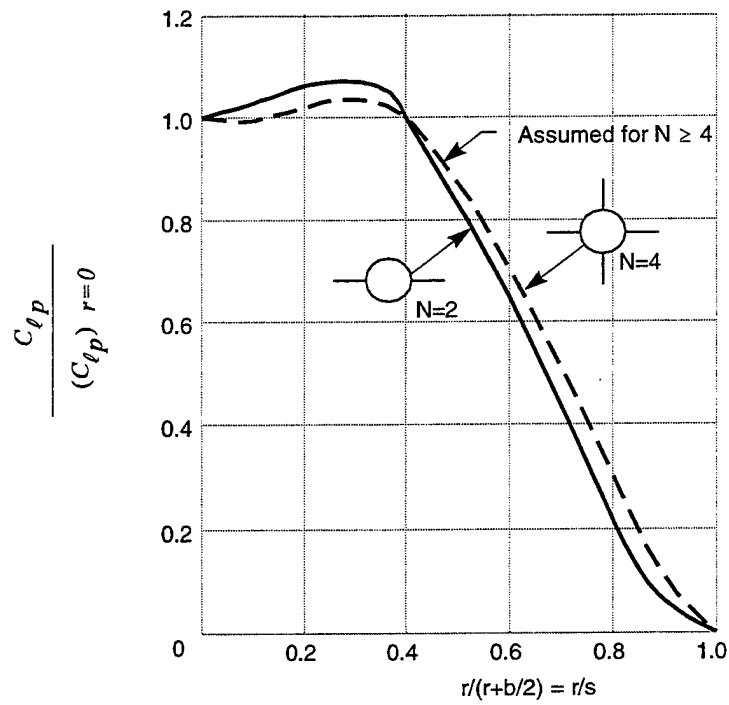


FIGURE 9. EFFECT OF BODY RADIUS ON DAMPING IN ROLL FOR FIXED SPAN  
(TAKEN FROM REFERENCE 24)

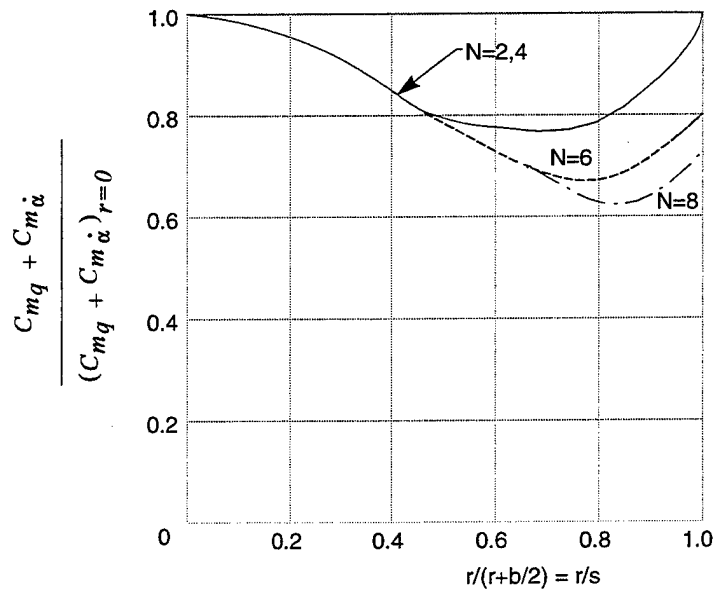


FIGURE 10. EFFECT OF BODY RADIUS ON DAMPING IN PITCH FOR FIXED SPAN WINGS

### 3.2 COMPUTATIONAL FLUID DYNAMICS (CFD) PREDICTIONS FOR MULTIFIN AERODYNAMICS

The SBT of Section 3.1 was limited to low AOA for slender wing-body configurations. The results do not account for wing-to-wing shock interactions, wing-to-wing blockage effects that occur at high AOA and Mach number, or wing geometry effects. In order to address these issues, and either confirm SBT (which says the multi-wing aerodynamics are independent of these effects) or to develop an estimate of multifin aerodynamics as a function of the above-mentioned SBT assumptions, CFD will be used.

Before discussing the actual CFD codes used to perform the multifin aerodynamic calculations, it is believed appropriate to discuss some of the nonlinear physical phenomena involved that SBT does not account for. The first is wing blockage effects. To visualize wing blockage effects, several sketches of the configurations the flow would see, as AOA is increased from 0 to 90 deg, are shown in Figure 11 for four-, six-, and eight-fin configurations.

Figure 11A is for no sweepback of fins that have a large span and small chord. Notice that at AOA 0 deg, no blockage effects occur between fins, only fin-to-fin interference from shock waves. Note that at AOA 90 deg, there appears to be little or no difference between the four-, six-, and eight-fin cases. Thus, to assume that the SBT factors on normal force for the six-fin (1.5) and eight-fin (2.0) cases go to the four-fin value (1.0) at  $\alpha = 90$  deg appears reasonable. Also notice that for AOA 45 deg, there still does not appear to be blockage of the air flow for either the six- or eight-fin cases from the adjacent fins, but the body does adversely impact the leeward plane fins. The implication of these comments is that for short chord configurations, blockage occurs at fairly high AOA for the windward plane fins and at moderate AOA for the leeward plane fins.

Figure 11B illustrates a second case where the chord is longer and the leading edge is swept back. Note that for this case, the same statements hold true for the  $\alpha = 0$  and 90 deg cases as for the short chord configuration. However, note that for the 45 deg AOA, blockage of the flow from one fin to another has started to occur. In other words, as the chord increases, blockage occurs at lower AOAs.

It should be noted that the SBT factors at low AOA assume the fins in both the leeward and windward planes as being effective in providing lift. At both the 45 deg and 90 deg AOA, it is clear from Figure 11A and 11B that even if the windward plane fins remain completely or partially effective, the leeward plane fins are mostly blocked by the body or fins. Hence, part of the additional lift factor will be reduced because of the fact that in the leeward plane, a good portion of the fin is shielded or blocked by the body or windward plane fins.

As a result of the differences in flow patterns on the leeward and windward plane fins, the slender body enhancement in normal force of the six-fin and eight-fin cases could be split equally and treated separately between the leeward and windward planes. At low AOA, say 10 deg or less, it seems reasonable to assume that both the leeward and windward plane fins are fully effective. Above about 10 deg AOA, the leeward plane fins degrade quite rapidly.

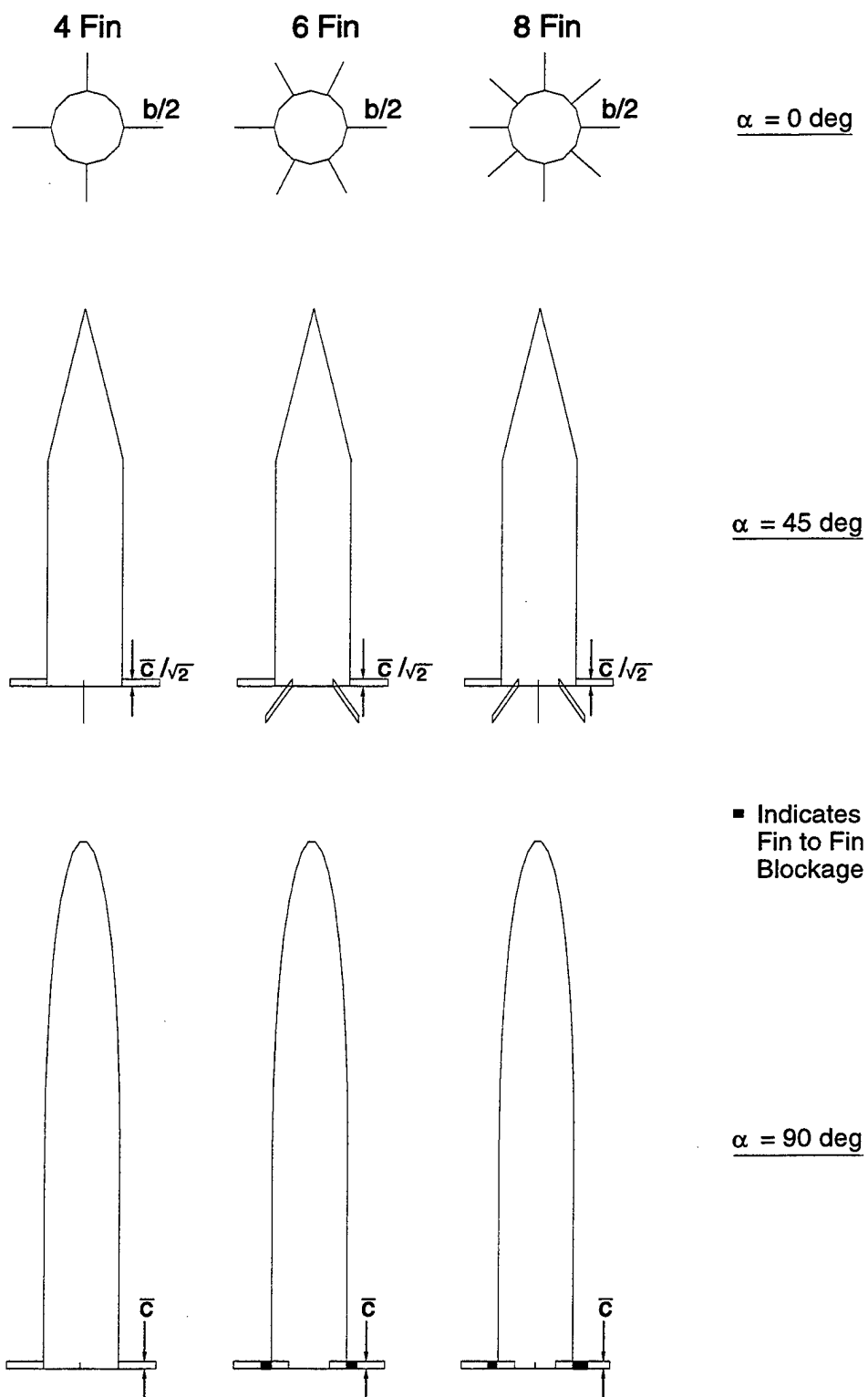


FIGURE 11A. FRONT VIEW OF MISSILE AS AOA GOES FROM 0 TO 90 DEG ILLUSTRATING WING-TO-WING BLOCKAGE EFFECTS ( $\Lambda_{LE} = 0 \text{ DEG}$ )

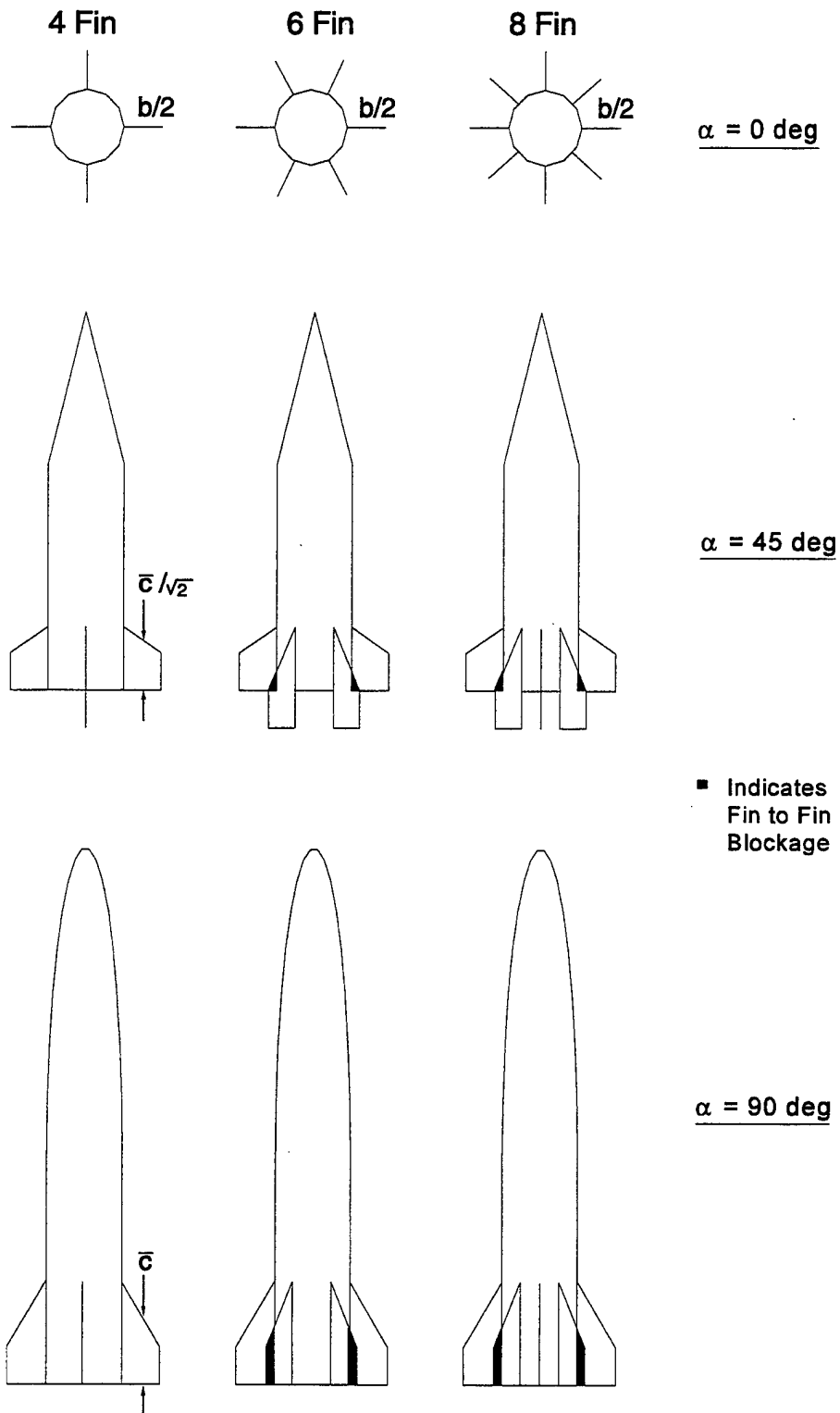


FIGURE 11B. FRONT VIEW OF MISSILE AS AOA GOES FROM 0 TO 90 DEG ILLUSTRATING WING-TO-WING BLOCKAGE EFFECTS ( $\Lambda_{LE} \neq 0 \text{ DEG}$ )

A possible way in which the normal force factors for six and eight fins degrade with AOA, as compared to that for two or four fins, is illustrated in Figure 12. Figure 12 breaks down the nonlinear degradation of the normal force factor with AOA into, first, the leeward and windward plane fins, and then the total or sum of the two. This figure is simply a qualitative representation of what is envisioned to occur as AOA increases. CFD computations will be used to verify or modify this qualitative view of multifin aerodynamics as a function of AOA.

Another physical phenomenon inherent in multifin aerodynamic computations is wing-to-wing shock interactions. Obviously, this phenomenon is also not accounted for by SBT, since the slender body theory allows for an isentropic flow assumption, which in turn means no shock waves are present. In reality, these shock interactions between wings in Figure 11 are functions of wing geometry, Mach number, and AOA. CFD codes can easily account for this physical phenomenon.

### 3.2.1 Computational Fluid Dynamics Computations

Two CFD codes will be used in the computational process. They are the ZEUS<sup>27</sup> and GASP<sup>28</sup> codes. The ZEUS code is a full Euler solver whereas the GASP code is a full Navier-Stokes solver with a subsonic Euler solver option. The ZEUS code uses a marching solution to the Euler equations. This means the flow along the axial plane must be supersonic in order for the code to have hyperbolic flow conditions throughout the computational region. This region encompasses the bow shock to the rear of the body. To ensure supersonic flow, the general operational boundary of the ZEUS code is shown in Figure 13. This boundary will vary somewhat depending on the particular configuration of interest but is an approximate boundary.

The ZEUS code has been recently downloaded to a personal computer with a pre- and post-processing interface developed.<sup>29</sup> This interface (referred to as ZEUS<sup>++</sup>) uses much of the logic as used in the AP98 personal computer interface<sup>30</sup> in terms of several options for available body geometries. This greatly simplifies the geometry inputs for many cases and thus decreases the set-up time significantly for the ZEUS code. Also, with the higher-speed personal computers now available, computational time for a sharp-nose, wing-body case are quite reasonable for many design computations.

The configuration chosen for the computation of the factors  $F_6$  and  $F_8$  of Equation (1) is the NASA Tri-service model.<sup>31</sup> The NASA Tri-service model was the basic configuration used since wind tunnel data was available for the four-fin case at a wide range of aspect ratio, Mach number, and AOA. Aspect ratios of 0.25, 0.5, 1.0, 2.0, and 4.0 were considered at Mach numbers of 1.5, 2.0, 3.0, and 4.5. For the six- and eight-fin computations, the same geometric configuration was used for each individual fin as in the four-fin case. The hinge line location on the body was held constant for all aspect ratios. The normal force for the body alone was determined first at each Mach number and AOA. This result was subtracted from the normal force values computed for the four-, six-, and eight-fin cases at the corresponding freestream conditions. It was assumed that this remainder was the fin normal-force contribution, including all interference effects. The ratio of the six-fin and eight-fin values to those for four fins gave the multiplying factor indicating the effectiveness of the extra fins.

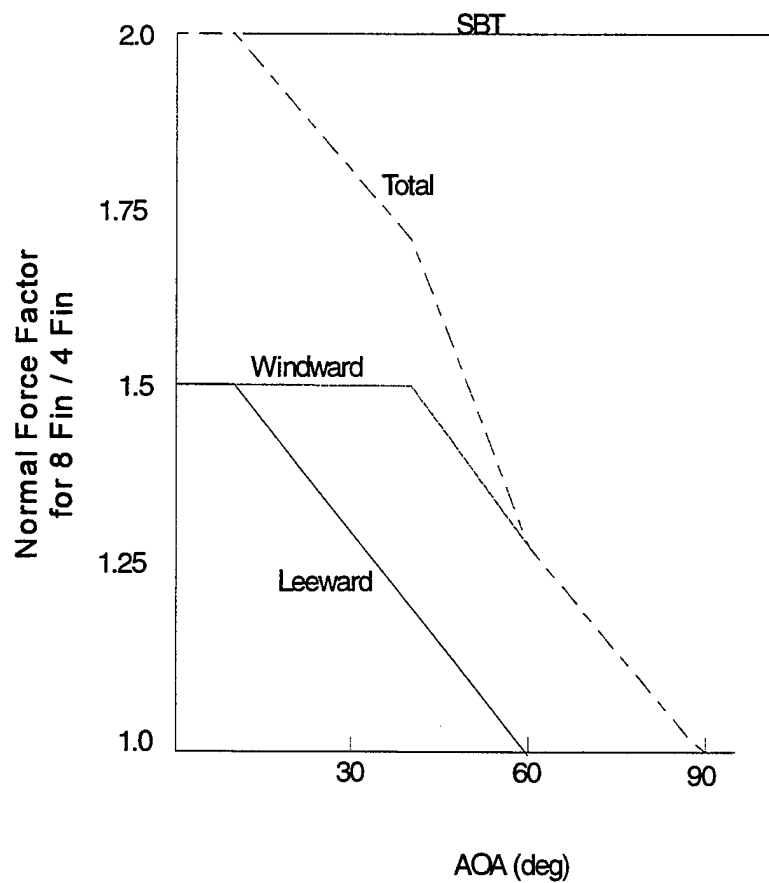
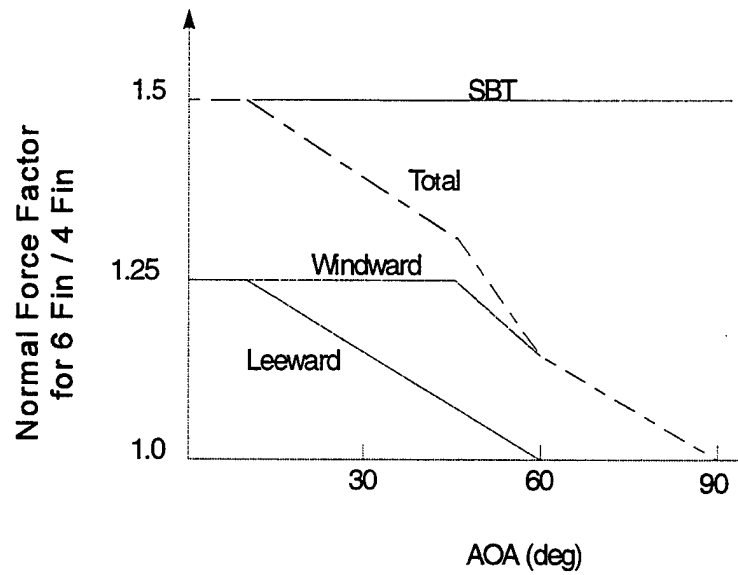


FIGURE 12. QUALITATIVE VIEW OF NORMAL FORCE FACTOR FOR MULTIPLE FINS



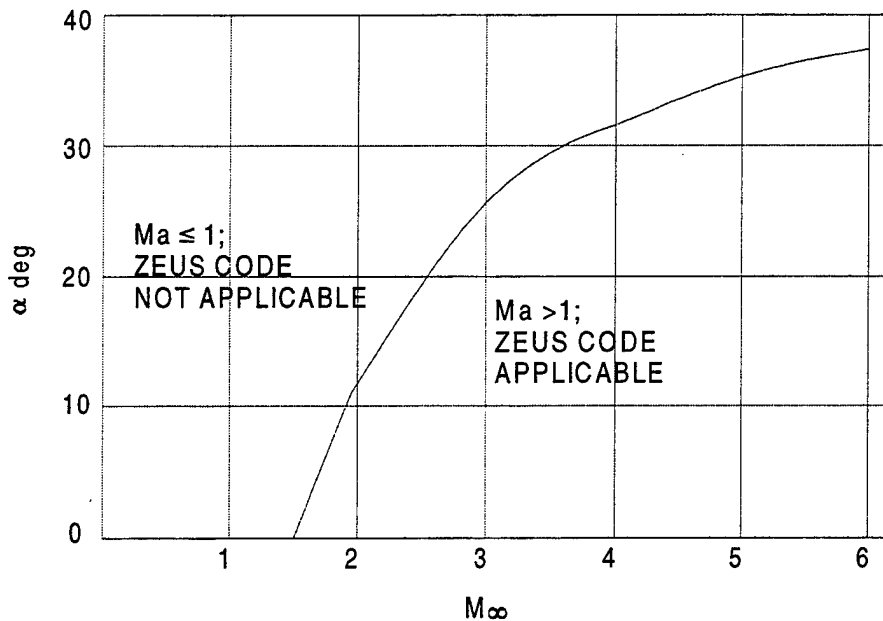
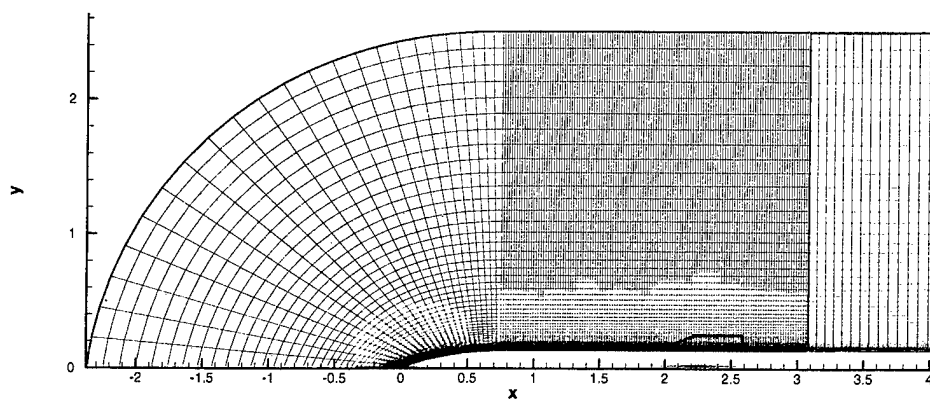


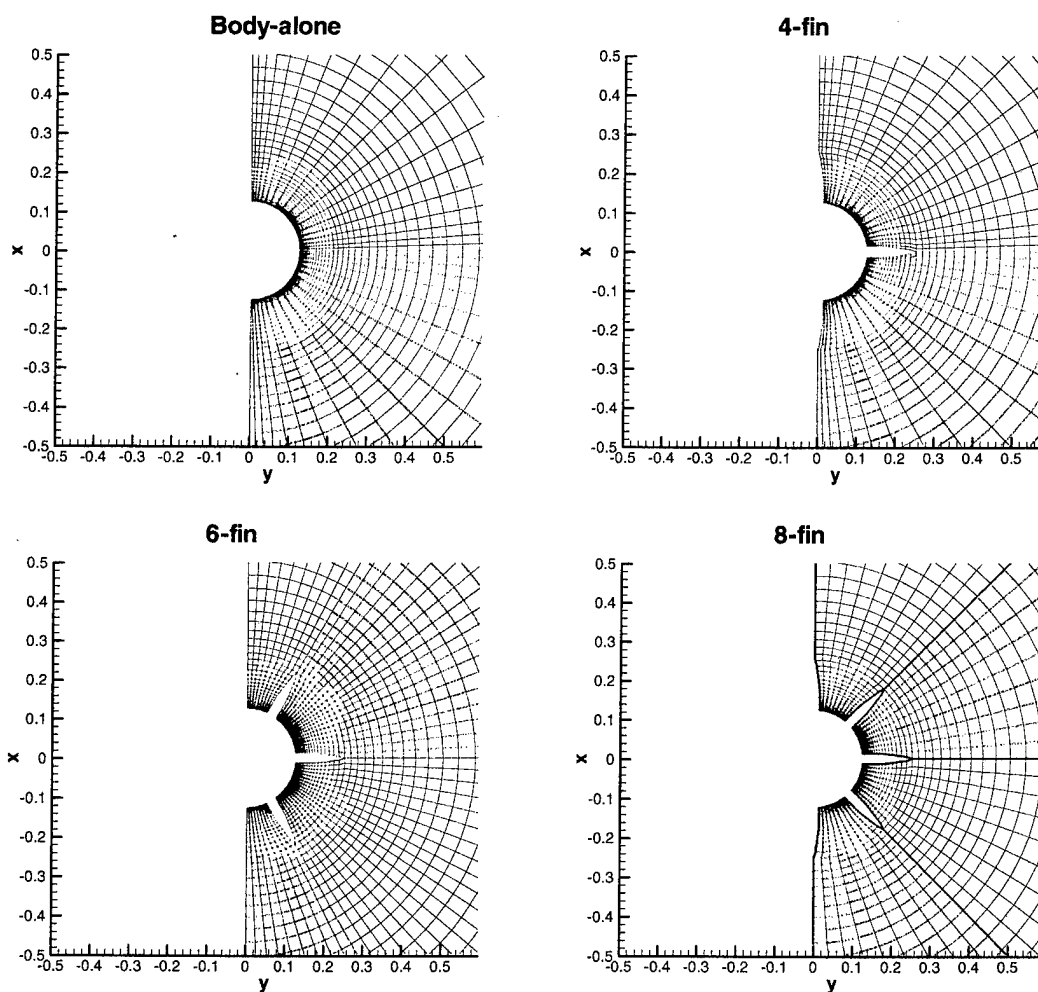
FIGURE 13. GENERAL OPERATIONAL BOUNDARY OF ZEUS CODE

The NASA Tri-service data base considered taper ratio as a configuration variable in addition to aspect ratio. However, after performing several computations for the factors  $F_6$  and  $F_8$  as a function of taper ratio, it was decided to drop this variable as secondary in importance compared to aspect ratio, Mach number, and AOA. Variations in the factors  $F_6$  and  $F_8$  as a function of taper ratio were less than 5 percent for the cases considered. Hence, a value of 0.5 was used for taper ratio in all the ZEUS<sup>++</sup> and GASP Euler calculations for the factors  $F_6$  and  $F_8$ . Computational times per data point for the ZEUS<sup>++</sup> varied from 3 to 15 minutes using a 200 megahertz Intel Pentium II computer chip. The higher the AOA, the larger the computational time. Computational times were not obtained for the GASP Euler solutions as they were run on a workstation in conjunction with other codes being run simultaneously. Times on the order of hours versus minutes were typical, however.

Note from Figure 13 that the ZEUS<sup>27</sup> Euler solver is limited by subsonic flow occurring anywhere in the flowfield. This is because the ZEUS code is a solution of the hyperbolic equations of motion, which means the axial flow ( $Ma$ ) must be supersonic throughout. To compute the normal force factors for the multifin cases where subsonic Mach numbers existed, the subsonic Euler solution option of the GASP<sup>28</sup> code was utilized. For these cases, the ZEUS<sup>++</sup> tool was used to generate three-dimensional grids that were then imported into the GASP flowfield software. The computational domains were (51×36×165), (51×36×165), (51×54×165), (51×36×165) for aspect ratios of 0.25, 0.5, 1.0, and 2.0, respectively. The first number indicates the number of grid points in the radial direction; the second and third, the number of points in the circumferential and axial directions, respectively. Note that all the cases are symmetric about the pitch plane, and therefore, only 180 deg of the circumferential plane was considered. Figure 14 shows the computational grid used for the axial and radial directions for the GASP computations. Results of the normal force computations of both the ZEUS<sup>++</sup> and GASP computations of the factors  $F_6$  and  $F_8$  are given in Table 1. A box is placed around the GASP computations so they can be distinguished from those



a) Axial Grid



b) Radial Grid

FIGURE 14. AXIAL AND RADIAL GRIDS USED IN GASP COMPUTATIONS

TABLE 1. EULER CFD CALCULATIONS FROM ZEUS<sup>++29</sup> AND GASP<sup>28</sup> CODES

AR = 0.25					
SIX FINS ( $F_6$ )					
$\alpha$	<u>M = 0.6</u>	<u>M = 1.5</u>	<u>M = 2.0</u>	<u>M = 3.0</u>	<u>M = 4.5</u>
1	1.260	1.365	1.274	1.232	1.232
2		1.295	1.260	1.221	1.234
3		1.288	1.248	1.216	1.235
4		1.278	1.238	1.206	1.244
5			1.223	1.199	1.255
6			1.209	1.194	1.268
7			1.196	1.188	1.281
8			1.186	1.186	1.289
9			1.171	1.182	1.296
10			1.160	1.178	1.302
15	0.921	1.011	1.104	1.174	1.360
20				1.204	1.379
25				1.203	1.318
30	0.694	0.976	0.987	1.201	1.222
45				0.926	0.948
EIGHT FINS ( $F_8$ )					
$\alpha$	<u>M = 0.6</u>	<u>M = 1.5</u>	<u>M = 2.0</u>	<u>M = 3.0</u>	<u>M = 4.5</u>
1	1.901	1.407	1.384	1.302	1.305
2		1.372	1.368	1.303	1.310
3		1.381	1.361	1.296	1.315
4		1.379	1.345	1.287	1.323
5			1.327	1.277	1.336
6			1.306	1.265	1.350
7			1.292	1.257	1.366
8			1.273	1.249	1.379
9			1.259	1.239	1.391
10			1.238	1.234	1.407
15	0.9247	0.995		1.235	1.469
20				1.261	1.477
25				1.259	1.408
30	0.609	0.992	1.005	1.255	1.307
45				0.926	0.948

TABLE 1. EULER CFD CALCULATIONS FROM ZEUS<sup>++29</sup> AND GASP<sup>28</sup> CODES (Continued)

AR = 0.5					
SIX FINS ( $F_6$ )					
$\alpha$	<u>M = 0.6</u>	<u>M = 1.5</u>	<u>M = 2.0</u>	<u>M = 3.0</u>	<u>M = 4.5</u>
1	1.336	1.235	1.201	1.321	1.485
2		1.232	1.191	1.322	1.487
3		1.215	1.188	1.315	1.486
4		1.211	1.179	1.314	1.484
5			1.180	1.312	1.494
6			1.176	1.308	1.507
7			1.175	1.308	1.522
8			1.174	1.304	1.491
9			1.174	1.300	1.480
10			1.169	1.293	1.479
11			1.171		
12			1.171		
15	1.050	1.087		1.270	1.527
20				1.292	1.533
25				1.294	1.483
30	0.794	0.944	1.070	1.291	1.354
45			0.952	1.002	
60				0.709	
EIGHT FINS ( $F_8$ )					
$\alpha$	<u>M = 0.6</u>	<u>M = 1.5</u>	<u>M = 2.0</u>	<u>M = 3.0</u>	<u>M = 4.5</u>
1	2.143	1.336	1.273	1.369	1.728
2		1.351	1.274	1.364	1.715
3		1.350	1.269	1.357	1.717
4		1.341	1.262	1.361	1.719
5			1.256	1.368	1.760
6			1.255	1.369	1.773
7			1.252	1.372	1.796
8			1.248	1.371	1.785
9			1.251	1.370	1.793
10			1.252	1.371	1.818
11			1.256		
12			1.258		
15	1.201	1.184		1.396	1.844
20				1.430	1.816
25				1.422	1.741
30	0.750	1.065	1.160	1.418	1.608
45			1.038	1.050	
60				0.943	

TABLE 1. EULER CFD CALCULATIONS FROM ZEUS<sup>++29</sup> AND GASP<sup>28</sup> CODES (Continued)

AR = 1.0					
SIX FINS ( $F_6$ )					
$\alpha$	$M = 0.6$	$M = 1.5$	$M = 2.0$	$M = 3.0$	$M = 4.5$
1	1.381	1.222	1.446	1.505	1.486
2		1.203	1.439	1.475	1.493
3			1.428	1.474	1.480
4			1.409	1.480	1.495
5			1.400	1.490	1.510
6			1.392	1.467	1.519
7			1.379	1.434	1.521
8			1.365	1.442	1.512
9			1.362	1.432	1.483
10				1.427	1.478
15	1.122	1.118	1.143	1.350	1.513
20				1.369	1.539
25				1.378	1.513
30	1.068	0.882	1.064	1.294	1.407
45					
60				0.806	0.763
EIGHT FINS ( $F_8$ )					
$\alpha$	$M = 0.6$	$M = 1.5$	$M = 2.0$	$M = 3.0$	$M = 4.5$
1	2.783	1.288	1.582	1.952	1.900
2		1.280	1.578	1.915	1.961
3		1.279	1.571	1.916	1.936
4			1.565	1.906	1.941
5			1.546	1.910	1.993
6			1.538	1.888	2.006
7			1.523	1.860	2.010
8			1.517	1.851	2.013
9			1.514	1.862	2.008
10				1.861	1.980
15	1.692	1.383	1.392	1.742	2.001
20				1.747	2.048
25				1.722	2.049
30	1.441	1.312	1.883	1.654	2.012
45					
60				1.332	1.237

TABLE 1. EULER CFD CALCULATIONS FROM ZEUS<sup>++29</sup> AND GASP<sup>28</sup> CODES (Continued)

AR = 2.0					
SIX FINS ( $F_6$ )					
$\alpha$	<u>M = 0.6</u>	<u>M = 1.5</u>	<u>M = 2.0</u>	<u>M = 3.0</u>	<u>M = 4.5</u>
1	1.468	1.512	1.524	1.519	1.524
2		1.503	1.495	1.481	1.495
3		1.522	1.468	1.477	1.486
4			1.470	1.497	1.487
5			1.457	1.482	1.498
6			1.473	1.439	1.506
7			1.464	1.419	1.500
8			1.444	1.422	1.512
9			1.447	1.397	1.480
10			1.432	1.416	1.478
11			1.418		
15	1.204	1.412	1.196	1.364	1.516
20				1.401	1.530
25				1.437	1.505
30	1.300	0.859	1.055		1.448
45	-0.533	0.776	0.966	1.118	
60				0.883	0.865
EIGHT FINS ( $F_8$ )					
$\alpha$	<u>M = 0.6</u>	<u>M = 1.5</u>	<u>M = 2.0</u>	<u>M = 3.0</u>	<u>M = 4.5</u>
1	3.681	1.730	1.940	1.913	1.910
2		1.756	1.954	1.901	1.926
3		1.775	1.912	1.930	1.901
4		1.728	1.928	1.948	1.889
5			1.927	1.911	1.948
6			1.915	1.868	1.977
7			1.893	1.870	1.953
8			1.874	1.856	1.956
9			1.860	1.858	1.957
10			1.859	1.839	1.950
11			1.846		
12			1.899		
15	2.339	1.946	1.732	1.761	2.021
20				1.830	2.043
25				1.842	
30	2.952	1.507	1.521		2.094
45	0.885	1.430	1.909	1.503	
60				1.829	1.653

of the ZEUS computations. As with the ZEUS<sup>++</sup> computations, the GASP computations were compared to the NASA Tri-service data base for the body alone and four-fin computations before proceeding to the six- and eight-fin computations. The results of these comparisons can be found in Table 2. Normal force coefficients are shown from the CFD computations and from the wind tunnel data base at each point where information was available for both. The percent difference between the two is also given. In the case of the CFD data, a box is placed around the GASP results as before. Results of the comparisons were within experimental errors in most cases, so it is believed the six- and eight-fin results of Table 1 should prove adequate for the development of a semiempirical model for multifin aerodynamics.

An exception to the computations being within experimental error occurred for the Mach 0.6 cases where the full Euler solution of the GASP code was used. Here, the GASP body-alone solution gave normal force coefficients that were higher than data for moderate angles of attack ( $\alpha = 15$  to  $30$  deg). In analyzing this with the AP98, it was concluded that the crossflow Reynolds number was supercritical, which meant that instead of a crossflow drag coefficient of 1.2, a value less than that was needed to match experiment. Physically, what is happening when the crossflow drag coefficient decreases rapidly is that the flow around the body remains more attached in the leeward plane as opposed to separating near the maximum diameter of the body in the crossflow plane. The inviscid Euler solution cannot model this without some help. The full Navier-Stokes solution from GASP, given the correct turbulence model, should be able to model this phenomena. However, at present, time does not permit this approach. As a result, engineering judgement will be used for the Euler solutions at low Mach numbers where the crossflow separation model is not accurate. This problem did not appear to occur with the ZEUS<sup>++</sup>, or with the GASP at higher Mach number, where the leeward plane pressures are fairly small in comparison to the windward plane pressures.

Another problem in the GASP Euler solutions occurred for the larger aspect ratio fin cases. Here the fins are very small and any errors in the body alone solution can produce fairly large errors in the factors  $F_6$  and  $F_8$ . As a result, engineering judgement must be used here as well.

Results from Table 1 were then plotted in Figure 15 for aspect ratio 0.25, 0.5, 1.0, 2.0 and Mach number 0.6, 1.5, 2.0, 3.0, and 4.5 as functions of AOA. Then curves were drawn through the data for use in the aeroprediction code. Data from these curves is given in Table 3. This then is the model that will be incorporated into the AP98 for multifin aerodynamics. Any Navier-Stokes calculations in the future or comparisons to wind tunnel data for configurations outside the data base can be used to fine-tune this model.

TABLE 2. COMPARISON OF CFD RESULTS TO NASA DATA BASE FOR  
FOUR-FIN CONFIGURATION

BODY ALONE				
<u>M</u>	<u><math>\alpha</math></u>	<u>C<sub>N</sub> (WIND TUNNEL)</u>	<u>C<sub>N</sub> (CFD)</u>	<u>% DIFFERENCE</u>
0.6	15	1.00	2.267	126.7
	30	3.09	4.658	50.7
1.5	15	1.39	1.629	17.2
	30	6.11	7.120	16.5
2.0	5	0.32	0.372	16.2
	10	0.82	0.835	1.8
	15	1.86	1.923	3.4
	30	6.47	7.222	11.6
4.5	5	0.43	0.381	-11.4
	10	1.21	1.129	-6.7
	15	2.21	1.997	-9.6
	20	3.28	3.039	-7.3
	25	4.62	4.251	-8.0
	30	6.00	5.565	-7.2

AR = 0.25				
<u>M</u>	<u><math>\alpha</math></u>	<u>C<sub>N</sub> (WIND TUNNEL)</u>	<u>C<sub>N</sub> (CFD)</u>	<u>% DIFFERENCE</u>
0.6	15	5.12	5.452	6.5
1.5	15	4.96	5.130	3.4
2.0	10	2.82	2.809	0.3
3.0	5	1.02	1.064	4.3
	10	2.46	2.442	-0.7
	15	4.13	4.111	-0.5
	20	6.00	5.929	-1.2
	25	8.14	7.984	-1.9
4.5	5	0.92	0.905	-1.6
	10	2.00	1.981	-1.0
	15	3.24	3.266	0.8
	20	4.96	4.876	-1.7
	25	6.92	6.782	-2.0
	30	9.05	8.889	-1.8



TABLE 2. COMPARISON OF CFD RESULTS TO NASA DATA BASE FOR  
FOUR-FIN CONFIGURATION (Continued)

AR = 0.5				
<u>M</u>	<u><math>\alpha</math></u>	<u>C<sub>N</sub> (WIND TUNNEL)</u>	<u>C<sub>N</sub> (CFD)</u>	<u>% DIFFERENCE</u>
0.6	15	3.62	4.129	14.1
	15	3.67	3.702	0.9
1.5	30	9.57	10.808	12.9
2.0	5	0.86	1.041	21.0
	10	2.00	2.184	9.2
	30	9.62	10.058	4.6
3.0	5	0.81	0.866	6.9
	10	1.95	1.959	0.5
	15	3.35	3.349	0.0
	20	4.81	4.882	1.5
	25	6.54	6.617	1.2
4.5	5	0.65	0.712	9.5
	10	1.62	1.611	-0.6
	15	2.70	2.672	-1.0
	20	4.05	4.017	-0.8
	25	5.68	5.597	-1.5
	30	7.51	7.347	-2.2

TABLE 2. COMPARISON OF CFD RESULTS TO NASA DATA BASE FOR  
FOUR-FIN CONFIGURATION (Continued)

AR = 1.0				
<u>M</u>	<u><math>\alpha</math></u>	<u>C<sub>N</sub> (WIND TUNNEL)</u>	<u>C<sub>N</sub> (CFD)</u>	<u>% DIFFERENCE</u>
0.6	15	2.54	3.252	29.0
	30	6.00	6.761	12.7
1.5	15	2.97	2.869	-3.4
	30	8.38	9.016	7.6
2.0	5	0.65	0.814	25.2
	15	2.92	3.040	4.1
	30	7.94	8.734	10.0
3.0	5	0.59	0.660	11.9
	10	1.51	1.569	1.8
	15	2.70	2.854	5.7
	20	4.05	4.262	5.2
	25	5.57	5.815	4.4
	30	7.29	7.588	4.1
4.5	5	0.59	0.574	2.7
	10	1.46	1.404	-3.8
	15	2.48	2.401	-3.2
	20	3.73	3.607	-3.3
	25	5.21	5.014	-3.8
	30	6.81	6.530	-4.1

TABLE 2. COMPARISON OF CFD RESULTS TO NASA DATA BASE FOR  
FOUR-FIN CONFIGURATION (Continued)

AR = 2.0				
<u>M</u>	<u><math>\alpha</math></u>	<u>C<sub>N</sub> (WIND TUNNEL)</u>	<u>C<sub>N</sub> (CFD)</u>	<u>% DIFFERENCE</u>
0.6	15	1.67	2.762	65.4
	30	6.32	5.281	-16.4
1.5	15	2.43	2.317	-4.6
	30	7.35	8.169	11.1
2.0	5	0.48	0.634	32.1
	10	1.18	1.362	15.4
	15	2.43	2.566	5.6
	30	7.35	8.048	9.5
3.0	5	0.48	0.518	7.9
	10	1.35	1.334	-1.2
	15	2.43	2.582	6.2
	20	3.73	3.925	5.2
	25	5.19	5.394	3.9
4.5	5	0.54	0.482	-10.7
	10	1.35	1.272	-5.8
	15	2.38	2.213	-7.0
	20	3.51	3.348	-4.6
	25	4.97	4.668	-6.1
	30	6.43	6.094	-5.2

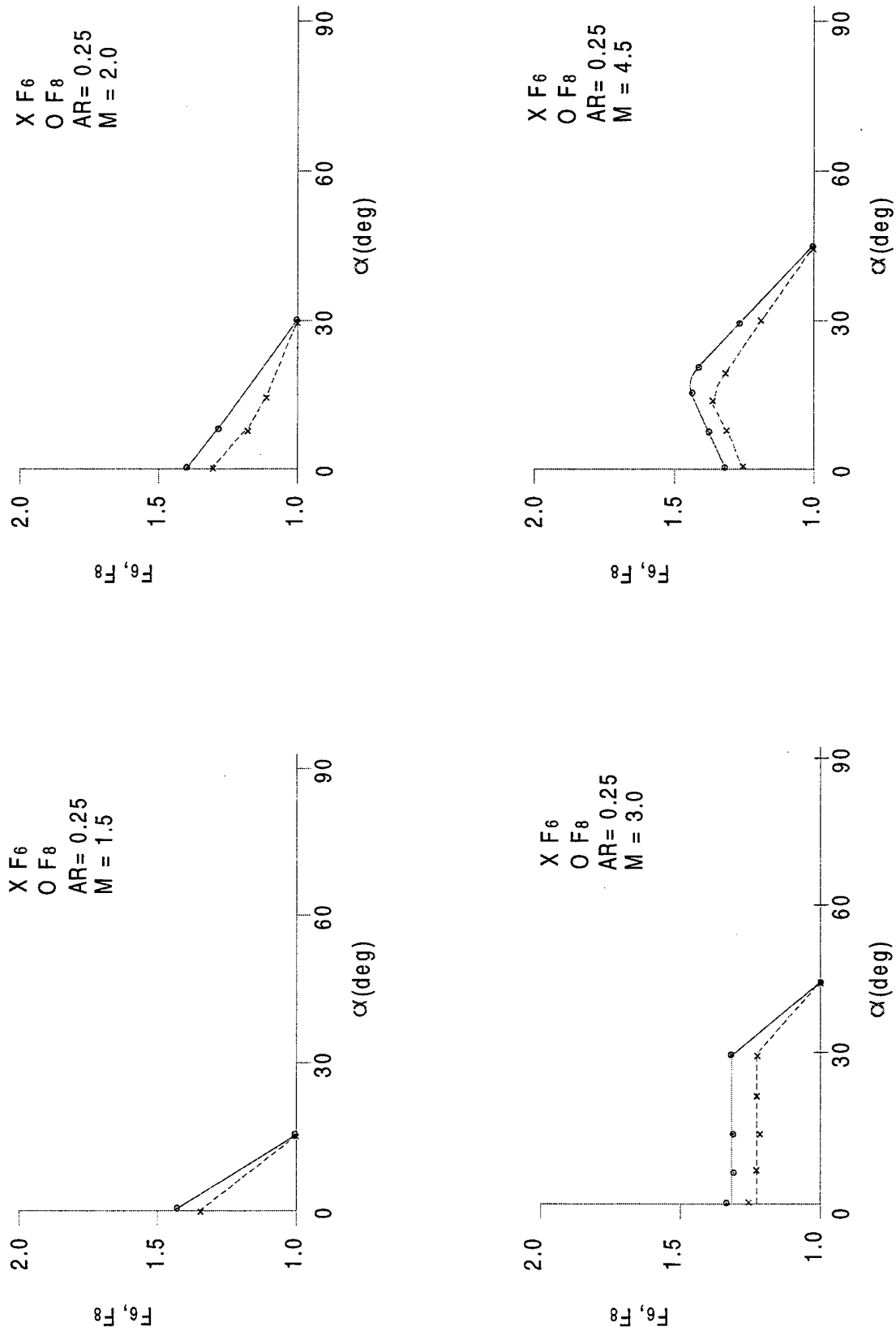


FIGURE 15. RATIO OF NORMAL FORCE OF SIX AND EIGHT FINS TO THAT OF FOUR FINS BASED ON CFD

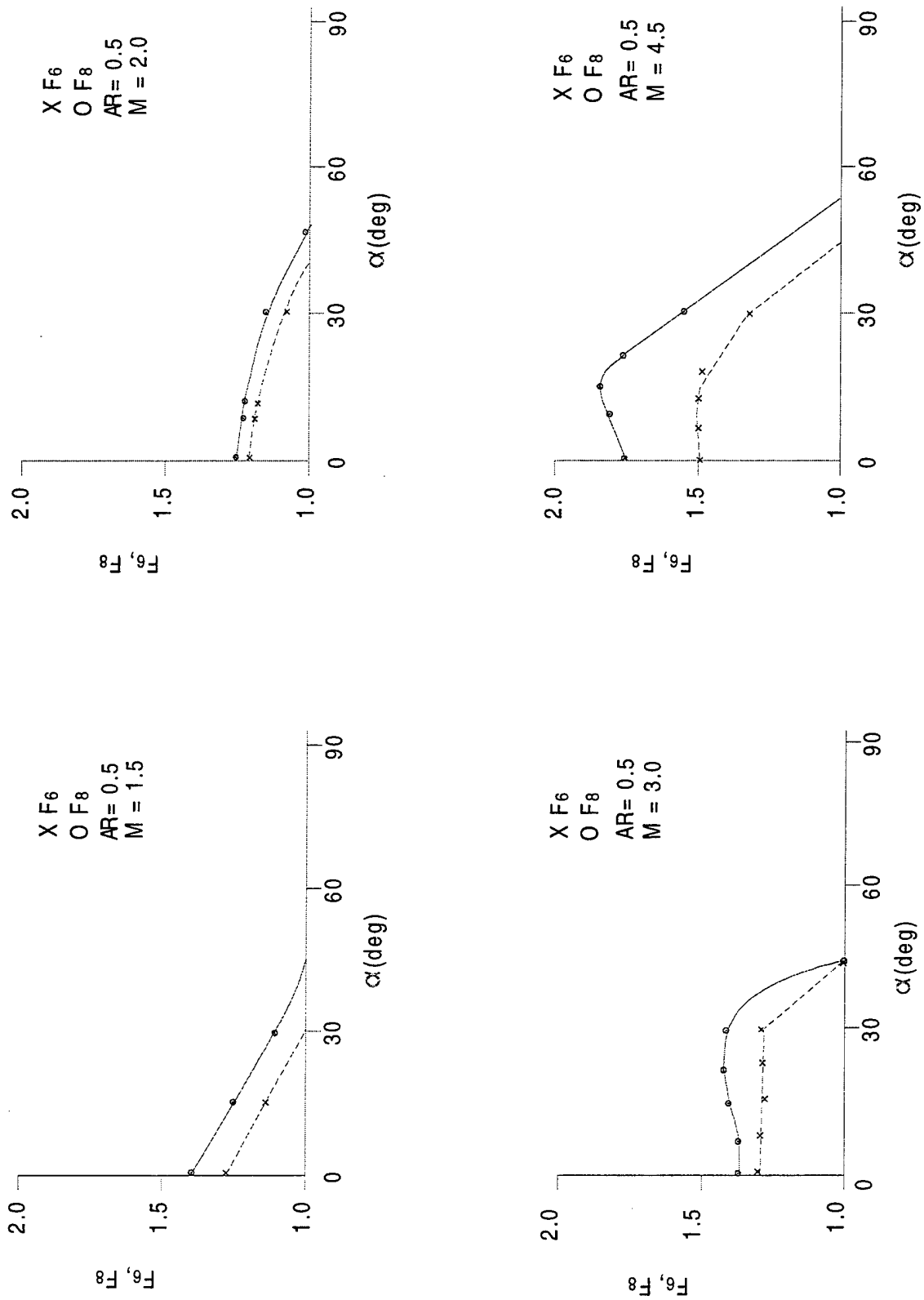


FIGURE 15. RATIO OF NORMAL FORCE OF SIX AND EIGHT FINS TO THAT OF FOUR FINS BASED ON CFD (Continued)

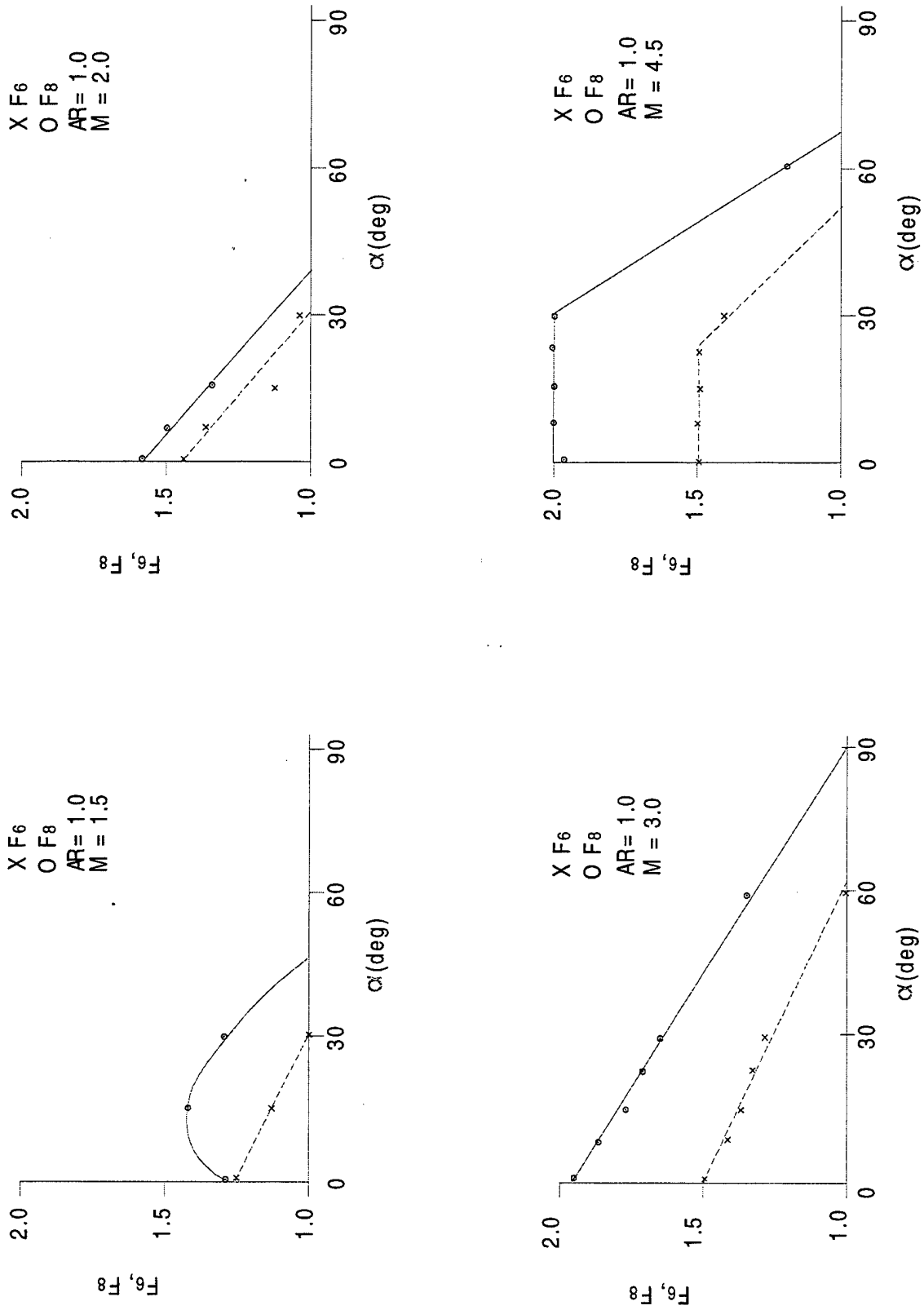


FIGURE 15. RATIO OF NORMAL FORCE OF SIX AND EIGHT FINS TO THAT OF FOUR FINS BASED ON CFD (Continued)

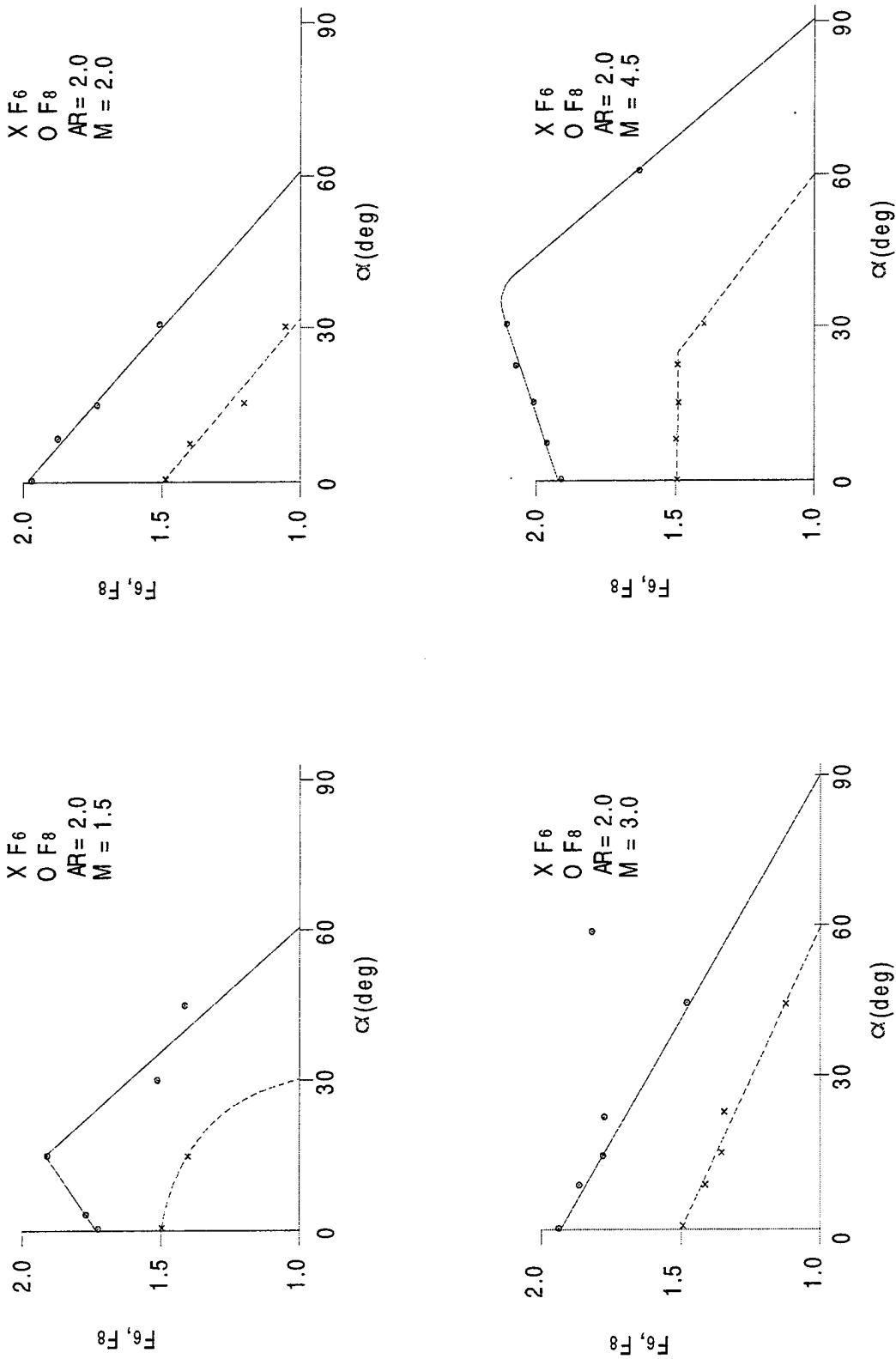


FIGURE 15. RATIO OF NORMAL FORCE OF SIX AND EIGHT FINS TO THAT OF FOUR FINS BASED ON CFD (Continued)

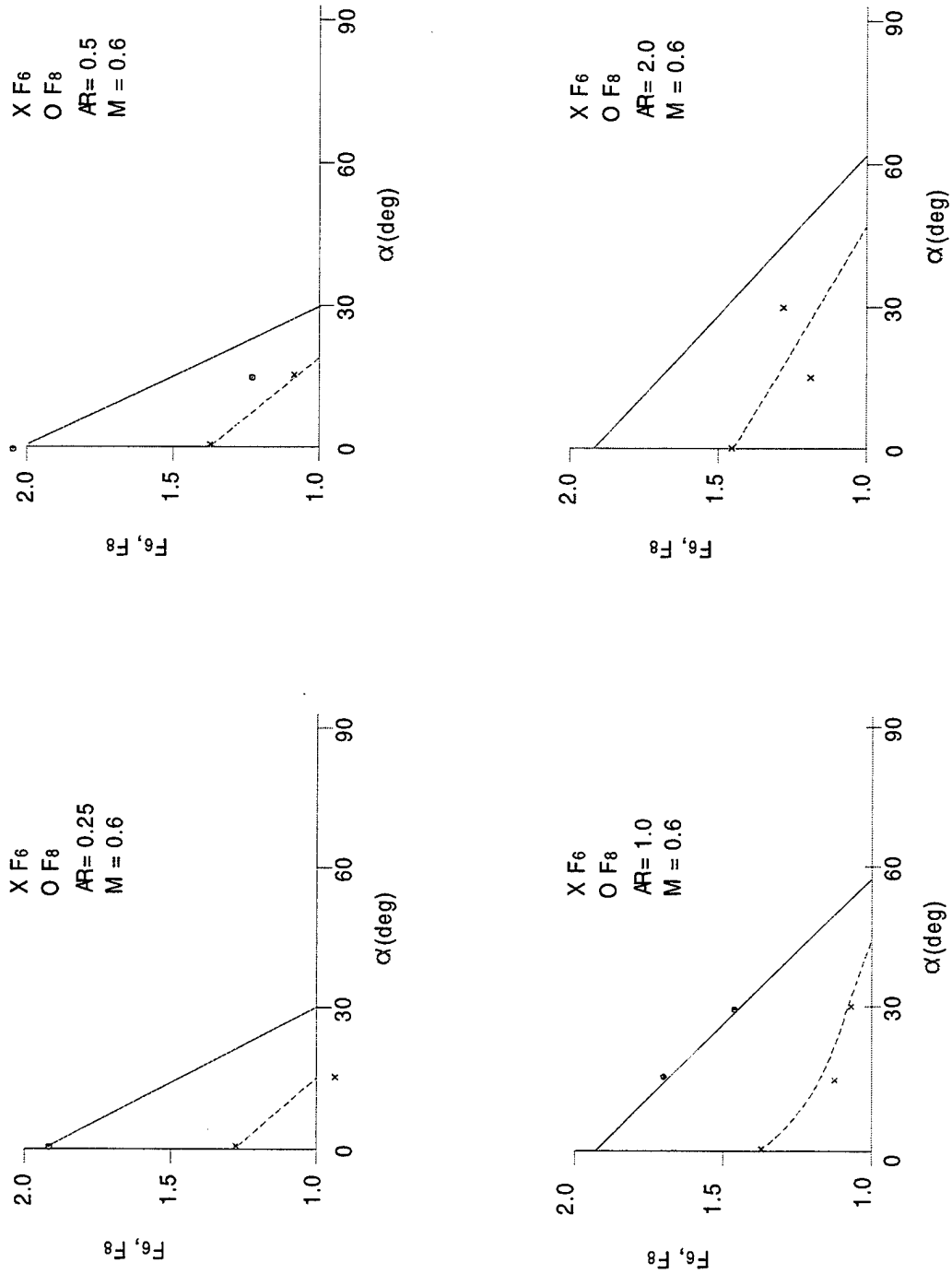


FIGURE 15. RATIO OF NORMAL FORCE OF SIX AND EIGHT FINS TO THAT OF FOUR FINS BASED ON CFD (Continued)



TABLE 3. APPROXIMATED VALUES OF THE FACTORS  $F_6$  AND  $F_8$  OBTAINED FROM SMOOTHED VALUES OF THE ZEUS++ AND GASP CODE COMPUTATIONS AND ENGINEERING JUDGEMENT

AR	$\alpha$	$F_6$ MACH NUMBER					$F_8$ MACH NUMBER				
		0.6	1.5	2.0	3.0	4.5	0.6	1.5	2.0	3.0	4.5
.25	0	1.26	1.37	1.27	1.19	1.22	1.90	1.42	1.4	1.27	1.30
	15	1.00	1.00	1.10	1.19	1.35	1.45	1.03	1.17	1.27	1.46
	30	1.00	1.00	1.00	1.19	1.22	1.00	1.00	1.01	1.27	1.32
	45	1.00	1.00	1.00	1.00	1.00	1.00	1.00	1.00	1.00	1.00
	60	1.00	1.00	1.00	1.00	1.00	1.00	1.00	1.00	1.00	1.00
	75	1.00	1.00	1.00	1.00	1.00	1.00	1.00	1.00	1.00	1.00
	90	1.00	1.00	1.00	1.00	1.00	1.00	1.00	1.00	1.00	1.00
.50	0	1.35	1.25	1.20	1.30	1.47	2.00	1.36	1.28	1.35	1.72
	15	1.06	1.10	1.15	1.29	1.50	1.50	1.18	1.24	1.40	1.83
	30	1.00	1.00	1.07	1.28	1.36	1.00	1.08	1.16	1.41	1.60
	45	1.00	1.00	1.00	1.00	1.00	1.00	1.00	1.04	1.06	1.20
	60	1.00	1.00	1.00	1.00	1.00	1.00	1.00	1.00	1.00	1.00
	75	1.00	1.00	1.00	1.00	1.00	1.00	1.00	1.00	1.00	1.00
	90	1.00	1.00	1.00	1.00	1.00	1.00	1.00	1.00	1.00	1.00
1.0	0	1.40	1.22	1.35	1.42	1.50	1.92	1.27	1.58	1.96	2.00
	15	1.15	1.13	1.23	1.32	1.50	1.69	1.38	1.38	1.80	2.00
	30	1.07	1.00	1.00	1.21	1.38	1.43	1.28	1.15	1.64	2.00
	45	1.02	1.00	1.00	1.10	1.13	1.20	1.05	1.00	1.48	1.61
	60	1.00	1.00	1.00	1.00	1.00	1.00	1.00	1.00	1.32	1.25
	75	1.00	1.00	1.00	1.00	1.00	1.00	1.00	1.00	1.16	1.00
	90	1.00	1.00	1.00	1.00	1.00	1.00	1.00	1.00	1.00	1.00
2.0	0	1.42	1.50	1.50	1.50	1.50	1.92	1.77	1.97	1.92	1.90
	15	1.31	1.41	1.27	1.39	1.50	1.70	1.95	1.75	1.77	2.00
	30	1.17	1.00	1.03	1.27	1.45	1.47	1.65	1.57	1.62	2.10
	45	1.03	1.00	1.00	1.14	1.23	1.25	1.32	1.27	1.47	1.95
	60	1.00	1.00	1.00	1.00	1.00	1.02	1.00	1.02	1.32	1.62
	75	1.00	1.00	1.00	1.00	1.00	1.00	1.00	1.00	1.17	1.32
	90	1.00	1.00	1.00	1.00	1.00	1.00	1.00	1.00	1.00	1.00

#### 4.0 AERODYNAMIC SMOOTHER

The aeroprediction code uses many different methods to predict aerodynamics at a given Mach number and angle of attack. These methods are illustrated in Figures 2 through 4. At Mach numbers 1.2, 2.0, and 6.0, where one method ends and another method takes over, discontinuities in aerodynamics can be obtained. The discontinuities are the result of different methods being used on either side of  $M_\infty = 1.2, 2.0, \text{ or } 6.0$ . The problem does not appear to be significant at  $M = 1.2$ , but at 2.0 and 6.0, these fictitious discontinuities can be misleading to an unsuspecting user of the APC when they plot out the aerodynamics as a function of Mach number. As an illustration of this problem, consider Figure 16. Figure 16 is an example of a 12-caliber, axisymmetric body, tangent ogive-cylinder configuration with a nose length of 3 calibers. It has aspect ratio 2.0 cruciform delta fins oriented in the  $\Phi = 0$  deg roll orientation with the leading edge located 7.8 calibers from the nose tip. The moments are taken about the center of gravity.

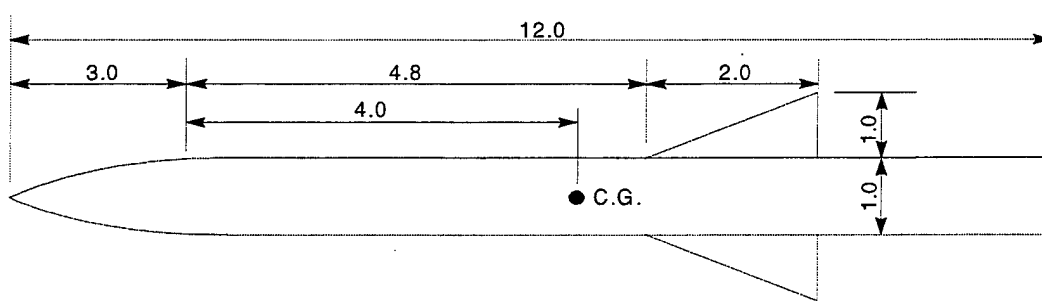
The static aerodynamics shown in Figure 16 are axial force, normal force, and pitching moment coefficients along with the center of pressure. Mach numbers for which the AP98 was executed were 0.6, 0.9, 1.2, 1.5, 1.99, 2.01, 2.4, 2.95, 3.95, 5.99, 6.0, and 10. The point where second-order Van Dyke (SOVD) ends and second-order shock expansion (SOSE) takes over was selected to be 2.0. The point where conventional second-order shock expansion ends and a modified form of shock expansion theory (MSOSE) takes over is automatically set at 6.0 in the AP98. Hence,  $M = 1.99$  data is from SOVD,  $M = 2.01$  and 5.99 data are from SOSE, and  $M = 6.0$  data is from MSOSE. Notice on the  $C_A$  plot that there is a discontinuity between SOVD and SOSE at  $M = 2.0$ . Also notice on the  $C_N$  plot there is a discontinuity at both  $M = 2.0$  and 6.0. For pitching moment and center of pressure, discontinuities occur only at  $M = 6.0$ . The discontinuities in Figure 16 appear small, but some cases considered in the past have shown discontinuities larger than these.

While the numbers in this particular example, due to the different aerodynamic methods, are less than 5 percent of the totals, the user of the APC is left with the question of which number to use. Experience has shown in comparison to data that an average of the two numbers is probably better than using either of the estimates alone. As a result, an aerodynamic smoother is developed that is based on an average of the values given by SOSE and SOVD at  $M = 2.0$  and an average of SOSE and MSOSE at  $M = 6.0$ . The smoother linearly goes to the SOVD value at  $M = 1.5$  and to the SOSE value of the particular coefficient at  $M = 2.5$ . Likewise, the value of the aerodynamic coefficient at  $M = 5.0$  is based fully on SOSE and at  $M = 7.0$  it is based on MSOSE. The average value of the two methods is used at  $M = 6.0$ .

The mathematics of the aerodynamic smoother at  $M = 2.0$  and  $M = 6.0$  are defined by Equations (2) and (3).

Smoother at  $M = 2.0$

$$(C_i)_{M=1.5} = (C_i)_{\text{SOVD}} ; (C_i)_{M=2.5} = (C_i)_{\text{SOSE}} \quad (2A)$$



BODY TAIL CONFIGURATION (DIMENSIONS IN CALIBERS WITH 1 CALIBER = 3.0 INCHES)

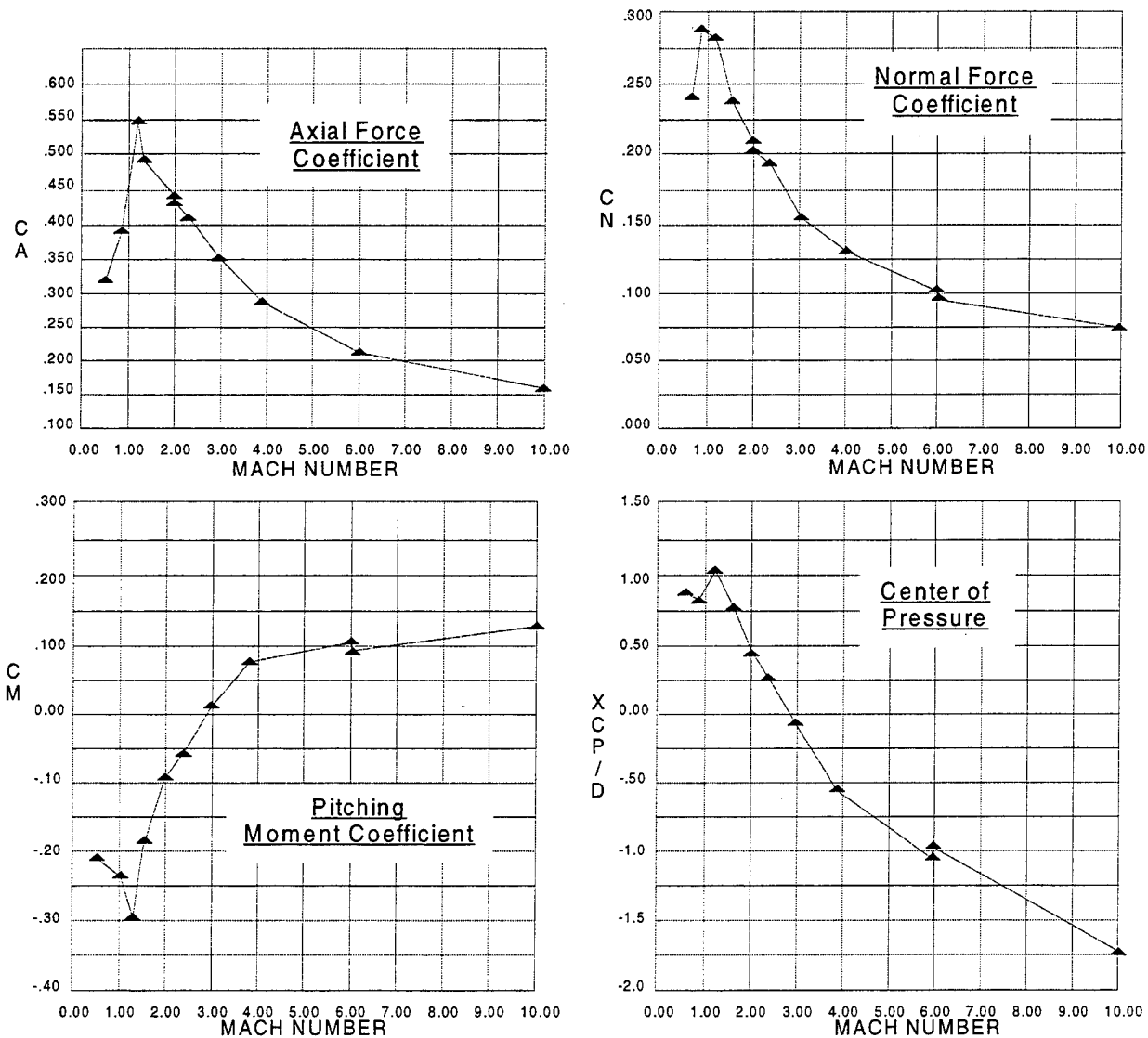


FIGURE 16. STATIC AERODYNAMICS OF A BODY-TAIL CONFIGURATION ILLUSTRATING DISCONTINUITIES AROUND  $M = 2.0$  AND  $6.0$  ( $\alpha = 1$  DEG,  $\Phi = 0$  DEG)

$$\underline{1.5 \leq M < 2.0}$$

$$(C_i)_M = (C_i)_{SOVD} + 2(M - 1.5) (\Delta C_i)_{M=2.0} \quad (2B)$$

$$\underline{2.0 \leq M \leq 2.5}$$

$$(C_i)_M = (C_i)_{SOSE} + 2(M - 2.5) (\Delta C_i)_{M=2.0} \quad (2C)$$

$$\text{where } (\Delta C_i)_{M=2.0} = ((C_i)_{SOSE} - (C_i)_{SOVD}) / 2$$

$$\underline{\text{Smoother at } M = 6.0}$$

$$(C_i)_{M=5.0} = (C_i)_{SOSE} ; (C_i)_{M=7.0} = (C_i)_{MSOSE} \quad (3A)$$

$$\underline{5.0 \leq M < 6.0}$$

$$(C_i)_M = (C_i)_{SOSE} + (M - 5.0) (\Delta C_i)_{M=6.0} \quad (3B)$$

$$\underline{6.0 \leq M < 7.0}$$

$$(C_i)_M = (C_i)_{MSOSE} + (M - 7.0) (\Delta C_i)_{M=6.0} \quad (3C)$$

$$\text{where } (\Delta C_i)_{M=6.0} = ((C_i)_{MSOSE} - (C_i)_{SOSE}) / 2$$

The term  $C_i$  of Equations (2) and (3) represents any of the static aerodynamic coefficients. Figure 17 is a qualitative view of what Equations (2) and (3) are doing in terms of modifying the values of the AP98 so as to eliminate the discontinuities shown in Figure 16.

Figure 18 shows the new values of normal force coefficient and center of pressure for the configuration of Figure 16 using the aerodynamic smoother. Note that the discontinuities of Figure 16 are no longer present in Figure 18 as a result of the aerodynamic smoother. The smoother only eliminates the discontinuity in value of the aerodynamic coefficient. It does not require that the slope of the aerodynamic coefficients ( i.e.,  $d C_i / d M$ ) be continuous in a mathematical sense.

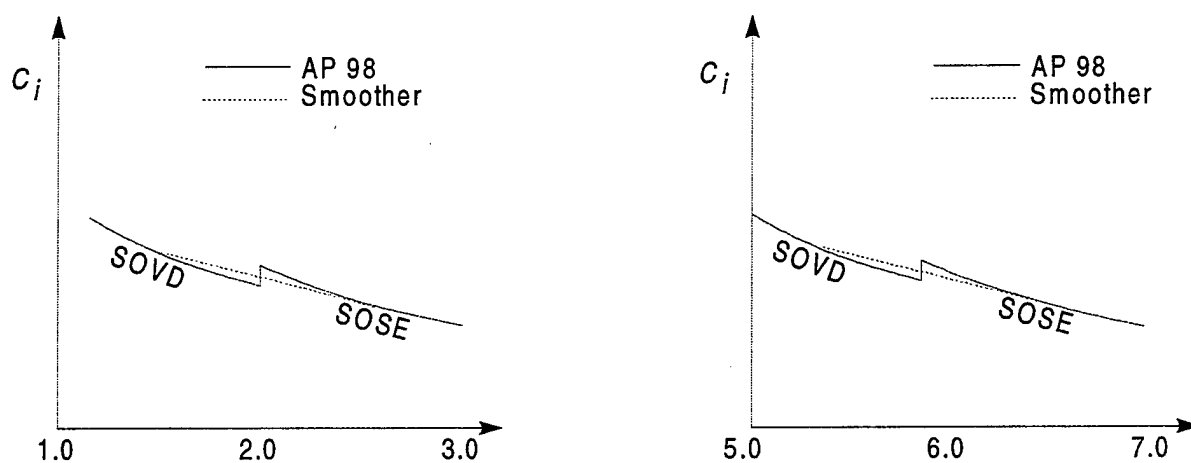


FIGURE 17. USE OF AERODYNAMIC SMOOTHER TO ELIMINATE DISCONTINUITY IN VALUE OF  $C_i$  AT  $M = 2$  AND  $6$

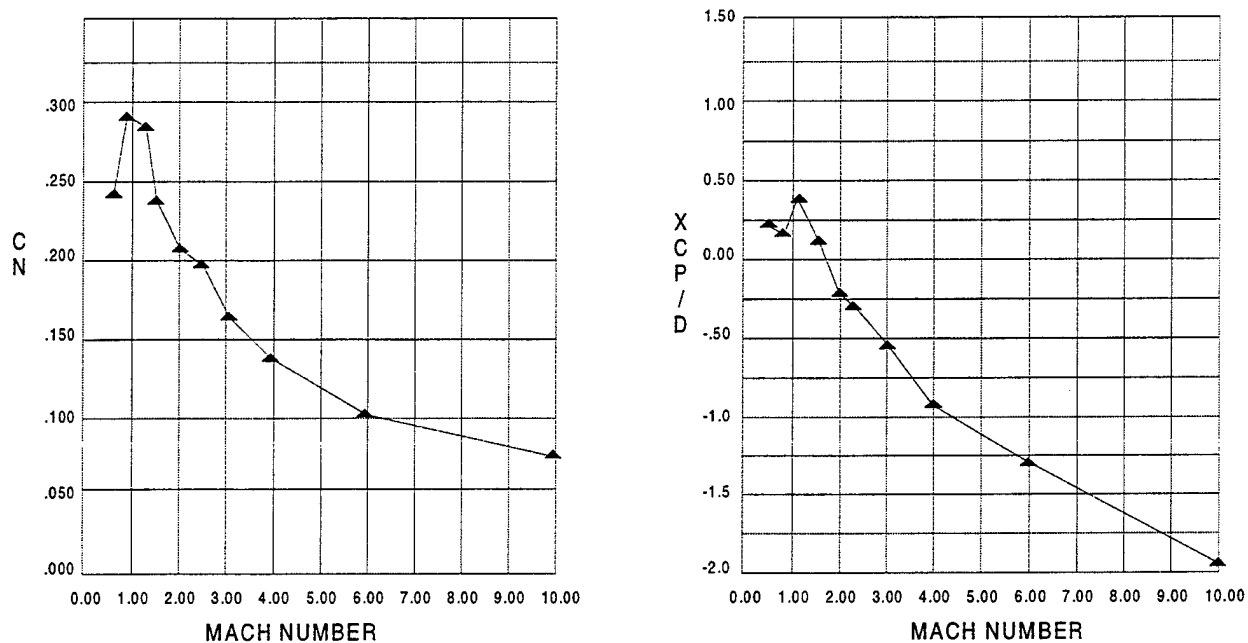


FIGURE 18. NORMAL FORCE COEFFICIENT AND CENTER OF PRESSURE FOR CONFIGURATION OF FIGURE 16 USING AERODYNAMIC SMOOTHER

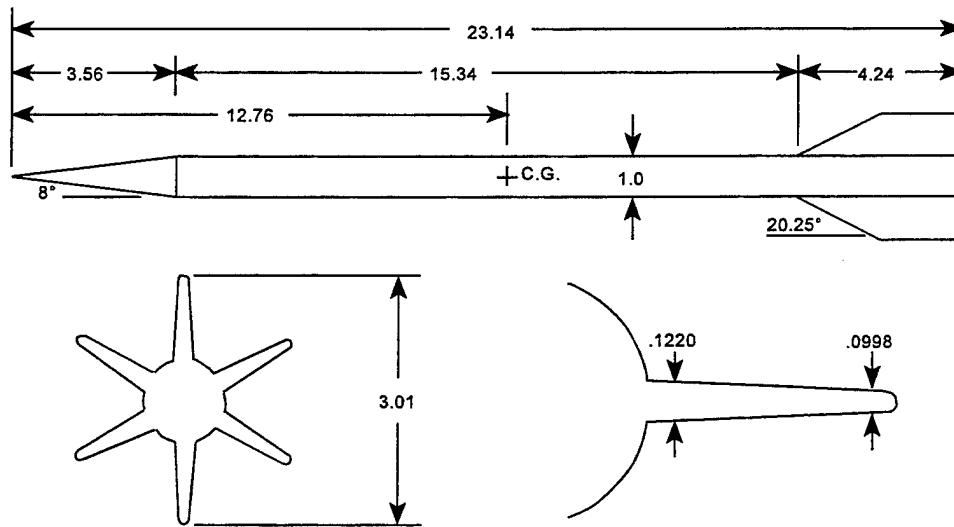
## 5.0 COMPARISON OF NEW METHOD FOR MULTIFIN AERODYNAMICS TO EXPERIMENT

The very limited availability of experimental data for normal force on missiles with more than four fins makes validation of the new methodology difficult. One set of ballistic range data for a six-finned projectile, along with accompanying CFD information, may be found in References 32 and 33. The geometric configuration of the model used in these tests is shown in Figure 19. It consists of a cone-cylinder body 23.14 calibers in total length with a diameter of 27.05 mm. The cone half angle is 8 deg and the leading and trailing edges of the fins are blunt. For the AP98 runs, Reynolds number was computed based on sea level conditions and the body diameter. The "wind tunnel model with no boundary layer trip" option was chosen for the viscous computations.

The comparisons for normal force coefficient slope at zero angle of attack, axial force coefficient, and center of pressure are shown in Figures 20A, 20B, and 20C, respectively. For these cases, range data was available from  $M_\infty = 3.5$  to 5.3 and CFD computations were done at  $M_\infty = 4.41$ , 5.0, and 5.88. AP98 results are shown for  $M_\infty = 2.0$  to 6.0. The large scatter in the range data could be the result of angle of attack motion that is not accounted for in either AP98 or the CFD runs. It can be seen that the AP98 results agree reasonably well with the CFD computations and both fall in the middle of the range data. Figures 20D, 20E, and 20F present comparisons for pitching moment coefficient slope at zero angle of attack, roll damping coefficient, and pitch damping coefficient, respectively. The range data is available for the same Mach number range as before, but the CFD and AP98 results are shown for  $M_\infty = 3.0$  to 5.5. Once again, the AP98 results are in fairly good agreement with the CFD computations except for pitching moment where they tend to be somewhat high. In general, both the AP98 and CFD results tend to be high compared to the range data.

A second set of experimental range data and CFD computations was available from References 32 and 33 for a similar six-finned projectile. In this instance, the cone-cylinder body is 13.94 calibers in length with a diameter of 35.2 mm. The cone half-angle is 8 deg and the leading and trailing edges of the fins are blunt. This configuration is shown in Figure 21. The same computational options were used as in the previous case. Ballistic data was available over a Mach number range from 3.0 to about 4.5. CFD data was given from  $M_\infty = 3.0$  to 5.5 and AP98 computations were performed over this same Mach number interval.

Comparisons for normal force coefficient and pitching moment coefficient slopes at zero angle of attack are shown in Figures 22A and 22B. The AP98 results at lower Mach numbers tend to be somewhat high compared to the CFD numbers in both cases, and both tend to lie above the range data. Figure 22C shows the comparison for axial force coefficient. Good agreement is obtained throughout in this instance. The comparison for pitch damping coefficient is shown in Figure 22D. Once again, the AP98 numbers are somewhat high relative to the CFD results and both tend to lie above the majority of the ballistic data.



All Dimensions in Calibers (One Caliber = 27.05 mm)

FIGURE 19. SCHEMATIC OF M829 PROJECTILE CONFIGURATION  
(FROM REFERENCE 32)

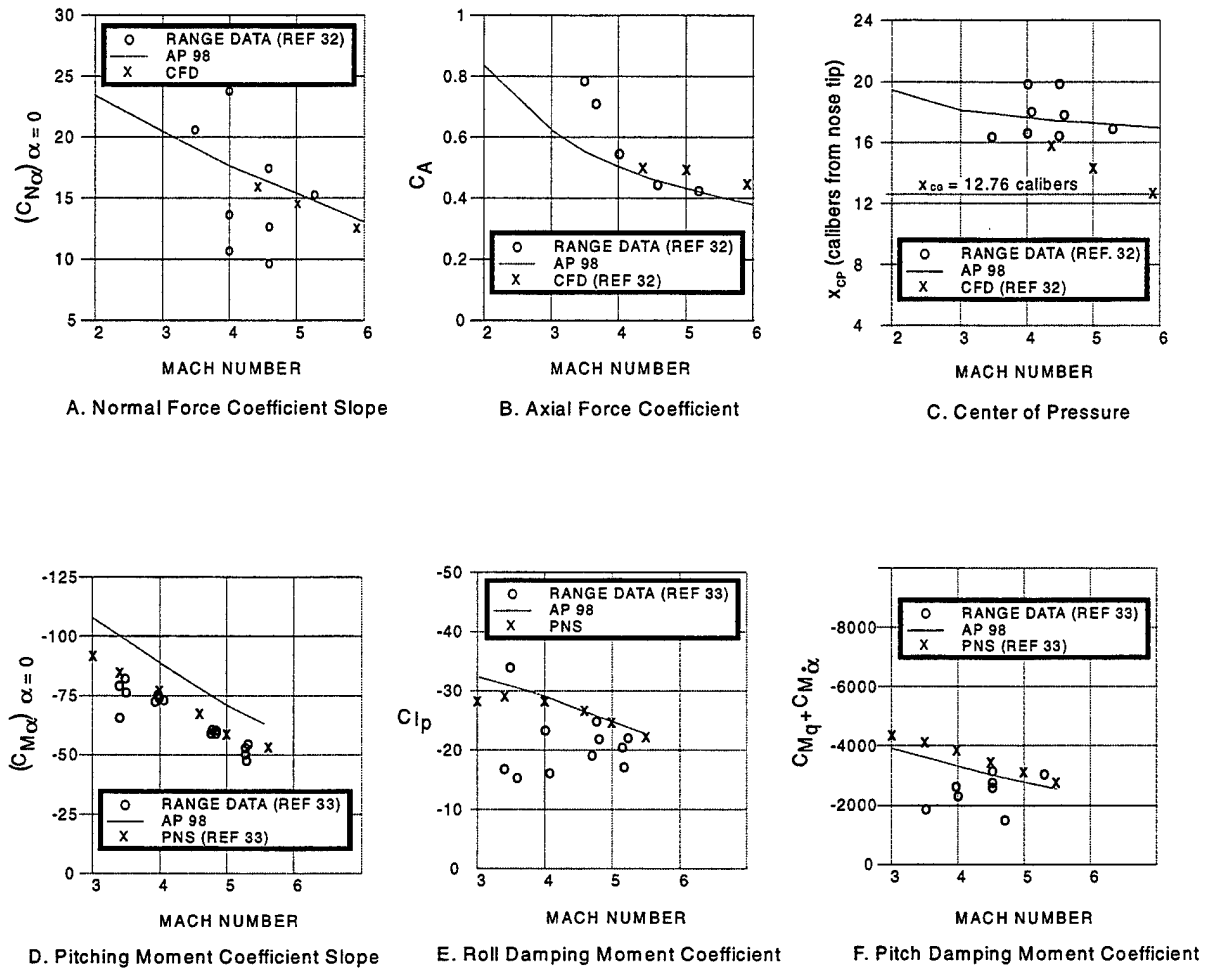
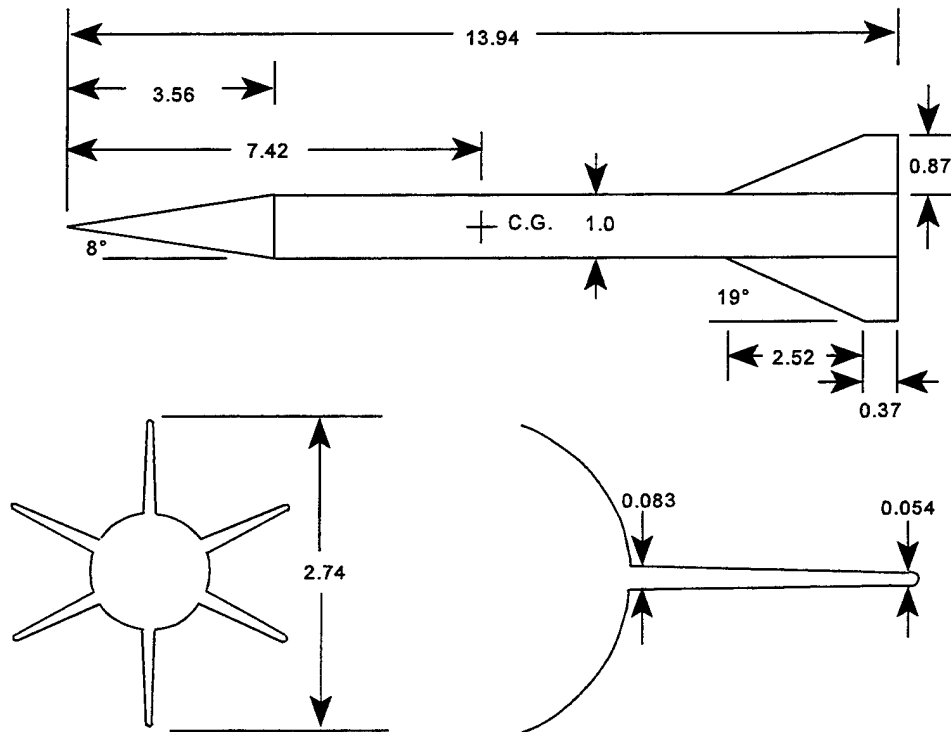


FIGURE 20. COMPARISON OF NEW MULTIFIN METHOD TO CFD AND EXPERIMENT FOR FIGURE 19 CONFIGURATION





All Dimensions in Calibers (One Caliber = 35.2 mm)

FIGURE 21. SCHEMATIC OF M735 PROJECTILE CONFIGURATION  
(FROM REFERENCE 34)

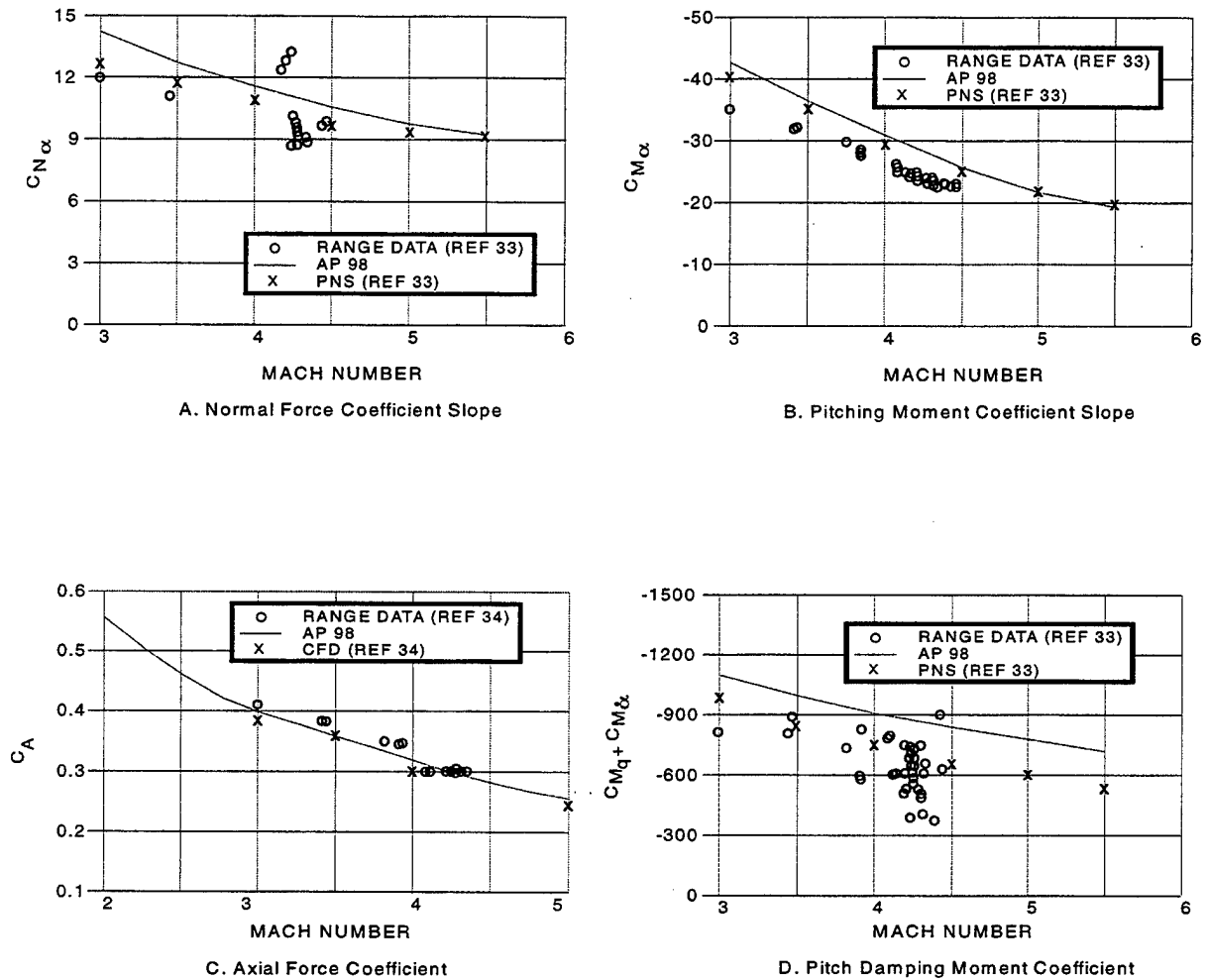


FIGURE 22. COMPARISON OF NEW MULTIFIN METHOD TO CFD AND EXPERIMENT  
FOR FIGURE 21 CONFIGURATION

A third set of data was available from the guided projectile wind tunnel tests of Reference 34. The model used is shown in Figure 23. It consists of a circular body, approximately 12.26 calibers in length, with a 3-caliber Von Karman ogive nose. The body diameter is 2.976 in. Eight small, high aspect ratio pop-out fins are located at the rear of a short boattail section. The model was also tested with four pop-out canards, but this configuration was not considered since the desire was to isolate the effects of the fins. It was necessary to modify the fin geometry to conform to the input requirements of AP98. The equivalent fin has a trapezoidal planform with the same area, sweep angle, and aspect ratio as the original. AP98 runs were done at the indicated Reynolds numbers for each case and the "wind tunnel model with no boundary layer trip" option was used.

Wind tunnel data was available in this case for the body alone, so it was used to adjust for the effects of crossflow separation and reattachment. This adjustment is made in AP98 by changing the critical crossflow Reynolds number and by shifting the value of crossflow Mach number at which the "drag bucket" starts. These two parameters are set to obtain a good fit to the experimental data at each Mach number and are then used for all further computations. The values that were determined are as follows:

M = 0.40:	Critical Reynolds Number = 179000 Crossflow Mach Number Shift = -0.05
M = 0.80:	Critical Reynolds Number = 285000 Crossflow Mach Number Shift = +0.05
M = 0.95:	Critical Reynolds Number = 304000 Crossflow Mach Number Shift = +0.09
M = 1.05:	Critical Reynolds Number = 318000 Crossflow Mach Number Shift = +0.12
M = 1.10:	Critical Reynolds Number = 326000 Crossflow Mach Number Shift = +0.13
M = 1.30:	Critical Reynolds Number = 365000 Crossflow Mach Number Shift = +0.15
M = 1.60:	Critical Reynolds Number = 390000 Crossflow Mach Number Shift = +0.15
M = 2.00:	Critical Reynolds Number = 390000 Crossflow Mach Number Shift = +0.15

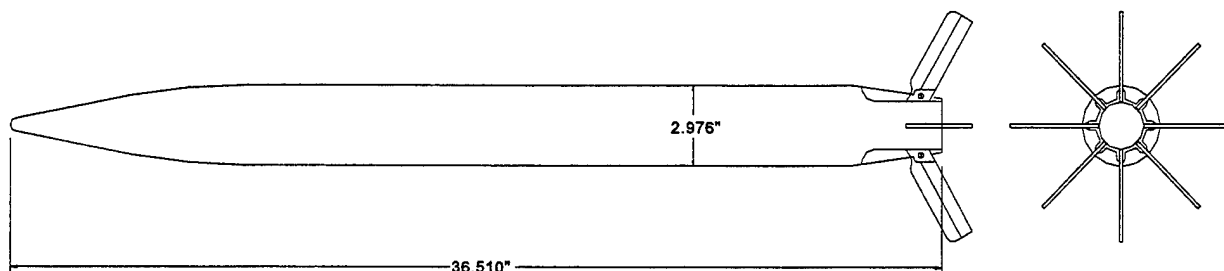


FIGURE 23. SCHEMATIC OF EIGHT-FIN GUIDED PROJECTILE  
(FROM REFERENCE 34)

Figures 24A–24H show the final results of this procedure for the body alone normal force. The very noticeable “kinks” in the curves at the lower Mach numbers are caused by the transition from subcritical to supercritical flow. It can be seen that these are more noticeable for the AP98 computations than for the wind tunnel data. The most likely cause of this difference lies in the incomplete modeling of this very complex phenomenon within AP98. While the critical crossflow Reynolds number and the location of the drag bucket can be varied, the width and shape of the reduced crossflow drag region cannot be changed in the AP98 model. In actuality, these latter parameters are likely to be highly dependent on both geometric and aerodynamic flow conditions.

Wind tunnel data was also available for this configuration with only four fins, and the normal force comparisons with AP98 for this case are shown in Figures 25A–25H. These results are included to provide information on how well AP98 does on these computations since they are used as a basis for the eight-fin model. If, for example, the AP98 predictions are low for a given case here, we would expect them to be low for the corresponding eight-fin case.

The comparisons for total normal force for the full eight-fin configuration are shown in Figures 26A–26H for Mach numbers of 0.4, 0.8, 0.95, 1.05, 1.1, 1.3, 1.6, and 2.0, respectively. Angles of attack range up to 15 deg. In general, the comparisons are quite good. The greatest disagreement occurs at the lower Mach numbers and higher angles of attack. The body aerodynamics under these conditions can be very sensitive to the subcritical or supercritical status of the flow in the leeward region, making accurate predictions difficult. The differences may be related primarily to this effect rather than to the fin modeling.

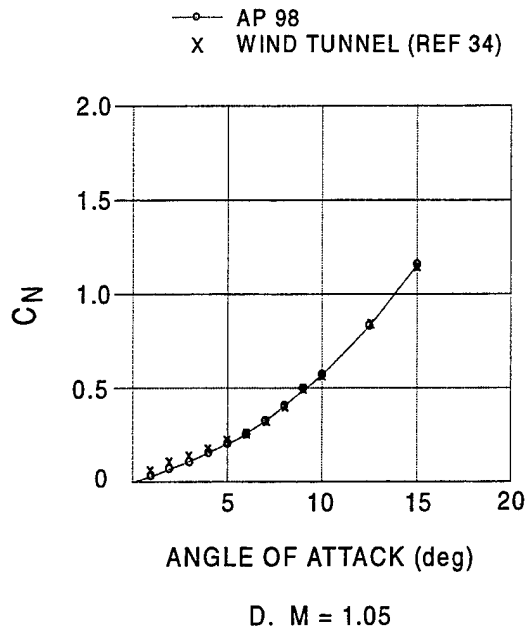
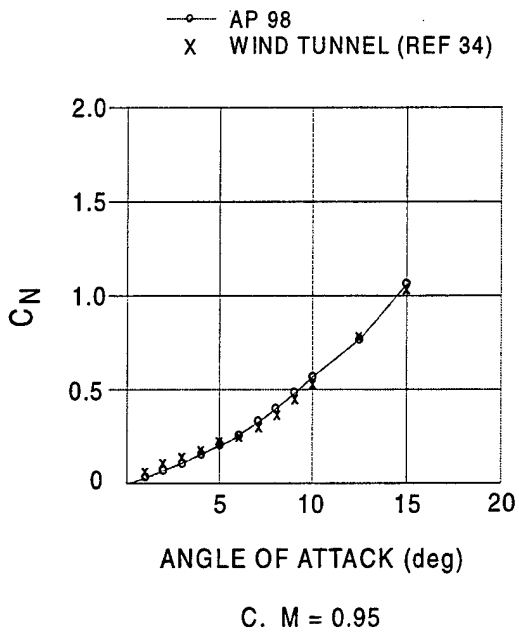
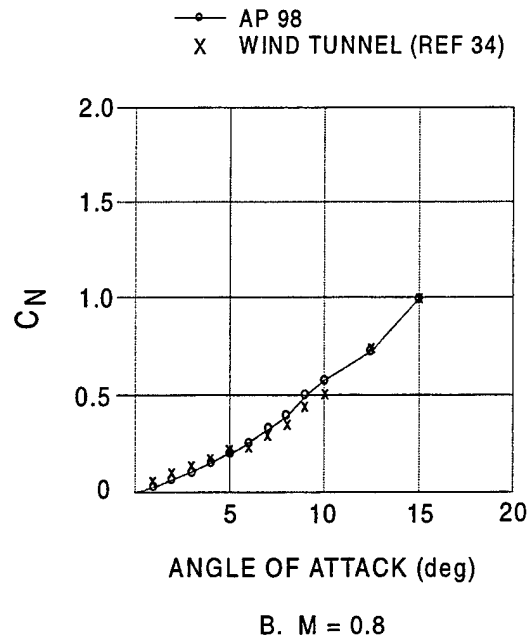
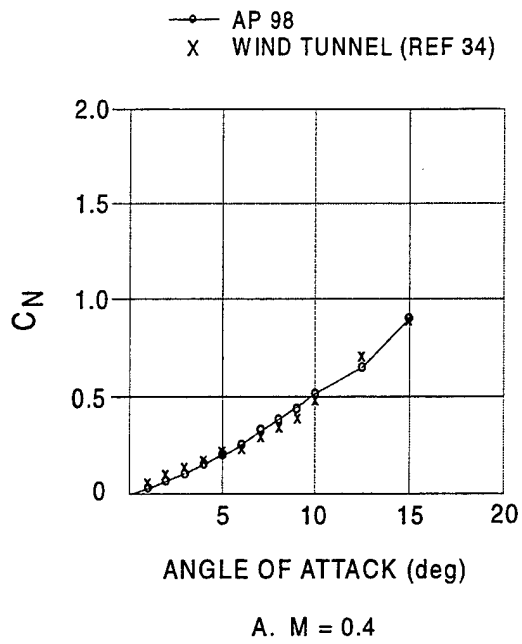


FIGURE 24. NORMAL FORCE COEFFICIENT COMPARISONS FOR BODY ALONE OF FIGURE 23

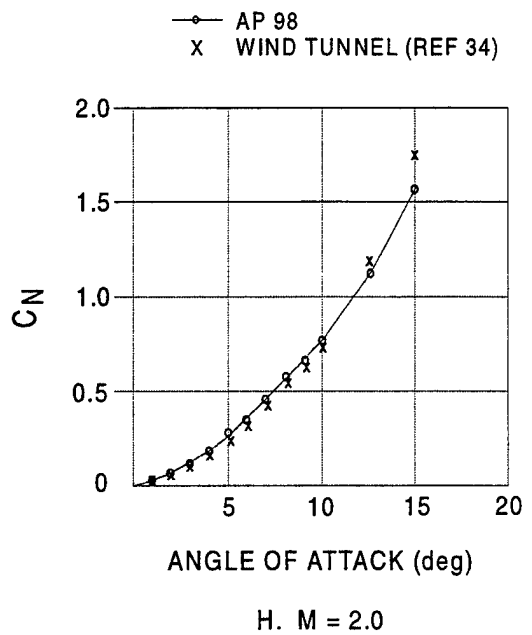
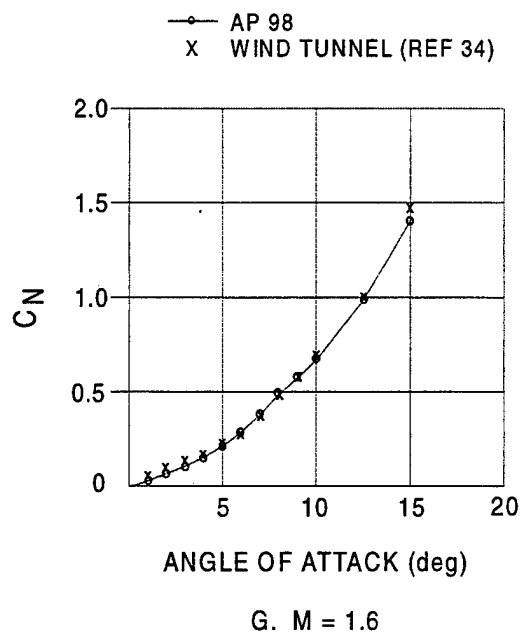
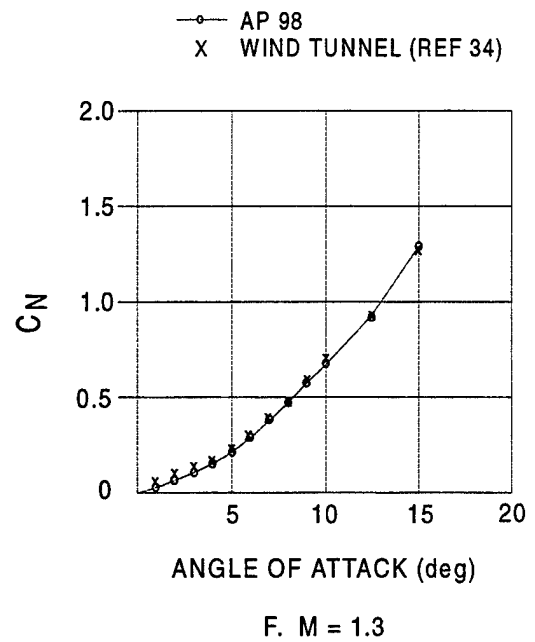
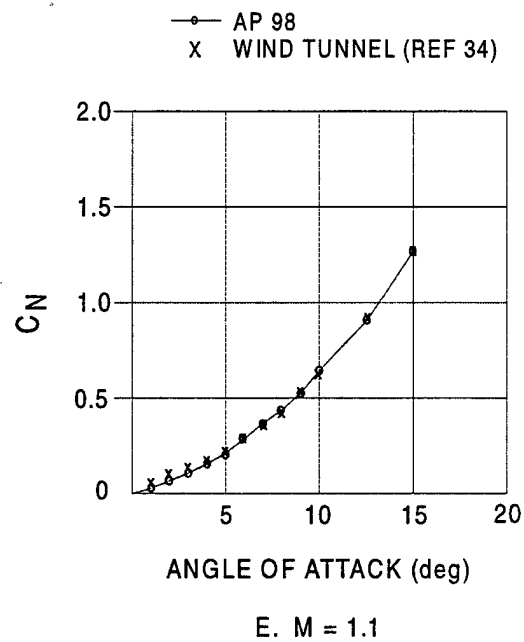


FIGURE 24. NORMAL FORCE COEFFICIENT COMPARISONS FOR  
BODY ALONE OF FIGURE 23 (Continued)

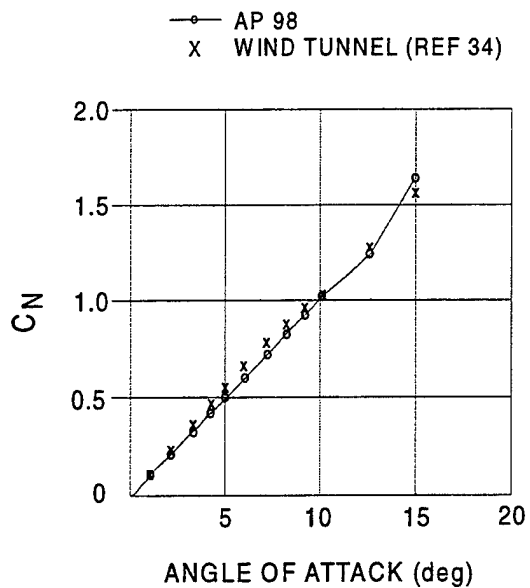
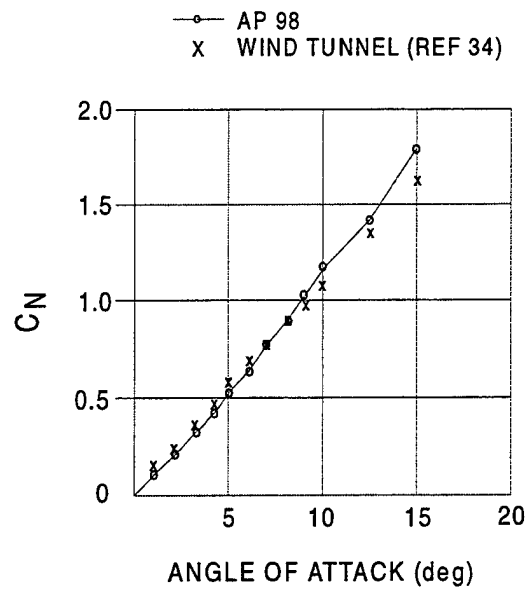
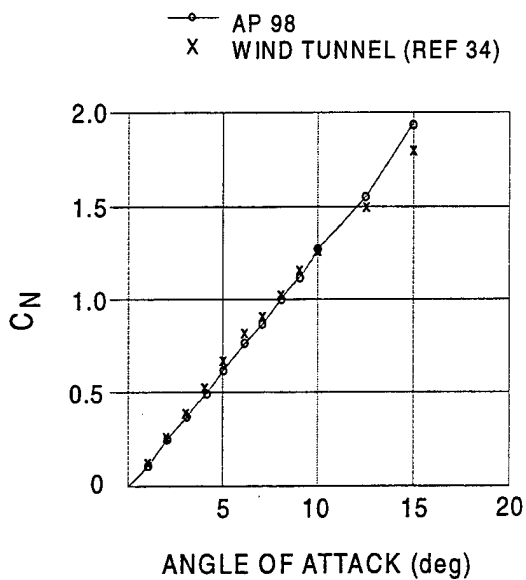
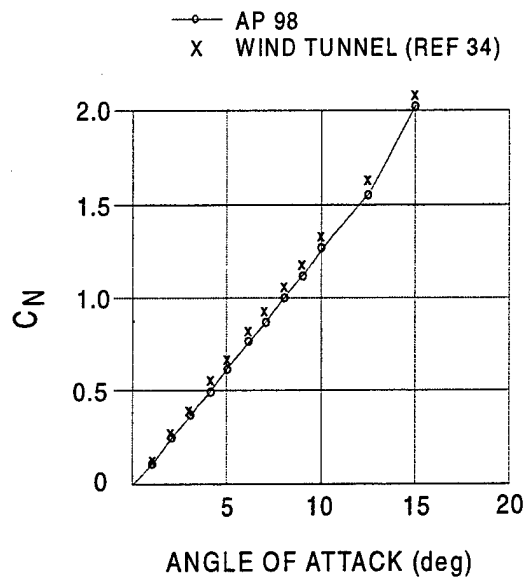
A.  $M = 0.4$ B.  $M = 0.8$ C.  $M = 0.95$ D.  $M = 1.05$ 

FIGURE 25. NORMAL FORCE COEFFICIENT COMPARISONS FOR FOUR-FIN GUIDED PROJECTILE OF FIGURE 23

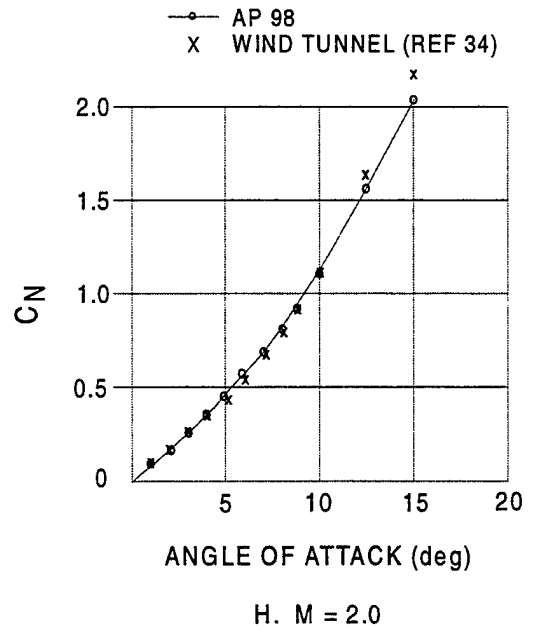
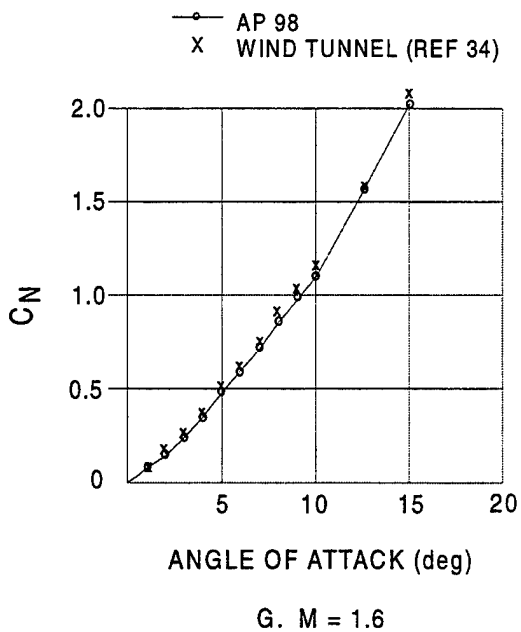
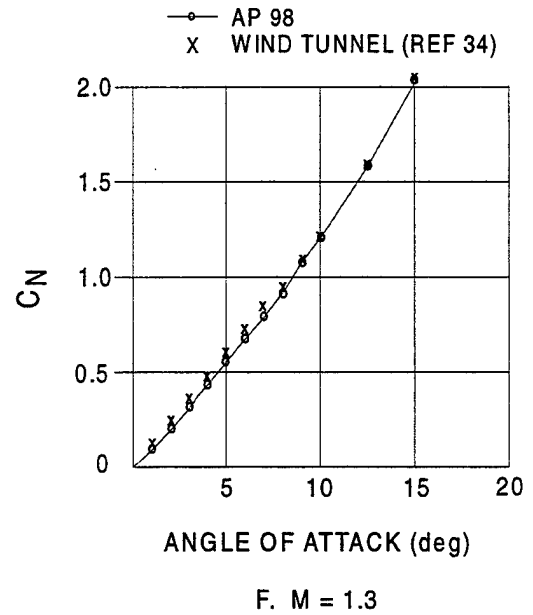
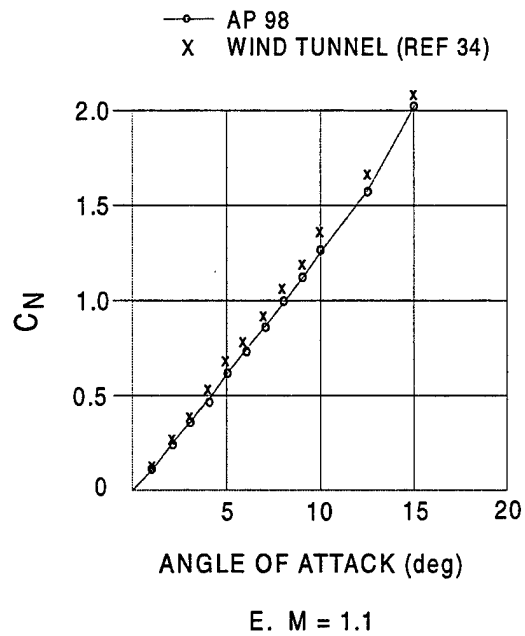


FIGURE 25. NORMAL FORCE COEFFICIENT COMPARISONS FOR FOUR-FIN GUIDED PROJECTILE OF FIGURE 23 (Continued)



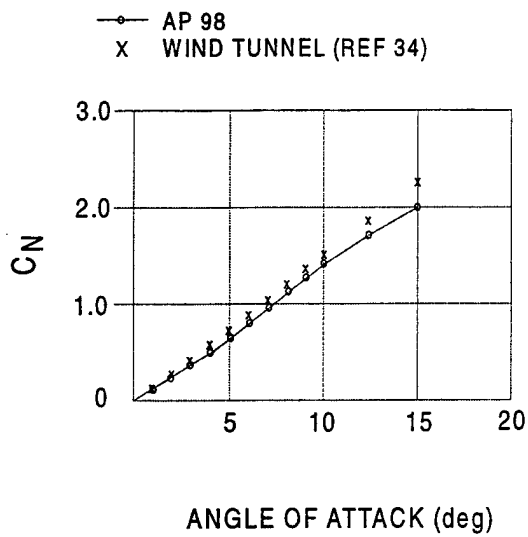
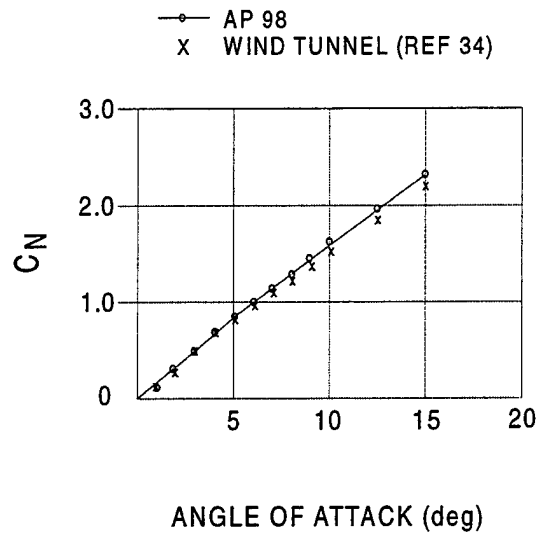
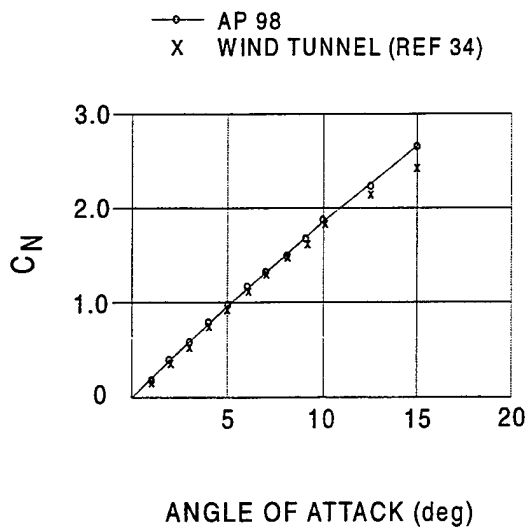
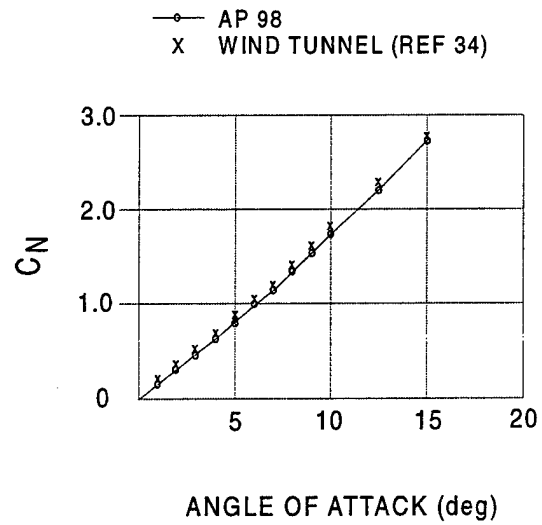
A.  $M = 0.4$ B.  $M = 0.8$ C.  $M = 0.95$ D.  $M = 1.05$ 

FIGURE 26. NORMAL FORCE COEFFICIENT COMPARISONS FOR EIGHT-FIN GUIDED PROJECTILE OF FIGURE 23

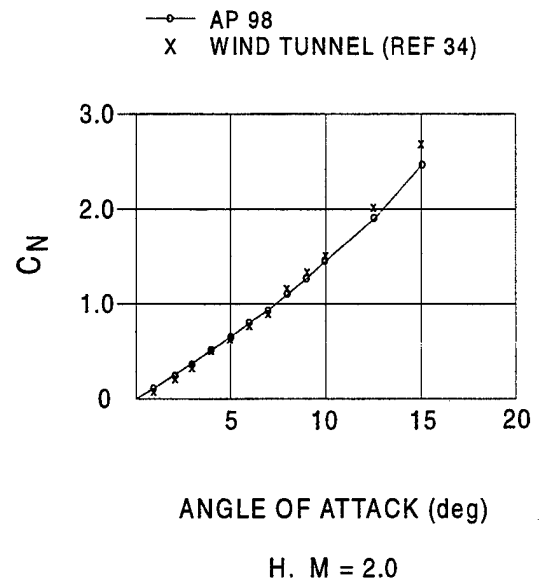
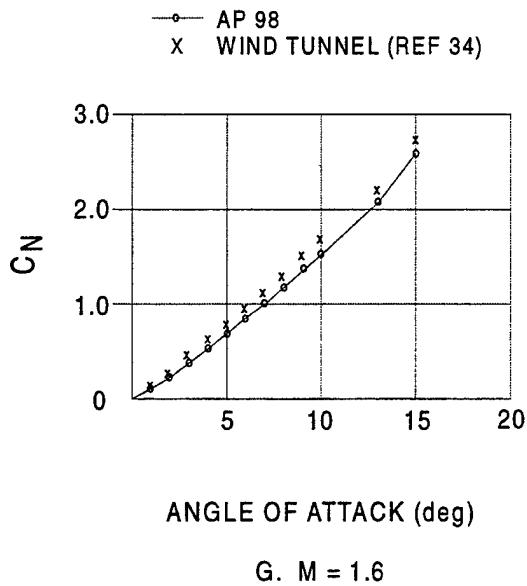
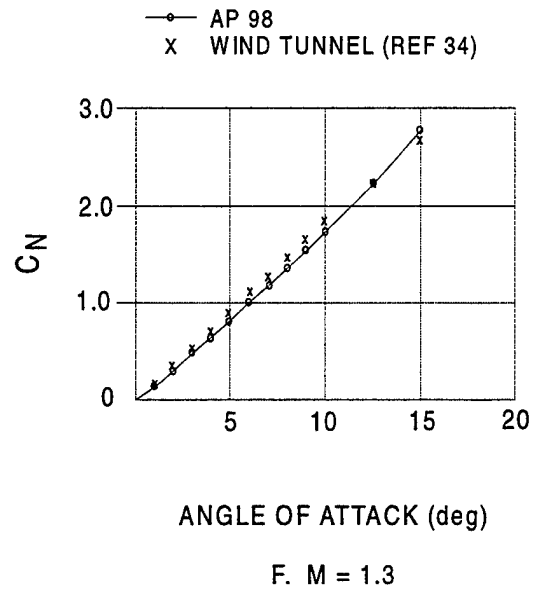
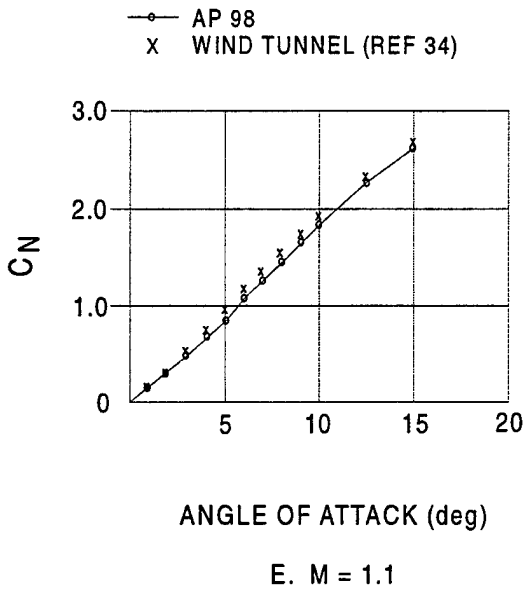


FIGURE 26. NORMAL FORCE COEFFICIENT COMPARISONS FOR EIGHT-FIN GUIDED PROJECTILE OF FIGURE 23 (Continued)

## 6.0 CONCLUSIONS

A new semiempirical method to compute aerodynamics of multifin missile configurations has been developed. The new method was developed using full Euler Computational Fluid Dynamics codes in conjunction with wind tunnel data bases. The Euler calculations were first compared to cruciform fin-body calculations from the NASA Tri-service data base. After this, factors for aerodynamics of configurations with six and eight fins were computed based on the four-fin results. Conclusions from this effort were as follows:

- i) Agreement between the NASA Tri-service data base and the CFD computations was quite good except at subsonic Mach numbers
- ii) It was concluded the major reason for the discrepancy at subsonic Mach numbers between the Euler computations and wind tunnel data was the failure of the Euler solution to adequately predict the correct flow in the leeward plane caused by viscous effects.
- iii) Full Navier-Stokes solutions, with the appropriate turbulence model, are necessary for adequate solutions of cruciform missile aerodynamics for subsonic Mach numbers as angle of attack increases. Comparisons with experiment could be improved upon at AOAs greater than 30 deg at all Mach numbers.
- iv) Without the time or funding to conduct full Navier-Stokes computations, it is believed the semiempirical model developed with the full Euler solutions in conjunction with engineering judgement is adequate.

A new aerodynamic smoother to smooth the static aerodynamics where different theoretical methods are used as a function of Mach number was also developed. It was concluded this new method worked well and should eliminate confusion on the part of users of future versions of the APC with respect to fictitious discontinuities in aerodynamics.

## 7.0 REFERENCES

1. Moore, F. G.; McInville, R. M.; and Hymer, T., *The 1998 Version of the NSWC Aeroprediction Code: Part I - Summary of New Theoretical Methodology*, NSWCDD/TR-98/1, April 1998.
2. Moore, F. G., *Body Alone Aerodynamics of Guided and Unguided Projectiles at Subsonic, Transonic, and Supersonic Mach Numbers*, NWL TR-2976, Nov 1972.
3. McInville, R. M.; Moore, F. G.; and Housh, C., *Nonlinear Structural Load Distribution Methodology for the Aeroprediction Code*, NSWCDD/TR-96/133, Sep 1996.
4. Moore, F. G. and Hymer, T., *An Improved Method for Predicting Axial Force at High Angle of Attack*, NSWCDD/TR-96/240, Feb 1997.
5. Tsien, H. S., "Supersonic Flow Over an Inclined Body of Revolution," *Journal of Aeronautical Sciences*, Vol. 5, No. 12, Oct 1938, pp. 480-483.
6. Moore, F. G.; Armistead, M. J.; Rowles, S. H.; and DeJarnette, F. R., *Second-Order Shock-Expansion Theory Extended to Include Real Gas Effects*, NAVSWC TR 90-683, Feb 1992.
7. Moore, F. G.; McInville, R. M.; and Hymer, T., *An Improved Semiempirical Method for Calculating Aerodynamics of Missiles with Noncircular Bodies*, NSWCDD/TR-97/20, Sep 1997.
8. Syvertson, C. A. and Dennis, D. H., *A Second-Order Shock-Expansion Method Applicable to Bodies of Revolution Near Zero Lift*, NACA TR 1323, 1957.
9. DeJarnette, F. R.; Ford, C. P.; and Young, D. E., "A New Method for Calculating Surface Pressures on Bodies at an Angle of Attack in Supersonic Flow," AIAA paper no. 79-1552, 12th Fluid and Plasma Dynamics Conference, Williamsburg, VA, Jul 1979.
10. Van Dyke, M. D., "First and Second-Order Theory of Supersonic Flow Past Bodies of Revolution," *Journal of Aeronautical Sciences*, Vol. 18, No. 3, Mar 1951, pp. 161-179.
11. Devan, L., *Aerodynamics of Tactical Weapons to Mach Number 8 and Angle of Attack 180 °: Part I, Theory and Application*, NSWC TR 80-346, Oct 1980.

## REFERENCES (Continued)

12. Van Driest, E. R., "Turbulent Boundary Layers in Compressible Fluids," *Journal of Aeronautical Sciences*, Vol. 18, No. 3, 1951, pp. 145-160, 216.
13. Moore, F. G.; Wilcox, F.; and Hymer, T., *Improved Empirical Model for Base Drag Prediction on Missile Configurations Based on New Wind Tunnel Data*, NSWCDD/TR-92/509, Oct 1992.
14. McInville, R. and Moore, F. G., *Incorporation of Boundary Layer Heating Predictive Methodology into the NAVSWC Aeroprediction Code*, NSWCDD/TR-93/29, Apr 1993.
15. Allen, J. H. and Perkins, E. W., *Characteristics of Flow Over Inclined Bodies of Revolution*, NACA RMA 50L07, Mar 1951.
16. Moore, F. G., *State-of-the-Art Engineering Aeroprediction Methods with Emphasis on New Semiempirical Techniques for Predicting Nonlinear Aerodynamics on Complete Missile Configurations*, NSWCDD/TR-93/551, Nov 1993.
17. Moore, F. G. and Swanson, R. C., *Aerodynamics of Tactical Weapons to Mach Number 3 and Angle of Attack 15 Degrees: Part I - Theory and Application*, NSWCDD, Dahlgren, VA, NSWCDD TR-3584, Feb 1977.
18. Moore, F. G., *Aerodynamics of Guided and Unguided Weapons: Part I - Theory and Application*, NSWCDD, Dahlgren, VA, NWL TR-3018, Dec 1973.
19. Moore, F. G.; McInville, R. M.; and Hymer, T., *The 1995 Version of the NSWC Aeroprediction Code: Part I - Summary of New Theoretical Methodology*, NSWCDD/TR-94/379, Feb 1995.
20. Moore, F. G. and McInville, R. M., *Extension of the NSWCDD Aeroprediction Code to the Roll Position of 45 Degrees*, NSWCDD/TR-95/160, Dec 1995.
21. McInville, R. and Moore, F. G., *Incorporation of Boundary Layer Heating Predictive Methodology into the NAVSWC Aeroprediction Code*, NSWCDD/TR-93/29, Apr 1993.
22. Nelson, H. F., "Wing-Body Interference Lift for Supersonic Missiles with Elliptical Cross-Section Fuselages," *JSR* Vol. 26, No. 5, Sep-Oct 1989, pp. 322-329.
23. Est, B. E. and Nelson, H. F., "Wing-Body Carryover and Fin Center of Pressure for Missiles with Noncircular Fuselage Cross Sections," AIAA 91-2856, Atmospheric Flight Mechanics Conference, New Orleans, LA, Aug 1991.
24. Nielsen, J. N., *Missile Aerodynamics*, NEAR Inc., Mountain View, CA, 1988.

## REFERENCES (Continued)

25. Ashley, H. and Landahl, M., *Aerodynamics of Wings and Bodies*, Addison-Wesley Publishing Company, Inc., Reading, MA, 1965, Chapter 7.
26. Bryson, A. E., "Stability Derivatives for a Slender Missile with Application to a Wing-Body Vertical Tail Configuration," *Journal of Aeronautical Sciences*, Vol. 20, No. 5, 1953.
27. Wardlaw, A. B. and Davis, S., *A Second-Order-Gudonov Method for Supersonic Tactical Missiles*, NSWC TR 86-506, 1986.
28. Walters, R. W.; Slack, D. C.; Cimmella, P.; Applebaum, M. P., and Frost, C., "A Users Guide to GASP," Virginia Polytechnic Institute and State University, Department of Aerospace and Ocean Engineering, Blacksburg, VA, Nov 1990.
29. Robinson, D. F, *ZEUS++ - A Graphical User Interface Flowfield Analysis Tool*, NSWCDD/TR-98/147, in publication.
30. Hymer, T. C.; Downs, C.; and Moore, F. G., *Users Guide for an Interactive Personal Computer Interface for the 1998 Aeroprediction Code (AP98)*, NSWCDD/TR-98/7, Jun 1998.
31. NASA Langley Research Center Tri-Service Missile Data Base, transmitted from NASA/LRC Jerry M. Allen to NSWCDD, 5 Nov 1991 (formal documentation of data base in process).
32. Guidos, B. J., *Static Aerodynamics CFD Analysis for 120 MM Hypersonic KE Projectile Design*, ARL-MR-84, U.S. Army Research Laboratory, Aberdeen Proving Ground, MD, Sep 1984.
33. Sturek, W. B.; Nietubicz, C. J.; Sahu, J.; and Weinacht, P., *Recent Application of CFD to the Aerodynamics of Army Projectiles*, ARL-TR-22, U.S. Army Research Laboratory, Aberdeen Proving Ground, MD, Dec 1992.
33. Guidos, B. J., "Navier-Stokes Computations of Finned Kinetic Energy Projectile Base Flow," *Journal of Spacecraft and Rockets*, Vol. 34, No. 4, Jul-Aug 1997.
34. DTRA/SAIC Projectile Development and Test Wind Tunnel Data, Defense Threat Reduction Agency, Alexandria, VA. Received through Darryl W. Hall, Science Applications International Corporation. (Unpublished)

## 8.0 SYMBOLS AND DEFINITIONS

AOA	Angle of Attack
APC	Aeroprediction Code
AP98	1998 version of the APC
AR	Aspect Ratio = $b^2/A_w$
CFD	Computational Fluid Dynamics
LT	Linear Theory
SBT	Slender-body Theory
b	Wing span (not including body)(ft)
$C_A$	Axial force coefficient
$C_{A_w}$	Axial force coefficient of wing alone
$C_{l_p}$	Roll damping moment coefficient
$C_M$	Pitching moment coefficient (based on reference area and body diameter, if body present, or mean aerodynamic chord, if wing alone)
$C_{M_q} + C_{M_{\dot{\alpha}}}$	Pitch damping moment coefficient
$\bar{c}$	Mean aerodynamic chord of wing or tail
$C_N$	Normal force coefficient
$C_{N_{B(w)}}$	Normal-force coefficient on body in presence of wing
$C_{N_{T(v)}}$	Negative normal-force coefficient component on tail due to wing or canard-shed vortex
$C_{N_w}$	Normal force coefficient of wing alone

$C_{N_{W(B)}}$	Normal-force coefficient of wing in presence of body
$C_Y$	Side force coefficient
$D$	Body diameter (ft) at base
$M_\infty$	Freestream Mach number
$r$	Local body radius (ft)
$s$	Wing or tail semispan plus the body radius in wing-body lift methodology
$V_\infty$	Freestream velocity
$X_{CP}$	Center of pressure (in feet or calibers from some reference point that can be specified) in x direction
$\alpha$	Angle of attack (deg)
$\Lambda_{LE}$	Leading edge sweep angle of wing or tail
$\Phi$	Roll position of missile fins ( $\Phi = 0$ deg corresponds to fins in the plus (+) orientation). $\Phi = 45$ deg corresponds to fins rolled to the cross (×) orientation



## DISTRIBUTION

	<u>Copies</u>		<u>Copies</u>
<b>DOD ACTIVITIES (CONUS)</b>		ATTN T C TAI	1
		M J MALIA	1
ATTN CODE 35 (ZIMET)	1	TECHNICAL LIBRARY	1
CODE 351 (SIEGEL)	1	COMMANDER	
CODE 351 (CHEW)	1	NSWC	
CODE 332FD (LEKOU DIS)	1	CARDEROCK DIVISION	
CHIEF OF NAVAL RESEARCH		WASHINGTON DC 20034	
BALLSTON CENTRE TOWER ONE			
800 NORTH QUINCY ST		ATTN R M HOWARD	1
ARLINGTON VA 22217-5660		TECHNICAL LIBRARY	1
		SUPERINTENDENT	
ATTN CODE 474T6OD (LOFTUS)	1	NAVAL POSTGRADUATE SCHOOL	
CODE 4732HOD (SMITH)	1	1 UNIVERSITY CIRCLE	
CODE 473COOD (PORTER)	1	MONTEREY CA 93943-5001	
CODE 47311OD (HOUSH)	1		
CODE 47311OD (GLEASON)	1	ATTN HEAD WEAPONS DEPT	1
CODE 4722EOD (JETER)	1	HEAD SCIENCE DEPT	1
TECHNICAL LIBRARY	1	SUPERINTENDENT	
COMMANDER		UNITED STATES NAVAL ACADEMY	
NAVAL AIR WARFARE CENTER		121 BLAKE RD	
WEAPONS DIVISION		ANNAPOLIS MD 21402-5000	
1 ADMINISTRATION CIRCLE			
CHINA LAKE CA 93555-6001		ATTN DIAG DT 4T (PAUL MURAD)	2
		DIRECTOR	
ATTN TECHNICAL LIBRARY	1	DEFENSE INTELLIGENCE AGENCY	
G RUDACILLE PMS 38012 7	1	WASHINGTON DC 20301	
COMMANDER			
NAVAL SEA SYSTEMS COMMAND		ATTN BRENT WAGGONER	1
2531 JEFFERSON DAVIS HWY		CODE 4072 BLDG 2540	
ARLINGTON VA 22242-5160		NAVAL WEAPONS SUPPORT CENTER	
		CRANE IN 47522-5000	
ATTN TECHNICAL LIBRARY	1		
COMMANDER		ATTN CODE 5252P (KRAUSE)	1
NAVAL AIR SYSTEMS COMMAND		TECHNICAL LIBRARY	1
47122 LILJENCRA NTZ ROAD UNIT 7		COMMANDER	
PATUXENT RIVER MD 20670-5440		INDIAN HEAD DIVISION	
		NAVAL SURFACE WARFARE CENTER	
ATTN C KLEIN	1	101 STRAUSS AVE	
TECHNICAL LIBRARY	1	INDIAN HEAD MD 20640-5035	
COMMANDER			
NAVAL AIR WARFARE CENTER			
WEAPONS DIVISION			
521 9TH ST			
POINT MUGU CA 93042-5001			

## DISTRIBUTION (Continued)

	<u>Copies</u>		<u>Copies</u>
ATTN TECHNICAL LIBRARY	1	ATTN H HUDGINS	1
COMMANDING GENERAL		G FRIEDMAN	1
MARINE CORPS COMBAT		TECHNICAL LIBRARY	1
DEVELOPMENT COMMAND		COMMANDING GENERAL	
2048 SOUTH ST		ARRADCOM PICATINNY ARSENAL	
QUANTICO VA 22134-5129		DOVER NJ 07801	
ATTN E SEARS	1	ATTN R PUHALLA JR	1
L E LIJEWSKI	1	W STUREK	1
C COTTRELL	1	C NIETUBICZ	1
TECHNICAL LIBRARY	1	A MIKHAIL	1
AFATL (ADLRA) (DLGC)	1	P PLOSTINS	1
EGLIN AFB FL 32542-5000		TECHNICAL LIBRARY	1
		COMMANDING GENERAL	
ATTN TECHNICAL LIBRARY	1	BALLISTIC RESEARCH LABORATORY	
USAF ACADEMY		ABERDEEN PROVING GROUND	
COLORADO SPRINGS CO 80912		ABERDEEN MD 21005-5066	
ATTN TECHNICAL LIBRARY	1	ATTN CODE TNC (BLACKLEDGE)	1
ADVANCED RESEARCH PROJECTS		RICH MATLOCK	1
AGENCY		DIRECTOR	
DEPARTMENT OF DEFENSE		INTERCEPTOR TECHNOLOGY	
WASHINGTON DC 20305		BALLISTIC MISSILE DEFENSE OFFICE	
		THE PENTAGON	
ATTN B BLAKE (BLD 146)	1	WASHINGTON DC 20350	
J JENKINS (BLD 146)	1		
TECHNICAL LIBRARY	1	ATTN SFAE SD ASP	1
COMMANDING OFFICER		SFAE SD HED	1
AFSC		DEPUTY COMMANDER	
2210 8TH STREET		US ARMY STRATEGIC DEFENSE COMMAND	
WRIGHT PATTERSON AFB OH 45433		P O BOX 1500	
		HUNTSVILLE AL 35807-3801	
ATTN EDWARD JENKINS	1		
NAIC TANW		ATTN D WASHINGTON	1
HQ NAIC TANW		W WALKER	1
4115 HEBBLE CREEK ROAD SUITE 28		R KRETZSCHMAR	1
WPAFB OH 45433-5623		D FERGUSON JR	1
		COMMAND GENERAL	
ATTN J USSELTON	1	US ARMY MISSILE COMMAND	
W B BAKER JR	1	AMSMI RD SS AT	
TECHNICAL LIBRARY	1	REDSTONE ARSENAL AL 35898-5252	
ARNOLD ENGINEERING DEVELOPMENT			
CENTER USAF		DEFENSE TECHNICAL INFORMATION	
TULLAHOMA TN 37389		CENTER	
		8725 JOHN J KINGMAN ROAD	
		SUITE 0944	
		FORT BELVOIR VA 22060-6218	2

**DISTRIBUTION (Continued)**

	<u>Copies</u>		<u>Copies</u>
DIRECTOR DEFENSE PRINTING SERVICE BLDG 176 WASHINGTON NAVY YARD 901 M ST E WASHINGTON DC 20374-5087	1	ATTN MICHAEL MUSACHIO DIRECTOR OFFICE OF NAVAL INTELLIGENCE 4251 SUITLAND ROAD (ONI 2321) WASHINGTON DC 20395	1
ATTN CODE A76 TECHNICAL LIBRARY COMMANDING OFFICER CSSDD NSWC 6703 W HIGHWAY 98 PANAMA CITY FL 32407-7001	1	ATTN DR ALAN NICHOLSON MSC 5B DEFENSE INTELLIGENCE AGENCY MISSILE AND SPACE INTELLIGENCE CTR REDSTONE ARSENAL AL 35898-5500	1
ATTN DR P WEINACHT AERODYNAMICS BRANCH PROPULSION AND FLIGHT DIV WTD AMSRL WT PB US ARMY RESEARCH LAB ABERDEEN PROVING GROUND MD 21005-5066	1	ATTN EDWARD HERBERT US ARMY MISSILE COMMAND AMSMI RD MG GA BLDG 5400 ROOM 250 REDSTONE ARSENAL AL 35898	1
ATTN GREGG ABATE US AIR FORCE WRIGHT LABORATORY WL MNAA 101 W EGLIN BLVD STE 219 EGLIN AFB FL 32542-5000	1	ATTN PAUL KOLODZIEJ NASA AMES RESEARCH CENTER MS 234 1 MOFFETT FIELD CA 94035	1
ATTN JOHN GRAU US ARMY ARDEC COMMANDER US ARMY ARDEC AMSTA AR AET A BLDG 3342 PICATINNY ARSENAL NJ 07806-5000	1	ATTN LCDR T HARTLINE USNR R NR ONI 2109 NAVAL RESERVE UNIT 112 CRESTVIEW CIRCLE MADISON AL 35758	1
ATTN FRANK MACDONALD NAWC CHINA LAKE COMMANDER CODE 473 20D NAVAIRWARCENNSDNDIV CHINA LAKE CA 93555	1	ATTN CODE 4732HOD DAVID HALL PROPULSION PERFORMANCE OFFICE NAVAL AIR WARFARE CTR WEAPONS DIV 1 ADMINISTRATIVE CIR CHINA LAKE CA 93555-6001	1
ATTN MARK LAMBERT NAWC CODE 4732HOD CHINA LAKE CA 93555	1	ATTN DONALD SHEREDA WL FIMA BLDG 450 2645 FIFTH ST STE 30 WRIGHT PATTERSON AFB OH 45433-7936	1
		ATTN ROBERT VAN DYKEN 473110D COMMANDER NAWC CHINA LAKE CA 93555	1
		BMDO AQS 1725 JEFFERSON DAVIS HWY STE 809 ARLINGTON VA 22202	1

## DISTRIBUTION (Continued)

	<u>Copies</u>		<u>Copies</u>
ATTN JEFFREY RANDORF	1	ATTN D G MILLER (L 219)	1
US ARMY SPACE AND STRATEGIC		TECHNICAL LIBRARY	1
DEFENSE COMMAND		LAWRENCE LIVERMORE NATIONAL	
P O BOX 1500 CSSD-BC-SS		LABORATORY	
106 WYNN DRIVE		EARTH SCIENCES DIVISION	
HUNTSVILLE AL 35807-3801		UNIVERSITY OF CALIFORNIA	
		P O BOX 808	
<b>NON-DOD ACTIVITIES (CONUS)</b>		LIVERMORE CA 94551	
NICHOLS RESEARCH CORPORATION		ATTN W RUTLEDGE (1635)	1
MS 912		R LAFARGE	1
P O BOX 400002		R EISLER	1
4040 S MEMORIAL PKWY		TECHNICAL LIBRARY	1
HUNTSVILLE AL 35815-1502	1	SANDIA NATIONAL LABORATORY	
		P O BOX 5800	
THE CNA CORPORATION		ALBUQUERQUE NM 87185-5800	
P O BOX 16268		ATTN WALT GUTIERREZ	1
ALEXANDRIA VA 22302-0268	1	SANDIA NATIONAL LABORATORIES	
GIDEP OPERATIONS OFFICE		MAIL STOP 0825	
CORONA CA 91720	1	P O BOX 5800	
		ALBUQUERQUE NM 87185-0825	
ATTN TECHNICAL LIBRARY	1	ATTN ASSISTANT DEFENSE	
NASA AMES RESEARCH CENTER		COOPERATION ATTACHE	1
MOFFETT CA 94035-1099		EMBASSY OF SPAIN	
		WASHINGTON DC 20016	
ATTN C SCOTT	1	DE/AVT	
D CURRY	1	DEFENSE EQUIPMENT STAFF	
NASA JOHNSON SPACE CENTER		BRITISH EMBASSY	
HOUSTON TX 77058		3100 MASSACHUSETTS AVE NW	
ATTN TECHNICAL LIBRARY	1	WASHINGTON DC 20008-3688	1
NASA		ATTN ASO LO IS	1
WASHINGTON DC 20546		ISRAEL AIR FORCE	
ATTN B HENDERSON	1	LIAISON OFFICER	
D MILLER	1	700 ROBBINS AVE	
J ALLEN	1	PHILADELPHIA PA 19111	
F WILCOX	1	ATTN GERMAN MILITARY REP US OA	1
TECHNICAL LIBRARY	2	GMR TRAFFIC AND TRANSPORTATION	
NASA LANGLEY RESEARCH CENTER		DIVISION	
HAMPTON VA 23365		10 SERVICES ROAD	
		DULLES INTERNATIONAL AP	
		WASHINGTON DC 20041	

## DISTRIBUTION (Continued)

	<u>Copies</u>		<u>Copies</u>
ATTN PROF F R DEJARNETTE	1	ATTN B BROOKS	1
NORTH CAROLINA STATE UNIVERSITY		R STANCIL	1
DEPT OF MECHANICAL AND		R ELKINS	1
AEROSPACE ENGINEERING		LORAL VUGHT SYSTEMS	
BOX 7921		P O BOX 650003	
RALEIGH NC 27695		M S EM 55	
		DALLAS TX 75265-0003	
ATTN PROF J A SCHETZ	1	ATTN PROF J D ANDERSON	1
VIRGINIA POLYTECHNIC AND STATE		DEPT OF AEROSPACE ENGINEERING	
UNIVERSITY		UNIVERSITY OF MARYLAND	
DEPT OF AEROSPACE ENGINEERING		COLLEGE PARK MD 20742	
BLACKSBURG VA 24060			
ATTN J M WU	1	ATTN TECHNICAL LIBRARY	1
C BALASUBRAMAYAN	1	HUGHES MISSILE SYSTEMS COMPANY	
TECHNICAL LIBRARY	1	P O BOX 11337 BLDG 802 MS A1	
THE UNIVERSITY OF TENNESSEE		OLD NOGALES HWY	
SPACE INSTITUTE		TUCSON AZ 83734-1337	
TULLAHOMA TN 37388			
ATTN R NELSON	1	ATTN M DILLENUS	1
TECHNICAL LIBRARY	1	NIELSEN ENGINEERING AND	
UNIVERSITY OF NOTRE DAME		RESEARCH INC	
DEPT OF AEROSPACE AND		526 CLYDE AVE	
MECHANICAL ENGINEERING		MOUNTAIN VIEW CA 95043	
BOX 537			
NOTRE DAME IN 46556		ATTN J XERIKOS	1
		N CAMPBELL	1
		TECHNICAL LIBRARY	1
ATTN PROF F NELSON	1	MCDONNELL DOUGLAS	
DEPT OF MECH AND AERO ENG		ASTRONAUTICS CO (WEST)	
UNIVERSITY OF MISSOURI ROLLA		5301 BOLSA AVE	
ROLLA MO 65401		HUNTINGTON BEACH CA 92647	
ATTN ROBERT ENGLAR	1	ATTN J WILLIAMS	1
GEORGIA TECH RESEARCH INSTITUTE		S VUKELICH	1
AEROSPACE SCIENCE AND		J FIVEL	1
TECHNOLOGY LAB		R GERBSCH (CODE 1111041)	1
ATLANTA GA 30332		TECHNICAL LIBRARY	1
		MCDONNELL DOUGLAS	
ATTN E LUCERO	1	ASTRONAUTICS CO (EAST)	
D FROSTBUTTER	1	BOX 516	
L PERINI	1	ST LOUIS MO 63166-0516	
TECHNICAL LIBRARY	1		
APPLIED PHYSICS LABORATORY		ATTN TECHNICAL LIBRARY	1
JOHNS HOPKINS UNIVERSITY		UNITED TECHNOLOGIES	
JOHNS HOPKINS ROAD		NORDEN SYSTEMS	
LAUREL MD 20723-6099		NORWALK CT 06856	

## DISTRIBUTION (Continued)

	<u>Copies</u>		<u>Copies</u>
ATTN T LUNDY	1	ATTN P REDING	1
D ANDREWS	1	G CHRUSCIEL	1
TECHNICAL LIBRARY	1	TECHNICAL LIBRARY	1
LOCKHEED MISSILES AND SPACE CO INC		LOCKHEED MISSILES AND SPACE CO INC	
P O BOX 1103		P O BOX 3504	
HUNTSVILLE AL 35807		SUNNYVALE CA 94088	
ATTN W CHRISTENSON	1	ATTN K C LEE	1
D WARNER	1	AEROTHERM CORP	
ALLIANT TECHSYSTEMS INC		580 CLYDE AVE	
600 SECOND ST NE		MOUNTAIN VIEW CA 94043	
HOPKINS MN 55343			
ATTN TECHNICAL LIBRARY	1	ATTN TECH LIBRARY	1
B SALEMI	1	FMC NAVAL SYSTEMS DIV	
J BOUDREAU	1	4800 E RIVER ROAD	
RAYTHEON COMPANY		MINNEAPOLIS MN 55421-1402	
MISSILE SYSTEMS DIVISION			
P O BOX 1201		ATTN DORIA GLADSTONE	1
TEWKSBURY MA 01876-0901		BATTELLE MEMORIAL INSTITUTE	
		COLUMBUS DIVISION	
		505 KING AVE	
ATTN LLOYD PRATT	1	COLUMBUS OH 43201-2693	
AEROJET TACTICAL SYSTEMS CO			
P O BOX 13400		ATTN JAMES SORENSON	1
SACRAMENTO CA 95813		VINCENT ALLEN	1
		ORBITAL SCIENCES	
ATTN JOSEPH ANDRZEJEWSKI	1	3380 SOUTH PRICE ROAD	
MEVATEC CORP		CHANDLER AZ 85248	
1525 PERIMETER PARKWAY			
SUITE 500		ATTN J FORKOIS	1
HUNTSVILLE AL 35806		KAMAN SCIENCES CORP	
		1500 GARDEN OF THE GODS ROAD	
ATTN DR G S SCHMIDT	1	P O BOX 7463	
LORAL DEFENSE SYSTEMS		COLORADO SPRINGS CO 80933	
1210 MASSILLON ROAD			
AKRON OH 44315-0001		ATTN RON EFROMSON	1
		MIT LINCOLN LABORATORY	
ATTN W NORDGREN 721	1	244 WOOD STREET	
GOULD INC OSD		LEXINGTON MA 02173-0073	
18901 EUCLID AVE			
CLEVELAND OH 44117		ATTN D J GIESE	1
		MAIL STOP 4C 61	
ATTN TECH LIBRARY	1	BOEING DEFENSE AND SPACE GROUP	
AEROJET ELECTRONIC SYSTEMS		P O BOX 3999	
P O BOX 296 III		SEATTLE WA 98124-2499	
AZUSA CA 91702			

**DISTRIBUTION (Continued)**

	<u>Copies</u>		<u>Copies</u>
ATTN BRIAN WALKUP ALLEGHENY BALLISTICS LAB 210 STATE ROUTE 956 WV01-13 ROCKET CENTER WV 26726-3548	1	ATTN WILLIAM FACINELLI ALLIED SIGNAL P O BOX 22200 MS 1207 3B TEMPE AZ 85285	1
ATTN DR T LIN TRW ELECTRONICS AND DEFENSE SECTOR BLDG 527/RM 706 P O BOX 1310 SAN BERNADINO CA 92402	1	ATTN DR T P SHIVANANDA TRW BMD P O BOX 1310 SAN BERNADINO CA 92402-1313	1
ATTN G VINCENT SPARTA INC 4901 CORPORATE DR HUNTSVILLE AL 35805	1	ATTN T R PEPITONE AEROSPACE TECHNOLOGY INC P O BOX 1809 DAHLGREN VA 22448	1
ATTN D P FORSMO TECHNICAL LIBRARY RAYTHEON COMPANY MISSILE SYSTEMS DIVISION HARTWELL RD BEDFORD MA 01730-2498	1 1	ATTN ERIC MOORE MAIL STOP MER 24 1281 LOCKHEED SANDERS P O BOX 868 NASHUA NH 03061	1
ATTN M S MILLER N R WALKER DYNETICS INC P O DRAWER B HUNTSVILLE AL 35814-5050	1 1	ATTN DR BRIAN LANDRUM RI BLDG E33 PROPULSION RESEARCH CENTER UNIVERSITY OF ALABAMA HUNTSVILLE AL 35899	1
ATTN H A MCELROY GENERAL DEFENSE CORP P O BOX 127 RED LION PA 17356	1	ATTN BRUCE NORTON MAIL STOP BL 1 RAYTHEON 100 VANCE TANK RD BRISTOL TN 37620	1
ATTN ENGINEERING LIBRARY ARMAMENT SYSTEMS DEPT GENERAL ELECTRIC CO BURLINGTON VT 05401	1	ATTN JIM ROBERTSON RESEARCH SOUTH INC 555 SPARKMAN DRIVE SUITE 818 HUNTSVILLE AL 35816-3423	1
ATTN TECHNICAL LIBRARY OAYNE AERONAUTICAL 2701 HARBOR DRIVE SAN DIEGO CA 92138	1	ATTN BOB WHYTE ARROW TECH ASSOCIATES INC 1233 SHELBURNE ROAD D8 SO BURLINGTON VT 05403	1
ATTN BRIAN EST BOEING ST LOUIS P O BOX 516 ST LOUIS MO 63166-0516	1	ATTN JUAN AMENABAR SAIC 4001 NORTH FAIRFAX DRIVE STE 800 ARLINGTON VA 22209	1

## DISTRIBUTION (Continued)

	<u>Copies</u>		<u>Copies</u>
ATTN TECHNICAL LIBRARY TELEDYNE RYAN AERONAUTICAL 2701 HARBOR DRIVE SAN DIEGO CA 92138	1	ATTN WILLIAM JOLLY KAMAN SCIENCES 600 BLVD SOUTH SUITE 208 HUNTSVILLE AL 35802	1
ATTN DR KIRIT PATEL SVERDRUP TECHNOLOGY INC TEAS GROUP BLDG 260 P O BOX 1935 EGLIN AFB FL 32542	1	ATTN STEPHEN MALLETT KBM ENTERPRISES 15980 CHANEY THOMPSON RD HUNTSVILLE AL 35803	1
ATTN FRANK LANGHAM MICRO CRAFT TECHNOLOGY 740 4TH ST MS 6001 ARNOLD AFB TN 37389	1	ATTN DONALD MOORE NICHOLS RESEARCH CORPORATION 4040 SOUTH MEMORIAL PARKWAY P O BOX 400002 MS 920C HUNTSVILLE AL 35815-1502	1
ATTN LAURA AYERS DELTA RESEARCH INC 315 WYNN DRIVE SUITE 1 HUNTSVILLE AL 35805	1	ATTN NANCY SWINFORD LOCKHEED MISSILES & SPACE CO P O BOX 3504 ORG E5-40 BLDG 1575E SUNNYVALE CA 94088-3504	1
ATTN BRIAN BENNETT MCDONNELL DOUGLAS MC 064 2905 P O BOX 516 ST LOUIS MO 63166-0516	1	ATTN DAVID RESSLER TRW BALLISTIC MISSILES DIV MS 953 2420 P O BOX 1310 SAN BERNARDINO CA 92402	1
ATTN THOMAS FARISS LOCKHEED SANDERS P O BOX 868 MER24 1206 NASHUA NH 03061-0868	1	ATTN MARK SWENSON ALLIANT TECHSYSTEMS MN11 262B 600 SECOND STREET NE HOPKINS MN 55343	1
ATTN COREY FROST LOCKHEED MISSILES & SPACE CO INC P O BOX 070017 6767 OLD MADISON PIKE SUITE 220 HUNTSVILLE AL 35807	1	ATTN LEROY M HAIR COLEMAN RESEARCH CORP 6820 MOQUIN DRIVE HUNTSVILLE AL 35806	1
ATTN JEFFREY HUTH KAMAN SCIENCES CORPORATION 2560 HUNTINGTON AVE ALEXANDRIA VA 22303	1	ATTN SCOTT ALLEN ALLEN AERO RESEARCH 431 E SUNNY HILLS RD FULLERTON CA 92635	1



**DISTRIBUTION (Continued)**

	<u>Copies</u>		<u>Copies</u>
ATTN DARRYL HALL SAIC 997 OLD EAGLE SCHOOL RD SUITE 215 WAYNE PA 19087-1803	1	ATTN MICHAEL GLENN TASC 1992 LEWIS TURNER BLVD FT WALTON BEACH FL 32547	1
ATTN PETER ALEXANDER MCDONNELL DOUGLAS AEROSPACE 689 DISCOVERY DRIVE MS 11A1 HUNTSVILLE AL 35806	1	ADAPTIVE RESEARCH 4960 CORPORATE DRIVE SUITE 100 A HUNTSVILLE AL 35805-6229	1
ATTN SAMUEL HICKS III TEXAS INSTRUMENTS 6600 CHASE OAKS BLVD MS 8490 PLANO TX 75086	1	ATTN STEVEN MARTIN SYSTEMS ENGINEERING GROUP INC 9841 BROKEN LAND PARKWAY SUITE 214 COLUMBIA MD 21046-1120	1
ATTN BARRY LINDBLOM ALLIANT DEFENSE ELECTRONICS SYSTEMS INC P O BOX 4648 CLEARWATER FL 34618	1	ATTN C W GIBKE LOCKHEED MARTIN VOUGHT SYSTEMS MS SP 72 P O BOX 650003 DALLAS TX 75265-0003	1
ATTN DR SHIN CHEN THE AEROSPACE CORP M4 967 P O BOX 92957 LOS ANGELES CA 90009	1	ATTN CHRIS HUGHES EDO GOVERNMENT SYSTEMS DIV 14 04 111TH ST COLLEGE POINT NY 11356	1
ATTN ROBERT ACEBAL SAIC 1225 JOHNSON FERRY RD SUITE 100 MARIETTA GA 30068	1	ATTN DANIEL LESIEUTRE NIELSEN ENGINEERING & RES INC 526 CLYDE AVENUE MOUNTAIN VIEW CA 94043-2212	1
ATTN EUGENE HART SYSTEM PLANNING CORP 1000 WILSON BLVD ARLINGTON VA 22209	1	ATTN CARL HILL FRANCIS PRIOLO STANDARD MISSILE COMPANY LLC 1505 FARM CREDIT DRIVE SUITE 600 MCLEAN VA 22102	1
ATTN ELAINE POLHEMUS ROCKWELL AUTONETICS & MISSILE SYSTEMS DIVISION D611 DL23 1800 SATELLITE BLVD DULUTH GA 30136	1	ATTN THOMAS LOPEZ COLEMAN RESEARCH CORP 990 EXPLORER BLVD HUNTSVILLE AL 35806	1
		ATTN JENNIE FOX LOCKHEED MARTIN VOUGHT SYSTEMS P O BOX 650003 MS EM 55 DALLAS TX 75265-0003	1

## DISTRIBUTION (Continued)

	<u>Copies</u>		<u>Copies</u>
ATTN JOHN BURKHALTER AUBURN UNIVERSITY 211 AEROSPACE ENGR BLDG AUBURN UNIVERSITY AL 36849	1	ATTN THOMAS KLAUSE TRW P O BOX 80810 ALBUQUERQUE NM 87198	1
ATTN DR MAX PLATZER NAVAL POSTGRADUATE SCHOOL DEPT OF AERONAUTICS & ASTRONAUTICS CODE AA PL MONTEREY CA 93943	1	ATTN DAN PLATUS THE AEROSPACE CORPORATION P O BOX 92957 LOS ANGELES CA 90009	1
ATTN MIKE DANGELO MIT LINCOLN LABORATORY 1745 JEFFERSON DAVIS HWY 1100 ARLINGTON VA 22202	1	ATTN DR REX CHAMBERLAIN TETRA RESEARCH CORPORATION 2610 SPICEWOOD TR HUNTSVILLE AL 35811-2604	1
ATTN RICHARD HAMMER JOHNS HOPKINS APPLIED PHYSICS LAB JOHNS HOPKINS ROAD LAUREL MD 20723-6099	1	ATTN DR DANNY LIU ZONA TECHNOLOGY INC 2651 W GUADALUPE RD SUITE B 228 MESA AZ 85202	1
ATTN MAURICE TUCKER BATTELLE HUNTSVILLE OPERATIONS 7501 S MEMORIAL PKWY STE 101 HUNTSVILLE AL 35802	1	ATTN PERRY PETERSEN NORTHROP GRUMMAN CORP DEPT 9B51 MAIL ZONE XA 8900 EAST WASHINGTON BLVD PICO RIVERA CA 90660-3783	1
ATTN STEVE MULLINS SIMULATION AND ENGINEERING CO INC 8840 HWY 20 STE 200 N MADISON AL 35758	1	ATTN DR JAMES HAUSER AERO SPECTRA INC 2850 KENYON CIRCLE P O BOX 3006 BOULDER CO 80307	1
ATTN ROBERT BRAENDLEIU KAISER MARQUARDT 16555 SATICOY ST VAN NUYS CA 91406-1739	1	ATTN DARRELL AUSERMAN TRW SPACE AND DEFENSE ONE SPACE PARK MAIL STATION R1-1062 REDONDO BEACH CA 90278-1071	1
ATTN LAWRENCE FINK BOEING DEFENSE AND SPACE GROUP P O BOX 3999 MS 82-23 SEATTLE WA 98124	1	ATTN JAY EBERSOHL ADVATECH PACIFIC INC 2015 PARK AVENUE SUITE 8 REDLANDS CA 92373	1
ATTN ROY KLINE KLINE ENGINEERING CO INC 27 FREDON GREENDELL RD NEWTON NJ 07860-5213	1	ATTN EDWARD RAWLINSON SY TECHNOLOGY INC 4900 UNIVERSITY SQUARE SUITE 8 HUNTSVILLE AL 35816	1

**DISTRIBUTION (Continued)**

	<u>Copies</u>		<u>Copies</u>
ATTN LAYNE COOK UNIVERSAL SPACE LINES 8620 WOLFF CT SUITE 110 WESTMINSTER CO 80030	1	ATTN DR RICHARD HOWARD NAVAL POSTGRADUATE SCHOOL DEPT OF AERONAUTICS AND ASTRONAUTICS CODE AA HO NPS MONTEREY CA 93943	1
ATTN PAUL WILDE ACTA INC 2790 SKYPARK DR SUITE 310 TORRANCE CA 90505-5345	1	ATTN J BRENT RUMINE MIT LINCOLN LABORATORY 244 WOOD STREET BUILDING S ROOM 52-327 LEXINGTON MA 02173-9185	1
ATTN DR MICHAEL HOLDEN CALSPAN UB RESEARCH CENTER P O BOX 400 BUFFALO NY 14225	1	<b>NON-DOD ACTIVITIES (EX-CONUS)</b>	
ATTN RICHARD GRABOW SPACE VECTOR CORP 17330 BROOKHURST ST SUITE 150 FOUNTAIN VALLEY CA 92708	1	ATTN LOUIS CHAN INSTITUTE FOR AEROSPACE RESEARCH NATIONAL RESEARCH COUNCIL MONTREAL RD OTTAWA ONTARIO CANADA K1A0R6	1
ATTN BRENT APPLEBY DRAPER LABORATORY 555 TECHNOLOGY SQ MS77 CAMBRIDGE MA 02139	1	ATTN H B ASLUND SAAB MILITARY AIRCRAFT 581 88 LINKOEPING SWEDEN	1
ATTN JAMES JONES SPARTA INC 1901 N FORT MYER DR SUITE 600 ARLINGTON VA 22209	1	ATTN A BOOTH BRITISH AEROSPACE DEFENCE LTD MILITARY AIRCRAFT DIVISION WARTON AERODROME WARTON PRESTON LANCASHIRE PR4 1AX UNITED KINGDOM	1
ATTN SCOTT HOUSER PHOENIX INTEGRATION 1872 PRATT DRIVE SUITE 1835 BLACKSBURG VA 24060	1	ATTN R CAYZAC GIAT INDUSTRIES 7 ROUTE DE GUERCY 18023 BOURGES CEDEX FRANCE	1
ATTN S ROM MURTY TELEDYNE BROWN ENGINEERING MS 200 300 SPARKMAN DRIVE HUNTSVILLE AL 35807	1	ATTN MAJ F DE COCK ECOLE ROYALE MILITAIRE 30 AV DE LA RENAISSANCE 1040 BRUXELLES BELGIUM	1
ATTN STUART COULTER SVERDRUP TECHNOLOGY 670 2ND ST MS4001 ARNOLD AIR FORCE BASE TULLAHOMA TN 37389-4001	1		

## DISTRIBUTION (Continued)

	<u>Copies</u>		<u>Copies</u>
ATTN J EKEROOT BOFORS MISSILES 691 80 KARLSKOGA SWEDEN	1	ATTN A MICKELLIDES GEC MARCONI DEFENCE SYSTEMS LTD THE GROVE WARREN LANE STANMORE MIDDLESEX UNITED KINGDOM	1
ATTN CH FRANSSON NATIONAL DEFENCE RESEARCH ESTABLISHMENT DEPT OF WEAPON SYSTEMS EFFECTS AND PROTECTION KARLAVAGEN 106B 172 90 SUNDBYBERG SWEDEN	1	ATTN K MOELLER BODENSEEWERK GERAETETECHNIK GMBH POSTFACH 10 11 55 88641 UBERLINGEN GERMANY	1
ATTN M HARPER BOURNE DEFENCE RESEARCH AGENCY Q134 BUILDING RAE FARNBOROUGH HAMPSHIRE QU14 6TD UNITED KINGDOM	1	ATTN G MOSS ROYAL MILITARY COLLEGE AEROMECHANICAL SYSTEMS GROUP SHRIVENHAM SWINDON WILTS SN6 8LA UNITED KINGDOM	1
ATTN A H HASSELROT FFA P O BOX 11021 161 11 BROMMA SWEDEN	1	ATTN RIBADEAU DUMAS MATRA DEFENSE 37 AV LOUIS BREQUET BP 1 78146 VELIZY VILLACOUBLAY CEDEX FRANCE	1
ATTN B JONSSON DEFENCE MATERIAL ADMINISTRATION MISSILE TECHNOLOGY DIVISION 115 88 STOCKHOLM SWEDEN	1	ATTN R ROGERS DEFENCE RESEARCH AGENCY BLDG 37 TUNNEL SITE CLAPHAM BEDS MK 41 6AE UNITED KINGDOM	1
ATTN P LEZEAUD DASSAULT AVIATION 78 QUAI MARCEL DASSAULT 92214 SAINT CLOUD FRANCE	1	ATTN S SMITH DEFENCE RESEARCH AGENCY Q134 BUILDING RAE FARNBOROUGH HAMPSHIRE QU14 6TD UNITED KINGDOM	1
ATTN J LINDHOUT N L R ANTHONY FOKKERWEG 2 1059 CM AMSTERDAM THE NETHERLANDS	1	ATTN J SOWA SAAB MISSILES AB 581 88 LINKOPING SWEDEN	1

## DISTRIBUTION (Continued)

	<u>Copies</u>		<u>Copies</u>
ATTN D SPARROW	1	ATTN H G KNOCHE	1
HUNTING ENGINEERING LTD		DR GREGORIOU	1
REDDINGS WOOD		MESSERSCHMIDT BOLKOW BLOHM	
AMPTHILL		GMBH	
BEDFORDSHIRE MK452HD		UNTERNEHMENSBEREICH APPARATAE	
UNITED KINGDOM		MUNCHEN 80 POSTFACH 801149 BAYERN	
		GERMANY	
ATTN P STUDER	1	ATTN DR S J YOON	1
DEFENCE TECHNOLOGY AND		AGENCY FOR DEFENSE DEVELOPMENT	
PROCUREMENT AGENCY		AERODYNAMICS DIVISION (4-3-1)	
SYSTEMS ANALYSIS AND INFORMATION		P O BOX 35-4 YUSEONG TAEJON	
SYSTEMS DIVISION		KOREA	
PAPIERMUEHLESTRASSE 25			
3003 BERNE		ATTN PETER CAAP	1
SWITZERLAND		HD FLIGHT SYS DEPT	
ATTN DR R G LACAU	1	FAA AERONAUTICAL RESEARCH INST	
AEROSPATIALE MISSILE		OF SWEDEN	
DEPT E/ECN		BOX 11021	
CENTRE DES GATINES		BROMMA SWEDEN 16111	
91370 VERRIERE LE BUISSON			
FRANCE		ATTN DAVE BROWN	1
ATTN J M CHARBONNIER	1	WEAPON SYSTEMS DIVISION	
VON KARMAN INSTITUTE		AERONAUTICAL AND MARITIME	
72 CHAUSSEE DE WATERLOO		RESEARCH LABORATORY	
1640 RHODE SAINT GENESE		P O BOX 1500 SALISBURY	
BELGIUM		SOUTH AUSTRALIA 5108	
		INTERNAL	
ATTN P CHAMPIGNY	1	B	1
DIRECTION DE L AERONAUTIQUE		B04	1
ONERA		B04 (ZIEN)	1
29 AV DE LA DIVISION LECLERC		B05 (GRAFF)	1
92320 CHATILLON SOUS BAGNEUX CEDEX		B05 (STATON)	1
FRANCE		B10	1
ATTN DR P HENNIG	1	B10 (HSIEH)	1
DEUTSCHE AEROSPACE (DASA)		B51 (ARMISTEAD)	1
VAS 414		B60 (TECHNICAL LIBRARY)	3
ABWEHR AND SCHUTZ		C	1
POSTFACH 801149		D	1
8000 MUENCHEN 80		G	1
GERMANY		G02	1
		G04	5
		G20	1
		G205	1
		G23	1
		G23 (BIBEL)	1
		G23 (CHADWICK)	1

## DISTRIBUTION (Continued)

	<u>Copies</u>
G23 (COOK)	1
G23 (HANGER)	1
G23 (HARDY)	1
G23 (HYMER)	1
G23 (OHLMEYER)	1
G23 (ROWLES)	1
G23 (WEISEL)	1
G30	1
G305	1
G32 (DAY)	1
G33 (MELTON)	1
G33 (RINALDI)	1
G50	1
G50 (SOLOMON)	1
G60	1
G70	1
G72	1
G72 (ALEXOPOULOS)	1
G72 (CHEPREN)	1
G72 (JONES)	1
G72 (ROBINSON)	1
G72 (MCINVILLE)	5
K	1
K40	1
K44 (ICHNIOWSKI)	1
N	1
T	1
T406	1